NMR STUDY OF STRUCTURE AND MECHANISMS OF SUPERABSORBENT POLYMERS

Diane Masson

A Thesis Submitted for the Degree of PhD
at the
University of St Andrews

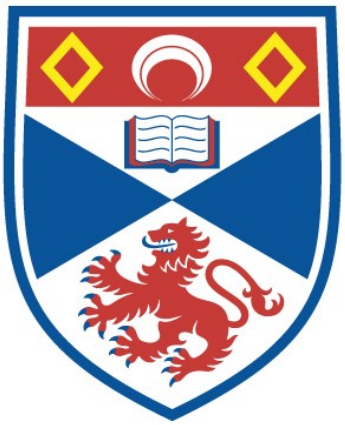

1999

Full metadata for this item is available in
St Andrews Research Repository
at:
http://research-repository.st-andrews.ac.uk/

Please use this identifier to cite or link to this item:
http://hdl.handle.net/10023/14798

This item is protected by original copyright

Lib

NMR Study of Structure and Mechanisms of Superabsorbent Polymers

Being a thesis by

Diane Masson

Submitted for the degree of
Doctor of Philosophy
in the Faculty of Science of the
University of St Andrews.

November 1998

ProQuest Number: 10171141

All rights reserved

INFORMATION TO ALL USERS
The quality of this reproduction is dependent upon the quality of the copy submitted.

In the unlikely event that the author did not send a complete manuscript
and there are missing pages, these will be noted. Also, if material had to be removed,
a note will indicate the deletion.

ProQuest 10171141

Published by ProQuest LLC (2017). Copyright of the Dissertation is held by the Author.

All rights reserved.
This work is protected against unauthorized copying under Title 17, United States Code
Microform Edition © ProQuest LLC.

ProQuest LLC.
789 East Eisenhower Parkway
P.O. Box 1346
Ann Arbor, MI 48106 – 1346

TL
D248.

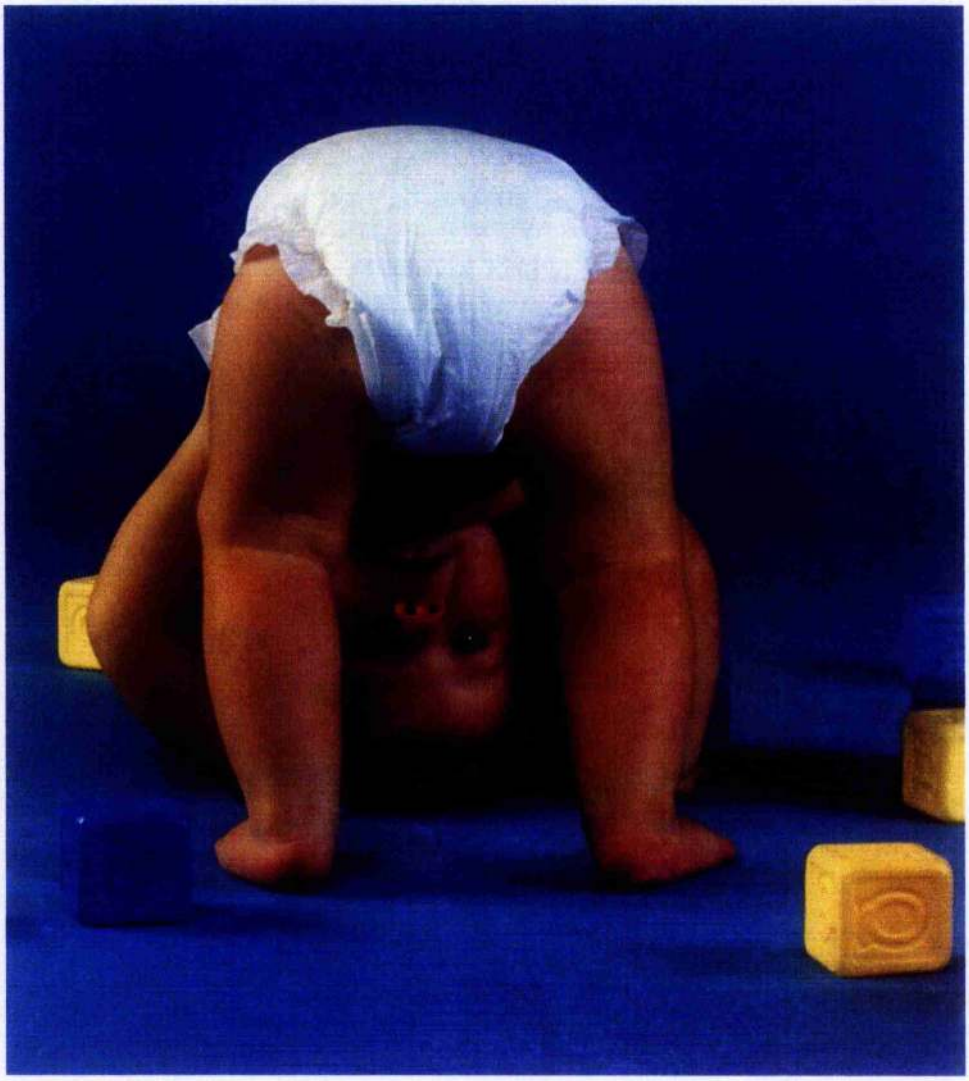

Declaration

I, Diane Masson, hereby certify that this thesis, which is approximately 30,000 words in length, has been written by me, that it is the record of work carried out by me and that it has not been submitted in any previous application for a higher degree.

Signed. (..... November 1998.

I was admitted as a research student in October 1995 and as a candidate for the degree of Doctor of Philosophy in October 1996; the higher study for which this is a record was carried out in the University of St Andrews between 1995 and 1998.

November 1998 Signature.

I hereby certify that the candidate has fulfilled the conditions of the Resolution and Regulations appropriate for the degree of Doctor of Philosophy in the University of St Andrews and that the candidate is qualified to submit this thesis in application for that degree.

November 1998 Signature. .....

Copyright

In submitting this thesis to the University of St. Andrews I wish it to be subject to the following conditions:

for a period of 5 years from the date of submission, the thesis shall be withheld from use;

I understand however, that the title and abstract of the thesis will be published during this period of restricted access; and that after the expiry of this period the thesis will be made available for use in accordance with the regulations of the University Library for the time being in force, subject to any copyright in the work not being affected thereby, and a copy of the work may be made and supplied to any bona fide library or research worker.

November 1998 Signature. .....

This work is dedicated to my mum, dad, Andrew, Fiona and Elaine

Contents

Chapter 2 - Experimental

Chapter 3 - Generations of Superabsorbent Polymer

Chapter 4 - Osmotic Ion-Exclusion Membrane

Chapter 5 - Nuclear Magnetic Resonance Imaging

Chapter 6 - Neutralisation Domains

Chapter 7 - Hydrogels of Superabsorbent Polymers

Chapter 8 - Sodium Relaxation of Superabsorbent Polymers

Abstract

Commercially important superabsorbent polymers are crosslinked polymers of partially neutralised acrylic acid which can typically absorb and retain up to a hundred times their own weight in water. Superabsorbent polymers are most widely used in the personal hygiene industry where they are found in the core of disposable nappies, external feminine sanitary products and adult incontinence pads as absorbents for bodily fluids. Many other applications have been found through their amazing absorptive properties including artificial snow, artificial muscles and the prevention of water leakage into underground transmission cables.

Superabsorbent polymers have many important industrial uses although little investigation into their structure and mechanisms has been done to date. As a result of superabsorbent polymers being totally insoluble in all NMR solvents solid state ^{13}C CP/MAS NMR was used to investigate various structural aspects of the polymer in both dry and hydrated states. The NMR work carried out on the structure of the superabsorbent polymers suggests differences in structure between polymers neutralised before and after polymerisation takes place. It also suggests different tacticity within the polymer, seen as the polymer becomes more hydrated. ^{23}Na relaxational studies have given an insight into the change in the sodium ion environment as the polymer becomes more hydrated. The effect of increasing neutralisation of the polymer was also investigated.

Nuclear Magnetic resonance imaging was also used to try and investigate the mechanism of absorption of liquid by the polymer. From the images produced it was seen that the liquid is not absorbed homogeneously throughout the polymer sample and a more intense region is seen at the front of the image suggesting a solvent front.

Commercial superabsorbent polymers are usually coated to enhance their absorptive

properties. Experiments were carried out using a sodium ion-selective electrode to try and determine whether or not this coating provided the polymer with an osmotic ion-exclusion membrane. The sodium ion-selective electrode allowed differences in $[Na^+]$ before and after the addition of polymer to a solution of NaCl to be detected, and consequently allowed the presence of an osmotic ion-exclusion membrane to be determined.

Chapter One

Introduction

History and Uses of Superabsorbent Polymers

Superabsorbent polymers (SAP's) were first commercially produced in Japan in 1978, although the idea and basic materials had been around for some time.[1] Superabsorbent polymers can typically absorb several hundred times their own weight in water.

Superabsorbent polymers were first described by W. Kern in 1938 where, using an aqueous solution of acrylic acid and divinylbenzene, he thermally synthesised crosslinked and swellable poly(acrylic acid).[2] During the 1950's Kuhn, Flory and Katchalsky described the kinetics and thermodynamics of crosslinked poly(methacrylic acid) and crosslinked poly(acrylic acid) gels swelling in water. A first practical use of these superabsorbents, as a water immobilising agent in fire fighting, was described in a patent by Bashaw and Harper (Dow Chemical) in 1966.[2] These synthetic superabsorbent polymers were synthesised by radiation induced polymerisation and crosslinking of potassium acrylate. In 1968 Harper and co-workers claimed that crosslinked polyacrylates would be useful as absorbents in nappies and similar materials, such as absorbent medical and personal care products. However, superabsorbents were only first used in disposable nappies in Japan in 1979, with the United States and Europe following in the late 1980's.[2]

Today throughout Japan, Europe and the United States, approximately 400,000 tonnes of superabsorbent polymer are manufactured every year, creating a one billion pound industry.[3]

The main use of superabsorbent polymers is to absorb body fluids in babies nappies, adult incontinence pads, child training pants and external feminine sanitary products.

The personal care industry uses 95% of the total amount of superabsorbent polymer produced.[4] Although nappies have evolved to thinner, lighter designs, the consumption of superabsorbent polymer has actually increased, since the weight loss has been achieved by removal of bulky cellulose fluff which was the traditional material of absorbent core construction.[4] The core of modern disposable nappies is manufactured by mixing the superabsorbent polymer with cellulose fluff. This mixture is then sandwiched between the porous top sheet and the impermeable back sheet.[2] While early disposable nappies contained 12 % superabsorbent polymer in their core, today it has increased to 60 %.[4] Superabsorbent polymers unlike cellulose fluff are able to absorb urine and retain it under pressure from the weight of the baby. Absorption capacities of thirty times their weight in urine are fairly typical for modern superabsorbent polymers. By absorbing and retaining the urine rather than keeping it in the spaces between the cellulose fibres, the urine is kept away from the baby's skin, leaving it dry and healthy.[4] Superabsorbent polymers are also good absorbers of ammonia and this is beneficial in nappies. The acid groups of the polymer react with alkaline substances, neutralising the ammonia in urine and possibly contributes to the prevention of nappy rash.[5]

As superabsorbent polymers are so efficient at absorbing and retaining liquids, many other applications outside the personal care industry have been developed. None of these new applications use nearly as large an amount of superabsorbent polymer as in the personal care industry, but they help solve many old problems.

Leaking water can effect the performance of buried fibre optic communication cables and power transmission cables. Where the outer core of the cable is damaged water blocking tape is used to prevent the intrusion of water.[2,3,4,5] This tape is prepared by applying a dispersion of superabsorbent polymer in a polymeric binder (styrene-butadiene-styrene resin) onto a nonwoven fabric that provides flexibility and a path for the water to reach the superabsorbent polymer. The recent building of the Channel

Tunnel used superabsorbent polymers in the making of superabsorbent rubber, also to help the prevention of water leakage.[2,4,5] The superabsorbent rubber, being made by blending hydrophilic superabsorbent powder into hydrophobic rubber, requires modification of the interface between the two materials. The superabsorbent rubber was placed on all sides of each concrete block which make up the wall of the structure. Once the superabsorbent rubber makes contact with the water, it swells, tightly filling the spaces between the blocks. The swollen polymer helps to make an impermeable barrier to the ingress of further water, keeping the tunnel dry.[2] Where the prevention of sea water leakage is important superabsorbent polymer containing sulfonate functional groups rather than carboxylic acid groups is required. This is due to the poor absorbency stability against polyvalent cations found in sea water.[4,5]

The food industry also benefits from the use of superabsorbent polymers in packaging, helping to stop fluids from leaking. Absorbent pads made by laminating the polymer powders between two tissue layers, are found in meat and poultry packages.[3,4] Sheets of polymerised monomers on nonwoven fabrics are used in fruit and vegetable storage to maintain constant humidity and to prevent condensed water from dripping onto the fruit and damaging it. Analysis of the water sorption isotherms of superabsorbent polymers using solution thermodynamics has recently been carried out. This gives important information on the transfer of water between food and the packaging in proportion to the water vapour pressure difference. Along with the affinity of the polymer for water (to prevent the leakage of water from the package during storage), this information allows an appropriate polymer to be chosen for use in food packaging.[6]

Swollen superabsorbent polymer also plays a very important part in agriculture and horticulture where it is mixed into the soil enabling the soil to retain moisture longer.[2,3,4,5,7,8] This helps plants live longer after germination and heavy soils to improve the air content. Research is currently being carried out to see if by mixing

superabsorbent polymer into deserts green fertile lands could be formed. The use of superabsorbent polymer in this way means that there can be longer intervals between watering, decreasing the accumulation of salts in the soil or water and helping the greening of deserts.[5] Usually only 0.1 weight% superabsorbent polymer is added to the soil, and recent tests have shown this to increase the yield of some vegetables up to 10 %.[2,5] Water is extracted from the gel by suction power exerted by the plant roots or by slow evaporation to the atmosphere.[7] Superabsorbent polymer powder used in this application requires to have particles with a larger diameter and higher gel strength. This prevents the gel filling the spaces between the soil, enabling the roots to breathe and the water to drain.[5,9]

In Tokyo, superabsorbent polymers are used in the manufacture of artificial snow for an indoor ski centre. The polymer is swollen to 100 times its original mass with water, frozen in place and the gel layer groomed to give realistic snow. By using these polymers the air temperature in the building can be as high as 15°C, higher than with conventional artificial snow, making life pleasanter for the skiers.[4,5]

Superabsorbent polymers have most recently been used in the active research of gel actuators, the key material for artificial muscles.[4,5,10] This could enable a robot to be built having human-like movement and touch. Gel actuators are polymeric gels which have a degree of swelling that is dependent on an external activator. The degree of swelling is used to control the actuator as the gel moves in response to a change in volume. The activator can be temperature, light, electrical field or a change of liquid. While the gel is acting as an actuator it requires a rapid response to the change in conditions, high force generation and high gel stability during repeated shrinking and swelling. Recent research by Kurauchi[5] has resulted in the construction of a "gel hand" with gel fingers which can grab an egg softly without breaking it, and a "gel fish" whose fin is made from gel.

Superabsorbent polymers can also be used as a medium for the detection of enzymes in enzyme assays as a result of their increased sensitivity over blotter paper. The superabsorbent polymer forms a clear colourless gel which allows any colour forming reaction to be seen throughout the gel giving increased sensitivity. Once the gel is formed it is restrictive to fluid and motion and only the enzyme and substrate in the vicinity will react. This has been used in the detection of alcohol in urine where levels below 0.01% have been detected.[11] Another use of superabsorbent polymers is controlling the flow of debris. The superabsorbent polymer thickens the debris flow, making it easier to clean up and preventing it from reaching residential areas.[5] Superabsorbent polymer can also be used to form a gel barrier for the containment of hazardous waste.[12]

Superabsorbent polymers have been shown to be more effective in controlling humidity than silica gel.[5] Walls and ceilings of humid buildings are protected from condensation using absorbent sheets and fibres. Due to the possibility of the gel moving, the sheets used in the food industry are not good enough for this purpose. Advanced superabsorbent sheets have to be manufactured by polymerising hydrophilic monomers in or on nonwoven fabrics.[5]

A recent patent application used a mixture of superabsorbent polymers to clean up blood spills in hospitals quickly and effectively. This use of superabsorbent polymers is very important as blood spills are not only hazardous by making the floor slippery, but can also pass on viral infections such as HIV and hepatitis.[13] The superabsorbent polymer mixture is used to convert the blood to a solid gel, where rose or pine oil is added to help stabilise the gel and remove any unpleasant odours. To make the gel safe to touch by those cleaning up the spill, chemical disinfectant is added. One major problem found with using superabsorbent polymers in this application was that it didn't solidify quickly enough. This was due to the free calcium ions in the blood interfering with the solidification process, and consequently an agent was added to

bind the free calcium ions.[13]

As well as cleaning up blood spills it was thought that the gel might also be used in surgery to help with the disposal of blood loss. Usually this blood is put into plastic bags for safe disposal. If the bag contained an amount of the solidifying mixture the gel filled bags would be easier to dispose of than a bag filled with liquid.[13]

Many new applications involving superabsorbent polymers are currently under development. These include drug delivery[14], oil explorations[14], dewatering of fine coal[15], material for semiconductor components and stabilisers for optically active media in high-capacity tuneable dye lasers.[16]

Chemistry of Superabsorbent Polymers

Commercially important superabsorbent polymers are crosslinked polymers of partially neutralised acrylic acid (Figure 1.1) and graft polymers of acrylic acid onto synthetic and natural macromolecules such as starch and cellulose.[2,3,17,18]

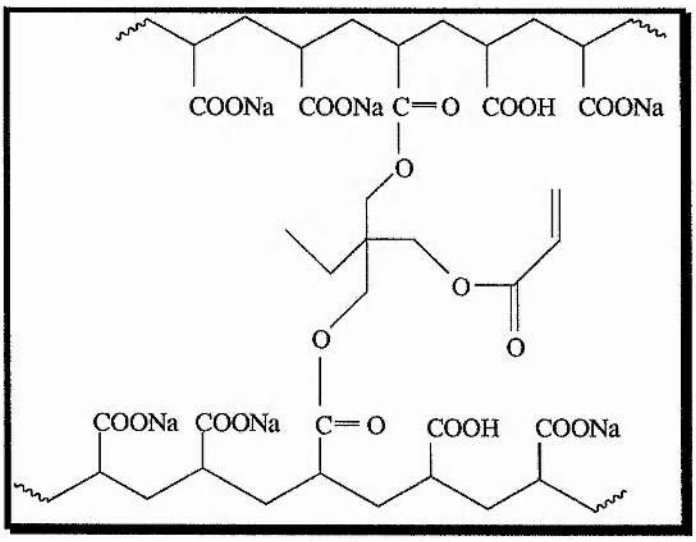

Figure 1.1 The structure of a crosslink in a typical superabsorbent polymer.

Due to the ease with which it is polymerised to high molecular weight, and to its being one of the cheapest water soluble monomers, acrylic acid is most commonly used.[19]

During a typical synthesis of a superabsorbent polymer, acrylic acid(1), sodium acrylate(2) and a crosslinker such as 1,1,1-trimethylolpropanetriacrylate(3) seen in figure 1.2 (the crosslinker is usually a monomer with more than one polymerisable vinyl double bond making it di or polyfunctional) react together in aqueous solution.[3,17] In a graft polymerisation the crosslinker is usually a reactive polyfunctional molecule, such as a diepoxide.[17]

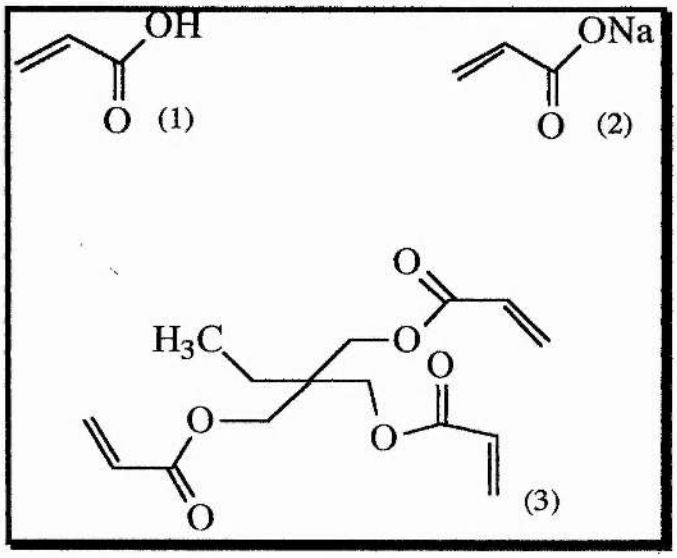

Figure 1.2 Main starting materials for the synthesis of Superabsorbent Polymers

The monomers react together by a free radical mechanism (Figure 1.3), to give a rubbery polymer gel.[3,17] During this sequence the initiator is split into two free radicals. The newly formed radicals then react with an acrylic acid or sodium acrylate monomer forming a new radical species. The crosslinker is incorporated during the propagation step where only one of the two double bonds is involved, leaving the other free to react with any further pendant chains. Propagation continues until the radicals recombine resulting in a high molecular weight three dimensional polymer.

The resulting rubbery polymer product is then cut into small pieces using a shredder. During the shredding procedure a secondary system redox initiating couple is added to capture any unreacted monomer.[20] The gel is then put through a mincing machine and the resulting small pieces are laid out and dried in an oven. The dried crumb tends to form a coral-like structure which is milled and sized disregarding any material that is over or under the required size of particle. Microparticles, which can be stored for a long time are produced with irregular shape (see photograph 1.1). These particles swell very quickly (5 to 10 seconds) although equilibrium swelling is not obtained till much later.[21]

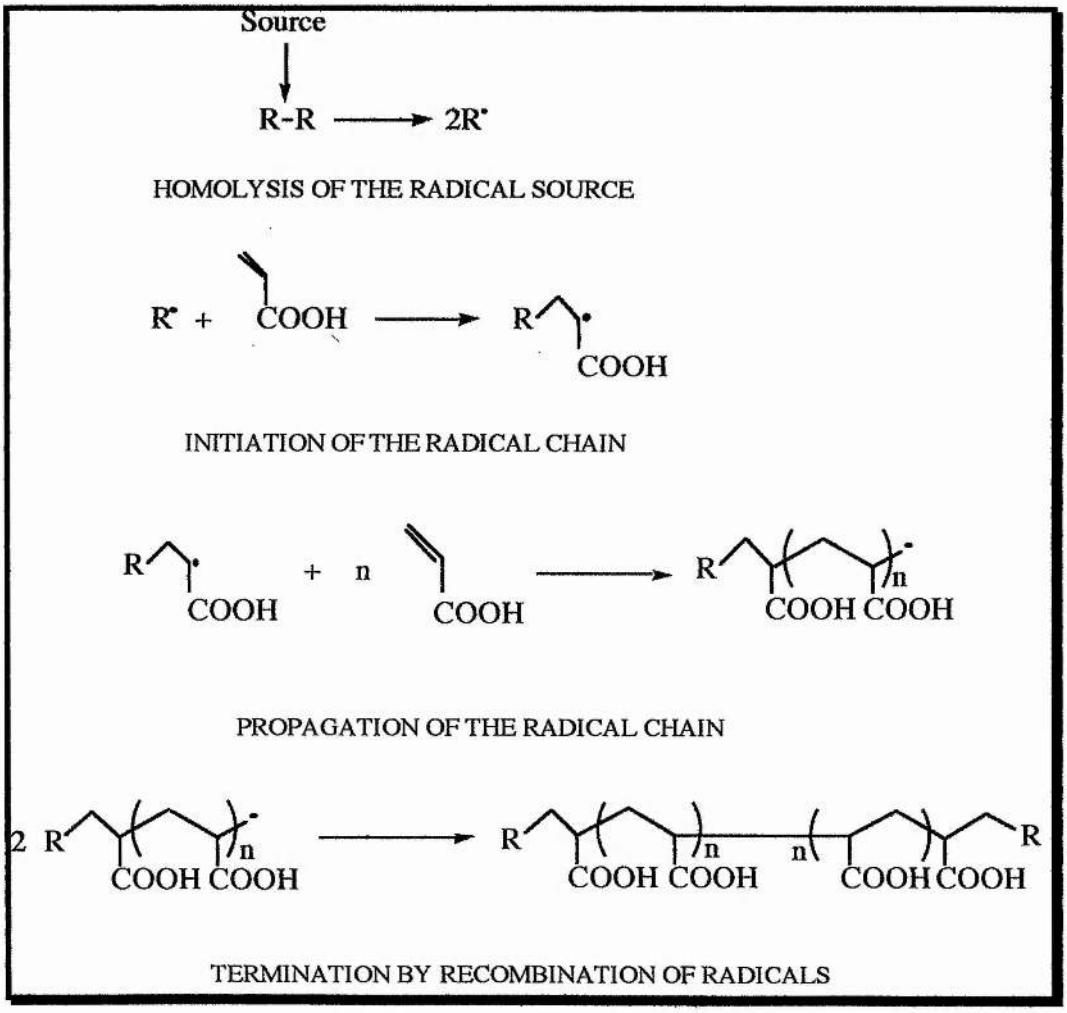

Figure 1.3 Free radical polymerisation.

Photograph 1.1. Electron microscope of polymer particles.

There are also other polymerisation routes by which superabsorbent granules can be synthesised. However, a typical laboratory aqueous gel polymerisation can be carried out by the above method.

Superabsorbent polymers can also be prepared by suspension polymerisation where small droplets of aqueous monomer solution are dispersed into an aliphatic or aromatic hydrocarbon, prior to polymerisation.[3,4,17] Free radical polymerisation of the monomers then takes place in a similar manner to that described in figure 1.3. This method of preparing superabsorbent polymers is advantageous in that no grinding of the product is required to obtain the required particle size and the heat of polymerisation is simply removed. This is due to the low viscosity of the suspension which aids agitation and heat removal.[17] Neutralisation needs to be higher using this

method of polymerisation because of the solubility of acrylic acid in the hydrocarbon phase which leads to difficulties with the reaction and handling of the product.

Another type of polymerisation used in the synthesis of superabsorbent polymers is emulsion polymerisation. In this polymerisation droplets of monomer are dispersed in water with the aid of an emulsifying agent which is usually a synthetic detergent. Small micelles are formed (1-100μm) which contain a small quantity of monomer, the rest of the monomer being suspended in the water without the aid of the surfactant. Emulsion polymerisation is initiated using a water soluble initiator, such as potassium persulfate which forms free radicals in solution which may initiate some growing chains. These radicals or growing chains then diffuse into the micelles and cause the bulk of the polymerisation to occur within the stabilised droplets.[22]

Superabsorbent polymers can also be synthesised by graft polymerisation. These use water soluble polymers such as starch, poly(vinylalcohol) and guargum[23] which are grafted into superabsorbent polymers. The introduction of rigid chains into the superabsorbent polymer is assumed to improve mechanical properties such as strength and elasticity in the swollen state. In this case the initiation is achieved by using a redox reaction between the oxidised form of a metal ion, and the oxidisable groups of the polysaccharides, helping to reduce the levels of unreacted monomer during the drying stage.[4,15]

Often to enhance its water absorptive and retention properties the polymer is further crosslinked at the surface of the particles. This is usually done using polyvalent metal ion salts, multifunctional organic crosslinkers, free radical initiators or monomer coatings that are then polymerised. The coating material is either added directly to the dry powder or as a solution in water or organic solvents. Heating is often required to promote the reaction of the crosslinker with the polymer surface.[16]

Behaviour of Superabsorbent Polymers

The behaviour of superabsorbent polymers is governed by the swelling capacity (the amount of liquid the dry polymer absorbs), and the modulus (the rigidity or stiffness of the resulting swollen gel).[4,17] These two properties depend on the crosslink density (the number of crosslinking functions per monomer function) which can be varied during the manufacture of the polymer. As the crosslinking density decreases the swelling capacity increases but the strength decreases. The final qualities of the polymer depend on the balance between the two properties. Crosslinking is also important in determining the amount of water in the polymer gel. From using the NMR values ^1H (T_1) spin-lattice relaxation, $^1H(T_2)$ spin-spin relaxation and the self diffusion coefficient (D_{H2O}) of water in a poly(methacrylic acid) gel, it was found that as the degree of crosslinking increased the above values for water in the gel decreased. This indicates that the molecular motion of water is restricted by the crosslinking.[24] Crosslinking in personal care products is of a very low level, so infra-red and NMR spectroscopy cannot be used in determining the crosslink density.

The properties of the superabsorbent polymer are dependent on the monomer concentration in the reaction solution, through the polymerisation kinetics which can lead to chain-branching, shorter primary chain molecular weight, less perfect network formation and hence poorer performance.[4,17] The efficiency of the crosslinker may be affected by the monomer concentration, as the solubility of the crosslinker (not very water soluble) often increases with an increasing organic content (increasing monomer concentration). At high monomer concentration there is a large heat of polymerisation of acrylic acid (monomer yields 18.5kcal/mole) so temperature control is important. The toughness of the intermediate polymer gel changes with the monomer concentration, affecting the design of the chemical plant used and the size of the gel particles produced during agitation of the reaction mass. If the monomer concentration is high chain transfer to the polymer will occur which leads to branching

and self crosslinking, affecting the properties of the polymer.

Another important factor in the preparation of superabsorbent polymers is neutralisation. This can take place prior to, or after polymerisation. Inexpensive bases such as sodium hydroxide and sodium carbonate are normally used as neutralising agents. The degree of neutralisation is normally in the range 60-80%[17] and can be determined using a sodium ion-selective electrode.[25]

Particle size may also affect the performance of superabsorbent polymers. This affects how rapidly the particle absorbs liquid and how easily the particle can be incorporated into the final product. Many new shapes of particle are currently being developed, one being an irregular cluster which can absorb liquid faster due to its extremely irregular shape and larger surface area.[3] Superabsorbent fibres are produced commercially and may present an attractive alternative absorbent form. Production costs for fibres are typically higher than for granular forms, and hence use of fibres has been mostly limited to specialist niche applications.

The choice of crosslinker used in the synthesis of superabsorbent polymers is also very important to the performance of the final product, although only a small amount of crosslinker is involved.[25] Usually, the crosslinker is in the form of an acrylate due to the reactivity being similar to that of acrylic acid.[26] If a crosslinker with very different reactivity ratios for homo- and co-polymerisation is used, then non-uniform crosslink distribution occurs. Chains formed late in the polymerisation tend to be less crosslinked and are either attached to the gel via grafting or contribute to the overall level of soluble polymer. This produces a gel with a nonuniform crosslink density which is detrimental to the properties of the final network.

In summary, superabsorbent polymers may be produced conveniently from widely available, aqueous compatible and attractively priced raw materials. The basic

polymerisation processes are fairly well understood, and much of the art of achieving technological advantage lies in variations of detail in preparation.

It was the primary objective of this project to enhance the understanding of the fundamental absorption processes occurring in superabsorbents by a study encompassing a variety of physical and spectroscopic methods, carried out on a range of commercial and laboratory prepared superabsorbent polymers.

The following sections will outline both the performance oriented, industrial tests used, and the more detailed analytical techniques employed.

Tests carried out on Superabsorbent Polymers

Many tests are carried out on superabsorbent polymers to try and make sure the polymer is as efficient as possible.[20,27,28] The European Disposables and Nonwoven Association (EDANA) is an industrial body which attempts to align test methodologies used within the superabsorbent polymer industry. Several patents are also available describing the different test methods.

Absorption under load (AUL)

Superabsorbent polymers used in personal care articles must resist deformation and deswelling under an external load as this ability has been correlated to improved performance in nappies. The absorption under load test has been carried out on superabsorbent polymers since 1977 and early methods indicate the use of the analysis for measuring absorption rates.[29] The test involves weighing a defined quantity of superabsorbent polymer into a cylindrical cell with mesh wire cloth fastened across the bottom. The apparatus is placed into a petri dish containing 0.9 % NaCl where it is left for a defined period. The results from the experiment are reported in grams of liquid absorbed per gram of polymer. A high AUL result indicates a high gel strength which results in a more porous gel mass. This leads to improved fluid acquisition and distribution during hydration.

Gel Volume

The gel volume test measures the swelling capacity of the polymer. Earlier industrial tests included the additional mass of interparticle unabsorbed liquid in the swelling ratios resulting in higher values. A colorimetric analysis described by Brandt et al.[30] has solved the problem of unabsorbed interparticle liquid. The concentration of a blue

macromolecular dye (blue dextran) is determined spectrophotometrically using UV/Visible in a known amount of liquid before and after swelling. This technique is known as the gel volume test and depends on the dye being rigorously excluded from the gel and concentrating in the free liquid as the polymer swells. The results are reported as a ratio of mass of liquid per mass of superabsorbent polymer.

Extractable polymer

The finished polymer may contain a proportion of polymer that is not crosslinked into the network and therefore remains soluble. This soluble portion (which does not have water absorptive properties) may leach from the superabsorbent polymer when swollen, decrease product yield and make the swollen superabsorbent polymer sticky.[17] The result is expressed as a weight % of the finished superabsorbent polymer.

Residual Monomer

Residual unreacted monomer may be left at the end of polymerisation, typically at very low (ppm) levels. As acrylic acid is an irritant and known to be toxic (LD50: 33.5 mg kg^{-1} oral, rat), residual monomer is rigorously controlled in commercial superabsorbent polymers to ensure product safety.[16] A portion of polymer is extracted in 0.9 % NaCl after which the sample containing the gel and soluble fraction is carefully filtered[30] to remove all traces of crosslinked polymer. The residual level is determined using HPLC and expressed as parts per million per gram of polymer.

Centrifuged capacity

This test measures the swelling capacity of the superabsorbent polymer.[31,32] This test

also excludes the interparticle liquid. The polymer powder is placed into a porous, heat sealable, water wettable fabric bag and placed into a bath of the desired test fluid. The polymer is left to absorb the fluid for a given length of time after which the bags are centrifuged to remove any unabsorbed fluid between the particles of the gel mass. The swelling capacity is measured as an increase in the mass of polymer sample and reported as a ratio of the weight of the fluid absorbed per weight of dry polymer.

Chemdal Ltd.

The samples used throughout this project were supplied by Chemdal Ltd., Birkenhead or synthesised by the author in their laboratories.

Chemdal Ltd. is a wholly owned subsidiary of AMCOL International Co-operation and was founded in 1986 to meet the growing demand for high-performance superabsorbent polymers. To give the company scientific expertise from North America to Europe, its laboratories are situated in Palatine, Illinois, USA and Birkenhead, UK. Chemdal is among the industry's top suppliers with an annual production capacity of 120,000 metric tons per year.

Superabsorbent Polymers manufactured by Chemdal have a wide range of performance characteristics, making them ideally suited for today's thinner nappies, feminine hygiene products and adult incontinence items. The technology for the manufacture of superabsorbent polymers was adapted from a patented process designed by the American Colloid Company (another subsidiary of AMCOL), for the manufacture of soluble polymers used in oil well drilling applications.

Nuclear Magnetic Resonance (NMR)

Most magnetic nuclei posses a nuclear spin which is described by a spin quantum number (I). The nuclear spin has an associated magnetic moment which will interact with a magnetic field B_o, generating 2I+1 energy levels. For example, the proton (^1H) and carbon (^{13}C) nuclei have spin $I = \frac{1}{2}$ which gives rise to two energy levels. These energy states can be characterised by the magnetic quantum number, m_I (where $m_I = I, (I-1).....-I$) and are separated by an amount ΔE, which is field dependent

$$\Delta E = h\gamma B_o/2\pi \qquad [\text{Eq 1.1}]$$

where γ is the magnetogyric ratio and B_o is the magnitude of the applied static magnetic field. The magnetogyric ratio is a proportionality constant relating the observation frequency for a particular nucleus to the applied magnetic field.[33,34,35]

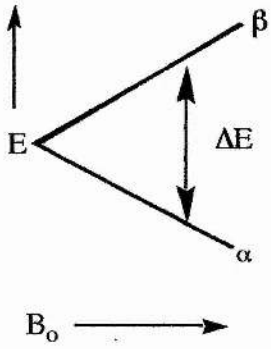

Figure 1.4. Energy level diagram spin $I=\frac{1}{2}$

The lower energy state, in which the nuclear magnetic moment is parallel to the applied magnetic field corresponds to $m_I = +\frac{1}{2}$ and is usually labelled the α state. The upper state which corresponds to $m_I = -\frac{1}{2}$, where the magnetic moment is antiparallel to the applied magnetic field is labelled β (see figure 1.4). The two energy states have the same energy and are said to be degenerate in the absence of a magnetic field. This degeneracy is lost in the presence of an applied magnetic field causing an extremely small excess of population in the lower energy state. This excess in population is given by the Boltzman equation:

$$N\beta/N\alpha = \exp(-\Delta E/kT) \qquad [\text{Eq 1.2}]$$

where Nβ and Nα are the numbers of nuclei in the excited and ground states respectively, ΔE is the energy difference between them, k is the Boltzman constant and T is the absolute temperature.[33,34,35] The population difference between the energy states is dependent both on the field and the nuclear species under observation. In the case of the proton at 200 MHz, the population difference is of the order 1 in 10^5. In the presence of the applied static magnetic field the spinning nuclei precess in a conical path around the z-axis, at the Larmor frequency (dependent on nucleus under observation). The sum of the magnetisations of all the spins causes a bulk magnetisation (M) along the z-axis[34] (see figure 1.5.)

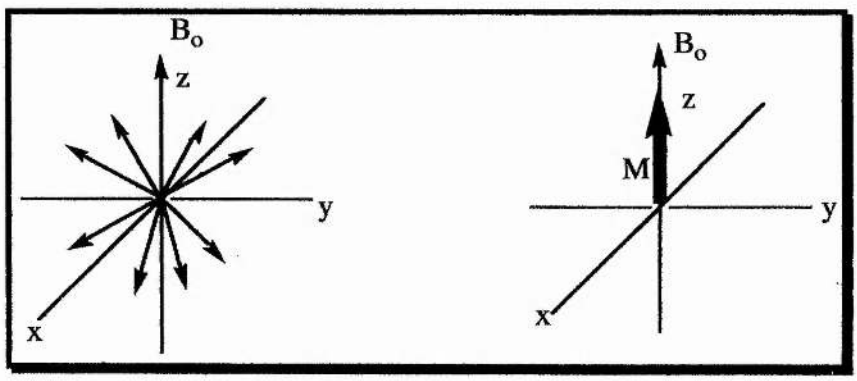

Figure 1.5. Magnetisation precessing around the z-axis.

Transitions between the two energy levels are possible when incoming radiofrequency (RF) is exactly matched to the energy difference between the two levels (the two are said to be in resonance). This radiofrequency is applied as a second rotating magnetic field (B_1) at right angles to the z-axis. This causes M to be tipped towards the xy plane through any number of degrees, according to the length of the application of the radiofrequency (pulse duration).[33,34] The radiofrequency pulse is applied over the desired range of frequencies, typically lasting a few microseconds. If for instance, a 90° pulse is applied along the x-axis the magnetisation will be tipped onto the y-axis. Here the signal is picked up by the receiver coil. The signal decays exponentially

with time due to relaxation of the spins back to their equilibrium position. Information on all the excited nuclei is contained within the signal. This is known as a free induction decay (FID). As a result of all the frequencies being recorded at the same time a Fourier transform operation using a computer is required to separate the individual frequencies.[33,34]

Rotating frame

NMR experiments can be simplified by considering them within a rotating frame of reference rather than a fixed laboratory reference frame. To overcome the problem of envisaging the precession of M around a magnetic field (B_1) which is itself rotating, we imagine ourselves to be rotating around the z-axis at the frequency of the radiofrequency field. As a result, the rotating radiofrequency field B_1 appears stationary along the rotating x-axis. The rotating frame axes are denoted as x' and y'. Two radiofrequency pulses of interest have flip angles of 90° and 180°. Applying a 90° pulse flips the bulk magnetisation into the xy plane along the y-axis of the rotating frame, where the signal has its maximum intensity. In contrast, applying a 180° pulse inverts the bulk magnetisation, flipping it onto the negative z-axis. This corresponds to an inverse polarisation of the spin system.[34]

Chemical Shift

Not all similar nuclei within a molecule have identical resonance frequencies. This is due to the frequency of an individual nucleus being influenced by the distribution of electrons in the chemical bonds of the molecule and the surroundings of the molecule.[34,35] Therefore, the resonance of a particular nucleus is dependent on molecular structure and environment. This effect is known as chemical shift. The interaction between the magnetic field B_o and the electron cloud around each nucleus produces an opposing magnetic field which is directly proportional to B_o. The local

magnetic field experienced by the nucleus is smaller than the magnetic field B_o which corresponds to a magnetic shielding of the nucleus, reducing B_o by an amount σ known as the shielding constant.[34,35]

$$B_{local} = B_o(1 - \sigma) \qquad \text{[Eq 1.3]}$$

The best way of defining the chemical shift (δ) is in terms of the difference in resonance frequencies between the nucleus of interest (υ) and a reference nucleus (υ_{ref}). In the case of ^1H and ^{13}C tetramethylsilane (TMS) is used as a reference which gives a single strong resonance from its identical twelve protons or four identical carbons. The additional advantage is that TMS resonates to low frequency (LHS of spectrum) of most other ^1H and ^{13}C resonances. This signal is set to resonate at 0 ppm and further chemical shifts are expressed in ppm from the TMS signal.

$$\delta = (\upsilon_{ref} - \upsilon) \times 10^6/\upsilon_{ref} \qquad \text{[Eq 1.4]}$$

Relaxation[33,34]

By irradiating the spins with radio frequency pulses the energy states eventually become equally populated (the system becomes saturated). In order for the system to relax back to its equilibrium position there has to be an interaction between the spins and their surroundings. There are two different relaxation processes by which this can happen, relaxation in the applied field direction (T_1) and relaxation in a direction perpendicular to the applied field (T_2). T_1 and T_2 are known as the spin-lattice relaxation and spin-spin relaxation, respectively. They are also known as longitudinal (T_1) and transverse (T_2) relaxation. During spin-lattice relaxation a change in the energy of the spin system occurs as the energy absorbed from the pulse must be removed. This energy is transferred to the "lattice" whose thermal energy increases. Dipole-dipole coupling is seen as the main contribution to spin-lattice relaxation and

arises from each nucleus being surrounded by other magnetic nuclei. The motion of the surrounding nuclei causes fluctuating magnetic fields positioned at the nucleus under observation. If these fluctuating fields have components of the appropriate frequency, then nuclear spin transitions can be induced. Immediately after irradiating with a radiofrequency pulse the z-component of the bulk magnetisation becomes zero and a transverse magnetisation component appears. Spin-spin relaxation determines how fast the transverse component of the magnetisation decays. The individual precessing nuclear spins which give rise to the bulk magnetisation, begin to lose their phase coherence and fan out. As this process continues the magnetisation becomes smaller and hence the induced signal in the receiver coil also decreases. Unlike spin-lattice relaxation, spin-spin relaxation may be regarded as an entropy process as the energy of the spin system is not altered. Spin-spin relaxation is therefore caused by energy being transferred from one nucleus to another via fluctuating fields. In this process the spin of one nucleus goes from a higher to a lower energy state, while another goes in the opposite direction. However, the main contribution to spin-spin relaxation is inhomogeneities in the magnetic field causing each nuclei to precess with slightly different Larmor frequencies.

Inversion Recovery[33,34]

T_1 relaxation is most commonly measured using a inversion recovery pulse sequence. This involves first applying a 180° pulse to flip the bulk magnetisation from the z-axis to the -z-axis. As there is no magnetisation in the xy plane we cannot directly observe the effect of this pulse and the magnetisation relaxes back to its equilibrium position. This relaxation can be monitored by making a component in the xy plane, achieved by applying a 90° pulse. This pulse flips any z magnetisation into the xy plane where it can be detected. The two pulses are separated by a delay (τ) and the intensity of the peak is measured as a function of the variable delay. See figure 1.6 for inversion recovery sequence diagram.

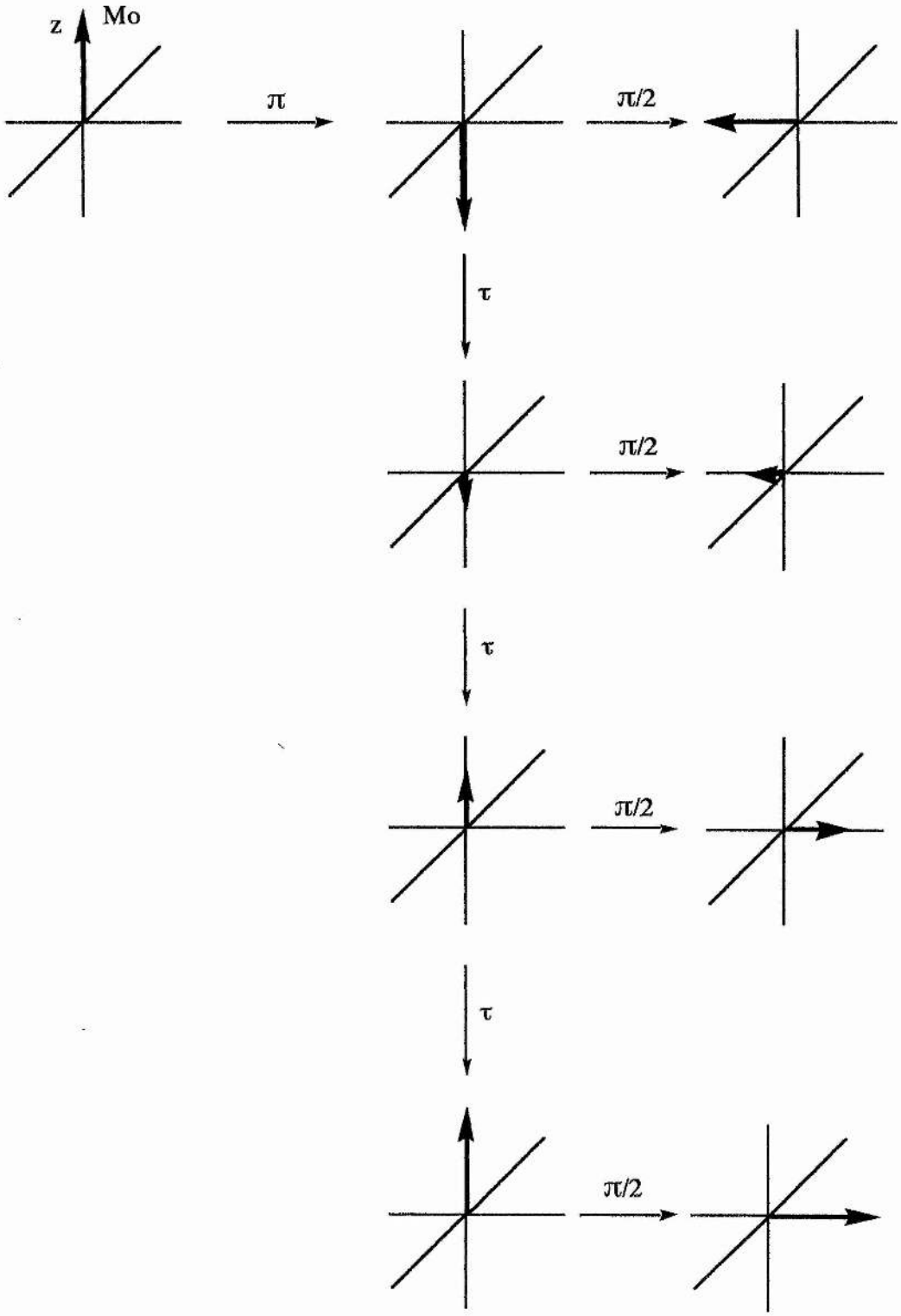

Figure 1.6. Vector diagram of an inversion recovery pulse sequence.

Saturation Recovery[33,34]

T_1 relaxation can also be measured using a saturation recovery pulse sequence. This involves saturating the system by subjecting it to a series of 90° pulses having very short delays between each one. This effectively reduces the nuclear magnetisation to zero. Once the system is saturated, it is allowed to evolve during the time delay (τ) and then detected using a 90° pulse. A variable delay is used and the intensity of the peak is measured for each delay. A graph is then plotted of ln(Ao-At) versus time where Ao is the infinity intensity value and At, the intensity value for each delay. This should give a straight line with slope $= 1/T_1$. See figure 1.7 for pulse sequence.

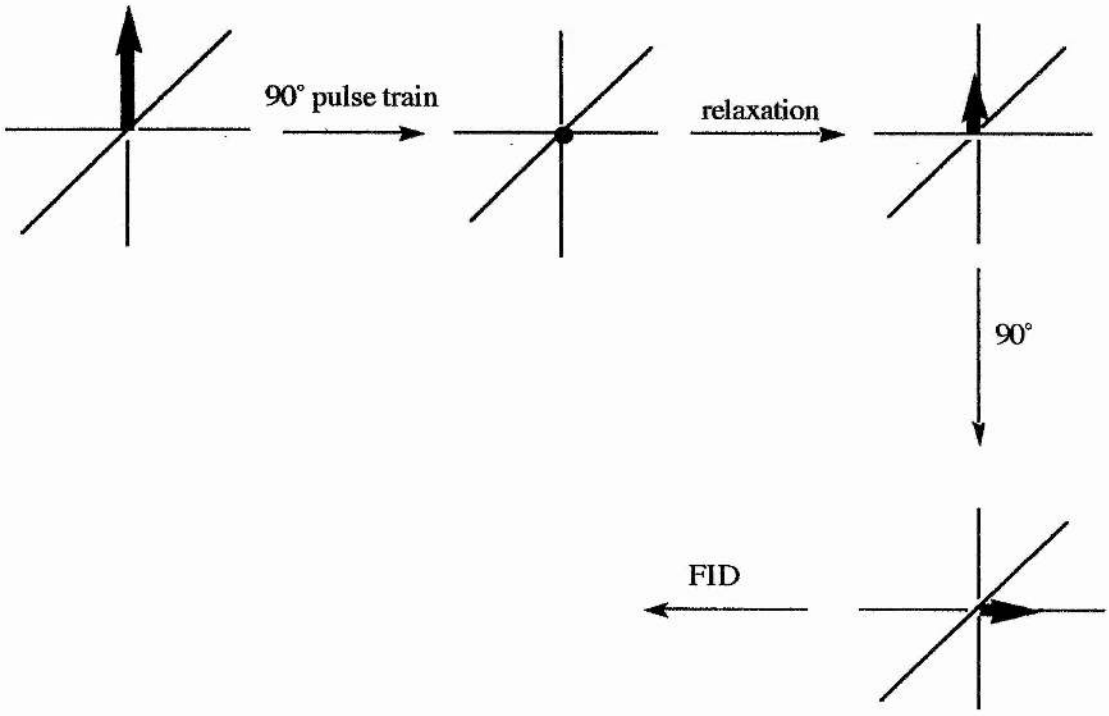

Figure 1.7. Vector diagram of saturation recovery pulse sequence.

Carr-Purcell-Meiboom and Gill pulse sequence[33,34]

T_2 relaxation can be measured by means of a modified spin echo pulse sequence, the Carr-Purcell-Meiboom and Gill pulse sequence. A spin echo pulse sequence is used to measure T_2 relaxation as it removes the contribution from the field inhomogeneities which are of little interest to the chemist. The spin echo pulse sequence first involves applying a 90° pulse along the x-axis, tipping the magnetisation onto the y-axis. As a result of the magnetic field inhomogeneities, each individual nuclear spin fans out decreasing the magnitude of the magnetisation vector. After a time delay (τ) a 180° pulse is applied so that all the vectors are along the -y direction. Due to the course followed by their relative motion, the vectors become focused in the -y direction after a time 2τ. The resultant magnetisation can now be detected by the receiver coil as a signal. The pulse sequence is shown in figure 1.8 along with the Carr-Purcell-Meiboom and Gill pulse sequence which uses a train of echoes.

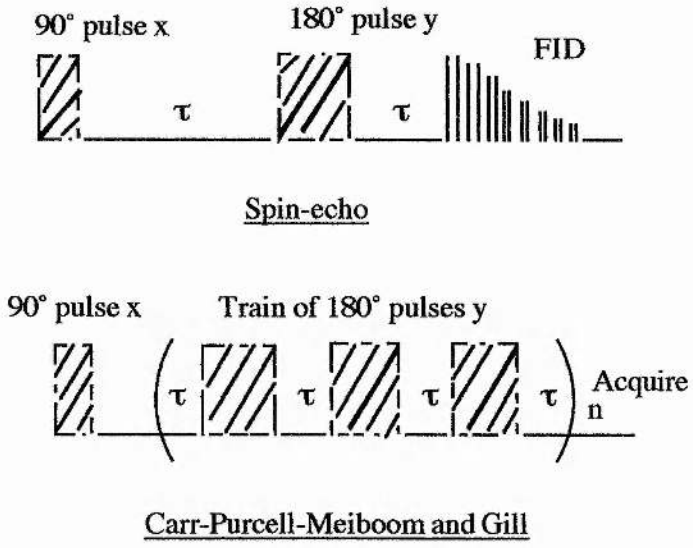

Figure 1.8. Spin-echo and CPMG pulse sequences.

Spin Coupling

Most NMR spectra contain signals which are split into many lines. The multiplicity of the splitting is dependent on the number of neighbouring nuclei plus one (n+1 rule). This splitting is caused by non-equivalent neighbouring nuclei influencing each others effective magnetic field.[33,34,35] This is usually observable when the distance between neighbouring nuclei is of three bonds lengths or less, and is known as spin-spin coupling or J-coupling. If for example we take two non-equivalent nuclei, A and B, the spin of each nuclei will be aligned with or opposed to the applied magnetic field. Therefore, the magnetic field at A for instance, will either be greater or less than the applied magnetic field. As a result A is experiencing two different applied fields and thus resonates at two different frequencies. The difference between the two frequencies is the coupling constant J. Coupling can also be through space, however, in solution the larger space coupling is averaged to zero by molecular tumbling.[33,34,35]

Decoupling

Spectra with multiple lines can be simplified by decoupling one nucleus from the other, whether they are the same nucleus or not. The splitting can only be seen if the lifetime of nucleus B, either aligned with or opposed to the applied magnetic field, is long enough. If the lifetime is shortened by irradiating with a separate radiofrequency source, then only a single line in the spectrum of nucleus A will be seen.[33,34]

Quadrupolar nuclei

Nuclei with spin quantum numbers greater than $I=\frac{1}{2}$ possess an electric quadrupole moment in addition to the magnetic dipole moment as a result of non-spherical distribution of nuclear charge.[33,34] These nuclei can interact with electrical field

gradients in the environment, especially those due to the electron shell in the molecule in which the nucleus is situated. The energy level diagram for a nucleus with I= $\frac{3}{2}$ is shown in figure 1.9.

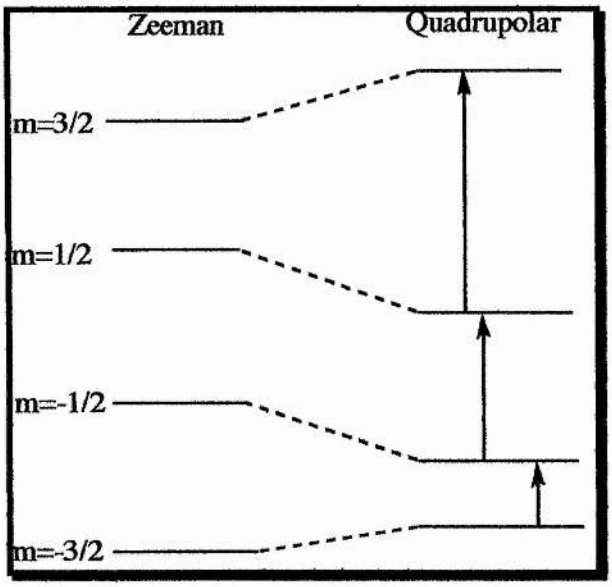

Figure 1.9. Schematic diagram of the energy levels I= $\frac{3}{2}$ resulting from the Zeeman interaction with the magnetic field and with the quadrupolar moment of the nucleus.

Solid-State NMR

In this thesis superabsorbent polymers will be investigated extensively using solid state NMR. This is because the insoluble nature of the superabsorbent polymers precludes their observation in solution and because we are interested in their solid-state properties.

Using the NMR conditions under which a liquid is investigated, a solid will give a broad signal, a rolling baseline or even nothing at all, making it very difficult to obtain clear, well resolved spectra.[33,34] This arises because many of the strong internuclear interactions present in solids have a directional dependency of the form $A(3\cos^2\theta-1)$ where θ is the angle between the internuclear vector and the magnetic field. In solution, unlike solids these interactions are averaged out by rapid molecular tumbling over a period of time $(3\cos^2\theta-1)=0$. In solids they are the main cause of line broadening.[33,34]

Dipole-dipole interactions between nearby magnetic nuclei, and chemical shielding anisotropy are the major factors causing broadening of peaks in solid state NMR.

Dipolar Broadening

In solids the dipole-dipole interaction becomes static with respect to the magnetic field and the major source of line broadening.

Dipolar coupling is dependent upon the local field (B_{loc}) at a nucleus **I** generated by a nucleus **S** (see figure 1.10). This is in turn, dependent on the magnetic moment of S (μ_S), the internuclear distance (r_{IS}) and the angle between I-S and B_O (θ_{IS}):

$$B_{loc}^{*} = \pm \mu_S \, r_{IS}^{-3} \, (3 \cos^2\theta_{IS} - 1) \qquad \text{[Eq 1.5]}$$

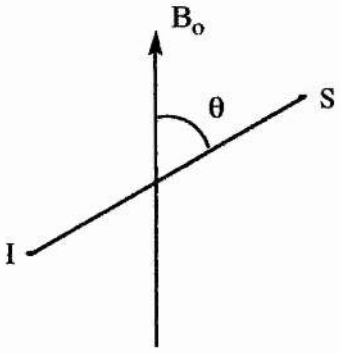

Figure 1.10. Definition of θ for dipolar interactions

Fortunately for ^{13}C NMR only 1 % of all carbons are ^{13}C. This means that on average each ^{13}C is surrounded by many ^{12}C reducing the ^{13}C-^{13}C dipolar interactions. Dipolar nuclei that are in such situations, where the nearest dipolar nucleus is well separated from it are called "dilute" spins. ^{1}H is clearly not a dilute spin whereas ^{13}C and e.g. ^{31}P in molecules containing only one phosphorous, are.

Chemical Shielding anisotropy

In solids, chemical shielding anisotropy is the second major source of line broadening.[33,34] In NMR the chemical shift is produced by electrons shielding the nucleus from the applied magnetic field. As a result of the electron distribution not being spherical or cubic (anisotropic), the chemical shielding also has directional properties. Like dipolar coupling, the chemical shielding depends on $(3\cos^2\theta-1)$ in absence of molecular tumbling.

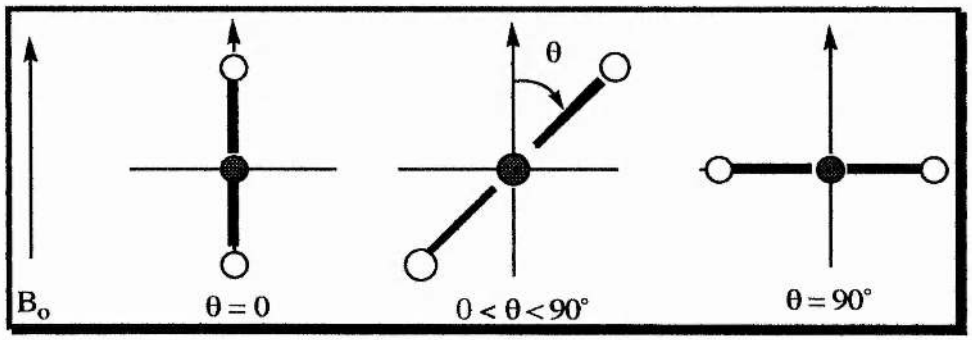

Figure 1.11. Orientations of a molecule in the applied magnetic field.

* B_{loc} can be positive or negative depending whether S is aligned with or against B_o

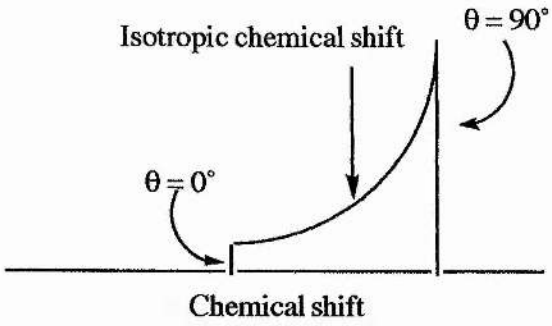

Figure 1.12. General lineshape due to chemical shielding anisotropy.

Many techniques are now available which allow the observation of narrow lines in solid-state spectra. These techniques rely on averaging the interactions described above on a timescale which is rapid compared to the linewidths.

Magic Angle Spinning

As we have seen both the dipolar coupling and the chemical shielding anisotropy have an angular dependence of the form $(3\cos^2\theta\text{-}1)$. If $(3\cos^2\theta\text{-}1)$ can be made = 0 the directional dependent terms can become vanishingly small. The angle at which this happens is referred to as the "magic angle" (θ_m).[33,34] Thus:

$$3\cos^2\theta_m - 1 = 0$$

$$\cos^2\theta_m = \frac{1}{3}$$

$$\cos\theta_m = \sqrt{\frac{1}{3}}$$

$$\theta_m = \cos^{-1}\left(\sqrt{\frac{1}{3}}\right)$$

$$\theta_m = 54.7° \text{ (see figure 1.13)}$$

If a sample is spun about an axis oriented at the magic angle to the magnetic field, the average orientation of the crystallite axes will equal the magic angle and the line will

become relatively sharp.

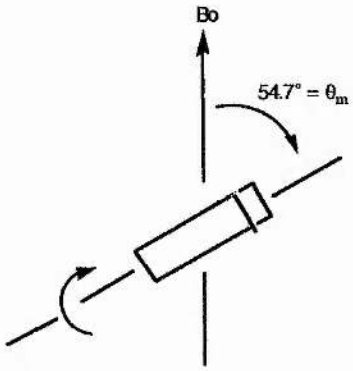

Figure 1.13. Sample spinning at the magic angle.

In order for magic angle spinning to eliminate the line broadening caused by chemical shielding anisotropy (CSA) the rotation frequency must be of the order of the CSA linewidth. If the sample is spun at the magic angle at a speed slower than the chemical shielding anisotropy envelope a series of side-bands separated by the spinning frequency is observed. As the speed is increased the spinning side-bands separate further. If the sample is spun faster than the chemical shielding anisotropy then only the centre band remains at the isotropic chemical shift.[33,34]

The more symmetrical the environment of a carbon atom is, the lower its chemical shielding anisotropy is. Thus aliphatic ^{13}C (sp^3) has a lower chemical shielding anisotropy than aromatic, alkene or carbonyl ^{13}C.

Dipolar decoupling

Much of the line broadening in solid-state spectra is due to dipolar coupling to protons. As these are strong interactions, linewidths of many kHz result. This coupling can be removed using high power heteronuclear decoupling which takes place during the acquisition of the FID.[33,34] This decoupling sharpens the lines of the spectrum. When dipolar coupling is combined with magic angle spinning both chemical shielding anisotropy and dipolar broadening can be essentially eliminated or at least greatly reduced.

Cross polarisation

Another difficulty in obtaining solid state spectra for dilute spins such as ^{13}C is that spin lattice relaxation times of ^{13}C can be very long, rendering conventional single pulse methods inefficient. The low γ and abundance of ^{13}C gives relatively weak signals. To overcome these difficulties a technique known as cross polarisation has been developed, which involves enhancing the intensity of NMR signals of low γ nuclei alternating the population distributions.[33,34] The dipolar interaction is used to transfer the population characteristics of high γ nuclei to low γ nuclei. The cross polarisation pulse sequence involves first applying a 90° pulse in the ^{1}H channel along the x' axis flipping the ^{13}C magnetisation vector onto the y' axis (see figure 1.14).

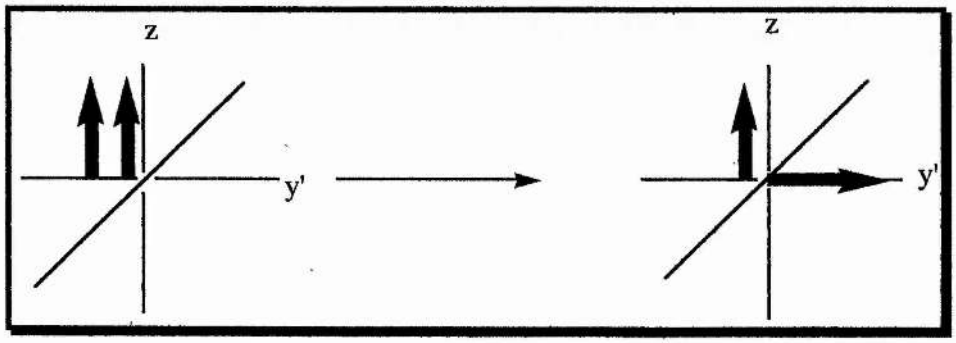

Figure 1.14. Vector Diagram for Cross Polarisation.

The transmitter is then switched to the y'axis which "spin-locks" the magnetisation vector in the rotating frame precessing about the y' axis at an angular frequency $\omega 1$:

$$\omega 1\,(^{1}H)=\gamma(^{1}H)B_1 \qquad \text{[Eq 1.5]}$$

If a radio frequency pulse is then applied along the y' axis for the ^{13}C spins it forces both sets of nuclei to precess in the rotating frame at a frequency $\omega 1$:

$$\omega 1(^{13}C) = \omega 1(^{1}H). \qquad \text{[Eq 1.6]}$$

At the ^{13}C nuclei there is an oscillating component of the ^{1}H magnetisation at the frequency $\omega 1(^{1}H)$ while at the protons there is an oscillating component of the ^{13}C magnetisation $\omega 1(^{13}C)$. Matching of the two frequencies meets the Hartmann-Hahn condition allowing the spins to "talk to each other" and permits mutual spin flips or mutual relaxations:

$$\gamma(^{13}C)B_1(^{13}C) = \gamma(H)B_1(H). \qquad \text{[Eq 1.7]}$$

As the ^{1}H magnetisation is larger than the ^{13}C magnetisation it allows rapid transfer of magnetisation from the large ^{1}H pool to the smaller ^{13}C pool by cross relaxation. During acquisition of the free induction decay the proton transmitter is left on for dipolar decoupling. The ^{13}C signal is derived from the value of γH rather than the lower γC, and the time delay required between successive acquisitions is governed by the ^{1}H spin-lattice relaxation rate rather than the slower ^{13}C relaxation rate. Using cross polarisation the ^{13}C nuclei are polarised up to a factor of four higher than by spin-lattice relaxation. The pulse sequence for cross polarisation can be seen in figure 1.15. During the contact time magnetisation is being transferred from ^{1}H to ^{13}C. It is also being lost by relaxation in the rotating frame from ^{1}H to ^{13}C. The contact time is varied to obtain the optimum transfer and is typically about 1 ms for ^{13}C in CPMAS NMR.

Using cross polarisation we can produce dipolar-decoupled ^{13}C spectra with significant improvement in sensitivity. Combining this sequence with a sample spinning at the magic angle gives us what is known as a CPMAS experiment.

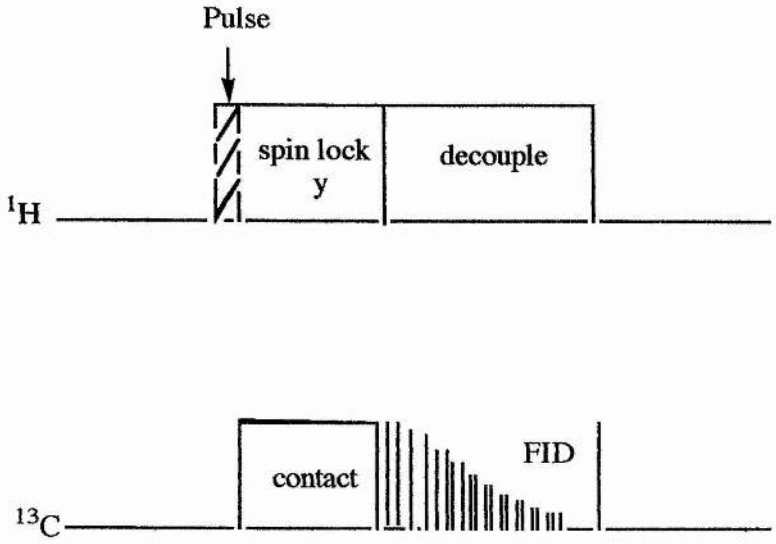

Figure 1.15. Pulse sequence for cross polarisation.

Flip Sequence

To improve the efficiency of the cross polarisation sequence the flip back pulse sequence was devised by Tegenfeldt and Harberlen in 1979.[33,34] This modified cross polarisation sequence introduces a 90°-x ^{1}H pulse immediately following the end of the decoupling pulse. The flip back pulse sequence is useful in the case of long proton relaxation times, where the extra 90° pulse flips the magnetisation remaining at the end of the observation period, back along the static magnetic field. Improved signal to noise ratio is also achieved using this pulse sequence. The pulse sequence is shown in figure 1.16.

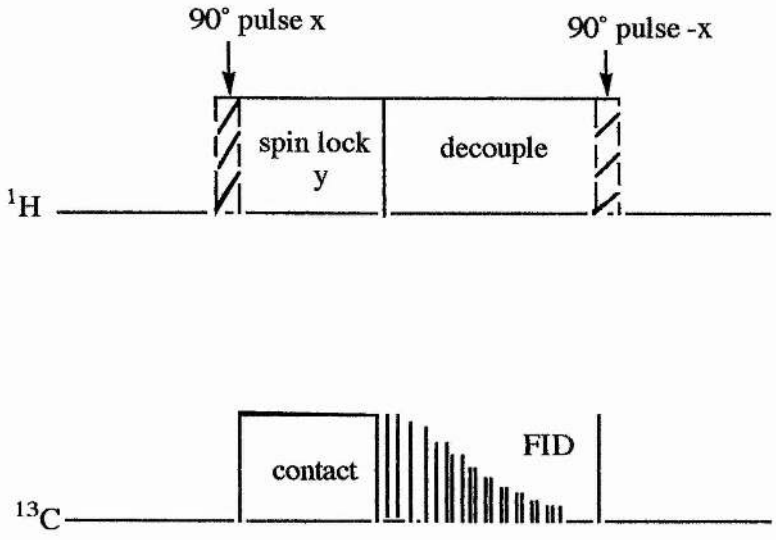

Figure 1.16. Flip back pulse sequence.

NMR of Polymers

Polymers are long chain molecules comprising a large number of basic repeating units. Usually they are organic materials involving elements such as carbon, oxygen, hydrogen, silicon, phosphorus, sulfur, chlorine and fluorine.[36] Polymers are high molecular weight molecules which can exist in crystalline, glassy or rubbery states (one or more can be present simultaneously). Many polymers have great commercial importance such as poly(ethylene), poly(styrene) and poly(vinyl chloride) and it is important to be able to control and design their physical and chemical responses.

It is important to understand structure and motion in polymers due to the manner in which they affect properties of practical interest such as the overall performance and potential applications of the polymer. Polymer characterisation has presented the analytical chemist with major difficulties, where new techniques have had to be developed to overcome the problem. NMR spectroscopy has become one of the most powerful techniques for the investigation of polymers, with new applications appearing constantly. The NMR of polymers was first reported by Bovey and Tiers in 1946.[37] No further advances were made for many years in this field as many thought the NMR spectra of macromolecules, due to their slow motions would give complicated and useless spectra.[38,39]

Polymers can be investigated by NMR both in solution and the solid-state. The nuclei most commonly used in the NMR study of polymers are ^{13}C, ^{1}H, ^{31}P, ^{29}Si and ^{19}F, although the use of ^{1}H NMR in polymers is restricted due to the lack of chemically unresolved information. When observed in the solid-state, polymers give very broad resonances which result from the direct interaction of the observed nuclei with the magnetic dipoles of the surrounding protons. These interactions are partially averaged by molecular motion and along with the techniques described on pages 33-37, narrower resonances are observed. The first ^{13}C solid-state NMR spectrum of a

polymer was reported by Schaefer in 1976[37], with further development leading to the introduction of MAS in the study of polymer characteristics. Due to many new synthetic polymers being not readily melted or being insoluble the development of solid-state NMR techniques for the study of polymers has greatly increased over the last decade.

One of the earliest and most useful applications of NMR in the study of polymers was the observation of the stereochemistry (tacticity).[38,40] Polymers containing a series of asymmetric carbon atoms along the molecule can exist in three distinct possible stereochemical arrangements. Firstly where all the asymmetric carbon atoms are in the same configuration, the polymer is described as isotatic. The other two configurations where the asymmetric carbons are in a regular alternating arrangement and where they are in a completely random arrangement are termed syndiotactic and atactic, respectively (see figure 1.17).

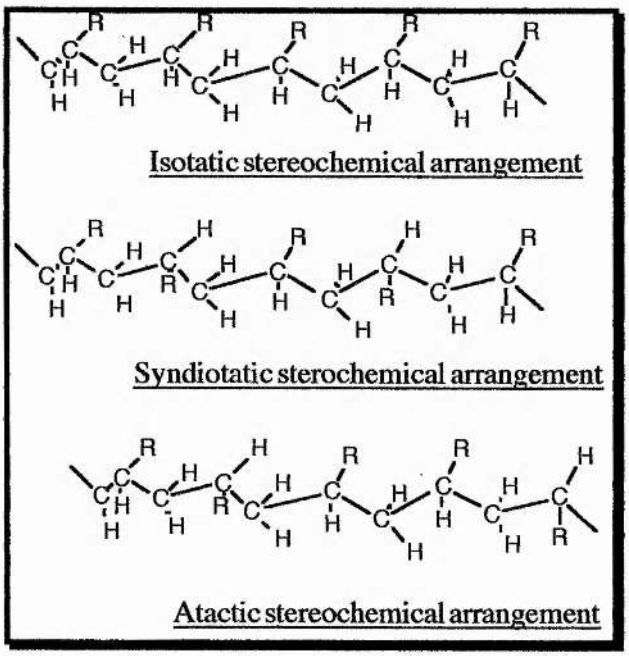

Figure 1.17. Stereochemical arrangements of polymers containing asymmetric carbon atoms

Spectral differences between various compounds reflect differences in stereochemistry. To interpret these differences the polymer chain is considered in terms of the shortest sequences which reflect the relative chirality of adjacent asymmetric carbon atoms i.e. monomer dyads. These dyads are termed rr in the syndiotatic chain and mm in the isotatic polymer chain. Further stereochemical differences can often be seen and this can be accounted for by looking at the pentad or even heptad sequences of the polymer chain.

The most widely used nucleus in the study of polymers by NMR is ^{13}C. It is thought that the chemical shift may be a function of the conformation of the polymer chain or molecule. In the liquid state, magnetically inequivalent nuclei will give a single signal if they are subject to the thermally activated exchange of the spins between different conformational sites. If the rate of exchange is fast relative to the difference in chemical shift a single signal is observed. However, in the solid-state the molecule is likely hindered and it is more likely to adopt only one of the conformations available, giving distinct signals.[41]

Many synthetic polymers are chemically crosslinked to from network structures which have limited solubility. High resolution solid-state NMR can be used to characterise the chemical structures of crosslinked systems, imply the mechanisms of network formation and characterise the segmental and chain motions at the molecular level.[42] Many polymer networks contain a variety of crosslinked structures. NMR can not only determine the types of crosslink present, but also the quantities of each type. Characterisation of the network structure of a polymer is important as it is responsible for the physical and mechanical properties.

NMR can also be used to measure relaxation times which are sensitive to the mobility of NMR active species.[43] The ability to distinguish chemical species based upon mobility is extremely useful in polymer reaction systems. This is due to a large

change in mobility occurring when unit is converted from monomer to polymer. Species that have high mobility have long relaxation times where species that have low mobility have short relaxation times. Kurtou looked at the bulk polymerisations of methylmethacrylate and methacrylic acid by measuring T_2 from the FID at various reaction conversions. Relaxational studies had also been carried out on the water inside hydrogels to try and obtain information about the network structure. Tanaka *et al.* used spin-echo experiments to analyse water in polyacrylamide networks.

NMR relaxational studies were also performed to characterise the complexes of poly(ethylene glycol) with poly(methylmethacrylate). The spin-spin relaxation time of the complexed poly(ethylene glycol) was found to be significantly shorter than for the uncomplexed chains.

NMR is therefore an extremely useful tool in the study of polymers allowing many structural and mechanistic details to be observed.

References

1. F. Masuda; ACS Symposium Series, (1994), **573**, Chapter 7.
2. F. L. Buchholz; *Journal of Chemical Education*, (1996), **73**, 512-515.
3. F. L. Buchholz; *Chemistry in Britain*, (1994), **30**, 652-656.
4. F. L. Buchholz; *Chemtech*, (1994), **September**, 38-43.
5. T. Shimomura, T. Namba; ACS Symposium Series, (1994), **573**, Chapter 9.
6. H. Kumagai, A. Mizuno, H. Kumagai, T. Yano; *Bioscience Biotechnology and Biochemistry*, (1997), **61**, 936-941.
7. J. Woodhouse, M. S. Johnson; *Agricultural Water Management*, (1991), **20**, 63-70.
8. K. S. Kazanskii, S. A. Dubrovskii; *Advances in Polymer Science*, (1992), **104**, 97-133.
9. A. V. Smagin, N. B. Sadovnikara; *Eurasian Soil Science*, (1995), **27**, 26-34.
10. H. Park, K. Park; Hydrogels and Biodegradable Polymers for Bioapplications, (1996), Chapter 1.
11. D. A. Kidwell; *Analytical Biochemistry*, (1989), **182**, 257-261.
12. E. Wilkins, Y. Lu; *Journal of Environmental Scientific Health*, (1994), **A29(9)**, 1829-1841.
13. European Patent Application, 0839539, (1997).
14. M. G. Kulkarni; *Indian Journal of Technology*, (1990), **28**, 343-353.
15. G. P .T. Dzinomwa, C. J. Wood; *Polymers for Advanced Technologies*, (1997), **8**, 767-772.
16. F. L. Buchholz; Absorbent Polymer Technology; Eds. L. Brannon-Peppas, R. S. Harland; Elsevier Science Publishing Company Inc.: New York, NY, 1990, Chapter 1.
17. F. L. Buchholz; ACS Symposium Series, (1994), **573**, Chapter 2.
18. C. M. Garner, M. Nething, P. Nguyen; *Journal of Chemical Education*, (1997), **74**, 95-96.

19. Z. S. Lui, G. L. Rempel; *Journal of Polymer Science A, Polymer Chemistry*, (1997), **64**, 1345-1353.

20. P. A. MacKenzie; Industrial Placement report, (1995).

21. N. A. Peppas, D. Hariharan; ACS Symposium Series, (1994), **573**, Chapter 3.

22. F. Askari, S. Natish, H. Omidian, S. A. Hashemi; *Journal of Applied Polymer Science*, (1993), **50**, 1851-1855.

23. H. T. Lokhande, P. V. Varadarajan, V. Iyer; *Journal of Applied Polymer Science*, (1992), **45**, 2031-2036.

24. H. Yasunga, I. Ando; *Journal of Molecular Structure*, (1993), **301**, 125-128.

25. S. S. Cutie, R. M. Van Effen, D. L. Rick, B. J. Duchane; *Analytica Chimica Acta*, (1992), **260**, 13-17.

26. P. B. Smith, C. Powell, S. S. Cutie, J. Koswan, D. E. Henton, B. A. Howell; *Journal of Applied Polymer Science A Polymer Chemistry*, (1997), **35**, 799-806.

27. F. Engelhardt, G. Ebert, R. Funk; *Advanced Materials*, (1992), **4**, 221-230.

28. H. Nagorski; ACS Symposium Series, (1994), **573**, Chapter 8.

29. A. R. Reid; US Patent, 4,051,086, (1977).

30. K. E. Brandt, S. A. Goldman, T. A. Inglin; US Patent, 32,649, (1988).

31. S. K. Byerly et al.; European Patent Application, 532,002, (1993).

32. F. H. Lahrman, C. J. Berg, D. C. Roe; US Patent, 5,149,334, (1992).

33. H. Gunther; NMR Spectroscopy Basic Principles, concepts, and applications in chemistry; John Wiley & Sons Ltd.: New York, NY, 1995, 2nd Edition, Chapters 1,7 and 10.

34. J. K. M. Sanders, B. K. Hunter; Modern NMR Spectroscopy A Guide for Chemists; Oxford University Press: Oxford, UK, 1993, 2nd Edition, Chapters 1,8 and 9.

35. P. J. Hore; Nuclear Magnetic Resonance; Oxford University Press: Oxford, UK, 1995, Chapters 1,2 and 3.

36. J. W. Nicholson; The Chemistry of Polymers; The Royal Society of Chemistry, Cambridge, 1997, 2nd Edition, Chapter 1.

37. J. L. Koenig; *Analytical Chemistry*, (1987), **59**, 1141-1154.

38. F. A. Bovey; *Arabian Journal for Science and Engineering*, (1988), **13**, 183-196.

39. R. K. Harris; Polymer Science; John Wiley and Sons Ltd.: New York, NY, 1996, Chapter 4.

40. F. A. Bovey; *Polymer Engineering and Science*, (1986), **26**, 1419-1429.

41. J. R. Havens, J. L. Koenig; *Applied Spectroscopy*, (1983), **37**, 226-249.

42. R. L. Silvestri, J. L. Koenig; *Analytica Chimica Acta*, (1993), **283**, 997-1005.

43. A. M. Marthur, A. B. Scranton; *Biomaterials*, (1996), **17**, 547-557.

Chapter Two

Experimental

Symbols and Abbreviations

Hz	hertz
MHz	Megahertz
kHz	kilohertz
ppm	parts per million
ms	milliseconds
s	seconds
μs	microseconds
NMR	nuclear magnetic resonance
o.d.	outer diameter
ASAP	advanced superabsorbent polymer
ml	millilitres
psi	pounds per square inch
rpm	revolutions per minute

NMR Spectra

All MAS NMR spectra were carried out on a Bruker MSL 500 spectrometer operating at 125.758 MHz for ^{13}C, 132.294 MHz for ^{23}Na and 500.130 MHz for ^{1}H. Samples were packed into 4 mm o.d. zirconia rotors and spun at approximately 6 kHz. Chemical shifts for ^{13}C were referenced to the CH_2 resonance in an external adamantane sample at 38.56 ppm. The following typical conditions were employed while using the CPMAS pulse sequence: contact time 1 ms, spectral width 35,000 Hz, acquisition time 14 ms, recycle delay 10 s. A high power decoupled (HPDEC) pulse sequence had to be used while investigating hydrogels of superabsorbent polymers. Typical conditions employed were similar to those used for CPMAS, although a recycle delay of 5 s was used. ^{23}Na chemical shifts were referenced to the single peak

in a solid NaCl sample at 0.00 ppm. ^{23}Na spectra and relaxation times were obtained using a saturation recovery pulse sequence.

Distilled water was used entirely throughout this project.

Osmotic Ion-exclusion Membrane

A sodium ion selective electrode housing its own reference electrode (Russell Electrodes), connected to a Griffin digital pH/voltage meter was used to measure $[Na^+]$ before and after the addition of superabsorbent polymer. Throughout these experiments 1 % NaCl was used (10 g NaCl made up to 1000 g with water). A calibration curve was set up measuring the voltage of various concentrations of NaCl (aq). Roughly 100 ml of each solution was placed into a beaker and the pH of the solution adjusted to 9 using 2 ml ionic strength adjuster (20 g NH_4Cl, 27 ml NH_4OH made up to 100 ml with distilled water). The solutions were stirred constantly during the readings. A solution of 1 % (0.17112 M) NaCl was also tested in the same way, although the solution was diluted 100 times to give a more accurate reading. Each different generation of superabsorbent polymer (including uncoated material) was tested by placing 0.19 - 0.21 g of the polymer in a beaker and adding 20 $\pm$ 0.03 g 1 % NaCl. The resulting gel mixtures were then stirred at approximately 108 rpm for 16 hours at room temperature. After this time any excess NaCl was filtered off, lightly squeezing the gel to remove any last traces. The weight of the gels were noted for further calculations. Voltage readings were then taken of the resultant solutions (again the pH was adjusted to 9) having been diluted 100 times to make the readings more accurate. To make sure that soluble polymers were not leaching out and affecting the results the experiments were repeated, first washing the polymers. Roughly 3 g of polymer was placed in a large conical flask and enough distilled water added (roughly 2 litres) so that constant stirring was maintained. The resulting gel solution was left stirring for approximately 24 hours, after which time it was filtered.

To remove any last traces of water, a vacuum pump was used. This procedure was repeated three times for each different polymer sample, each washing being tested for the presence of sodium (concentration levels found to be very low, typically less than 5×10^{-4} M). The reliability of this experiment was determined by repeating it three times with each different generation of polymer.

Synthesis of Superabsorbent Polymers with varying degrees of neutralisation.

To look at the difference in structure between superabsorbent polymers which were neutralised before and after polymerisation using NMR, a range of samples with varying degrees of neutralisation were synthesised. ASAP 2300, a pre-neutralised polymer was synthesised with degrees of neutralisation 0, 25, 50, 75, 100 % using both sodium hydroxide and sodium carbonate as the neutralising agent. DMRD1 was also synthesised with the same range of degrees of neutralisation, adding sodium carbonate after the polymerisation had taken place. To look at the effects of hydration on the structure of pre- and post-neutralised superabsorbent polymers, the samples were rehydrated using water and redried. These samples were also washed with hydrochloric acid to remove any sodium, bringing them back to having 0 % neutralisation.

Synthesis of ASAP 2300

Acrylic acid (90.0 g, 1.25 moles), water (221.0 g) and crosslinker* (0.077 g) were added to a beaker. The solution was then cooled to 18 °C and the required amount of aqueous sodium hydroxide (47 %) for the degree of neutralisation was added dropwise, maintaining the temperature throughout. If sodium carbonate was used the required amount was added as a solid and again the temperature was controlled

* Information commercially sensitive

throughout the neutralisation reaction. Solutions of the two initiators* were added (initiator 1, 0.824 g, 15 %; initiator 2, 1.832 g, 10 %) and the combined solution was transferred to a dish giving a monomer depth of 2 cm. Polymerisation was initiated* and the temperature noted at thirty second time intervals for roughly eighteen minutes. After the polymerisation was assumed to be complete (temperature stabilised) the resulting gel was removed from the dish and left to cool. The cooled gel was then added to a shredder where the required amount of sodium metabisulfite was added to remove any unreacted monomer. The shredded gel was then put through a mincing machine, the pieces laid out and dried in an oven. The resulting coral was then milled and sized, disregarding any material that was under or over the size required (standard size 180-710 microns). The polymer granules were then coated using a coating solution* and dried in an oven at 145 °C.

Synthesis of DMRD1

Acrylic acid (270.0 g, 3.75 moles), water (810.0 g) and crosslinker* (0.40 g) were added to a beaker. The solution was then cooled to 10 °C and solutions of the two initiators* were added (initiator 1, 2.304 g, 15%; initiator 2, 5.471 g, 10%). The combined solution was transferred to a dish giving a monomer depth of 5 cm. Polymerisation was initiated* and the temperature noted at thirty second time intervals for roughly ten minutes. When the temperature had stabilised (polymerisation assumed to be complete) the resulting gel was removed from the dish and left to cool. The gel was then added to a shredder where the required amount of sodium carbonate for the degree of neutralisation was added. Sodium metabisulfite (1% solution) was also added to capture any unreacted monomer. The polymer was then treated in the same way as ASAP 2300.

* Information commercially sensitive

Hydration of pre- and post- neutralised polymers

The polymer samples were hydrated using water to 1000 % (1 g polymer in 10 g H_2O), left for approximately one hour and then redried using a vacuum pump.

Washing of polymer samples with HCl

To wash the sodium out of the polymer samples, they were washed with excess 0.1 M HCl (1 g in 1 litre). The samples were then left for approximately twenty four hours, filtered and redried again using a vacuum pump. To check all the sodium had been removed, a ^{23}Na NMR spectrum was run for each sample. When no FID was seen, it was assumed that all the sodium had been successfully removed.

^1H NMR Imaging

Before any imaging experiments could be carried out the T_2 relaxation time of the protons within the polymer had to be measured, to check that they were of a suitable time length. These relaxation times were measured using a Carr-Purcell-Meiboom and Gill spin echo pulse sequence on the Bruker MSL 500 (see page 28 for pulse sequence). Conditions employed were 90° pulse = 3.5 μs, 180° pulse = 10.0 μs, n = 1 and τ ranged from 5 μs to 75 ms. For each individual delay the intensity of the peak was noted and a graph plotted of ln(intensity) versus time delay. Static samples of DMRD1 in various amounts of water were measured. T_2 relaxation times were calculated from the slope of the graph.

As the values for T_2 relaxation were acceptable to carry out NMR imaging the next problem was to find a way of feeding water to the polymer slowly enough to be able to produce images. A teflon (PTFE) device was devised (see figure 2.1) which would fit into a 25 mm NMR tube containing a few ml of water or 1 % NaCl. The sample

of polymer was housed within the PTFE device and water delivered through seven wicks attached to the device. These wicks were evenly spread below the sample and covered by a piece of filter paper to even out the delivery of water.

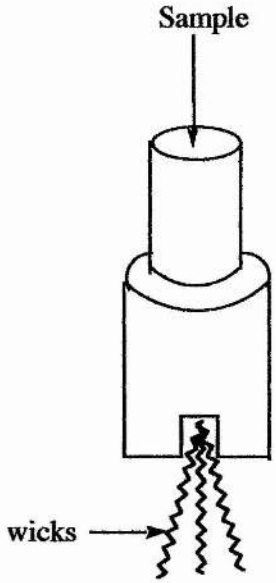

Figure 2.1. PTFE device constructed for imaging experiments.

All imaging experiments were carried out using a spin-echo pulse sequence (see page 28 for pulse sequence) on a Bruker AM300/WB FT NMR spectrometer operating at 300.05 MHz for ^{1}H. It was fitted with a Bruker microimaging accessory with a 25 mm saddlecoil resonator. Typical conditions employed can be seen in the table 2.1. below.

Several different experiments were carried out using both granules and pellets of superabsorbent polymer (see table 2.2.). The pellets were made using a KBr press and were roughly 13 mm in diameter and 2 mm in thickness. Homogeneous gel pellets were also synthesised. All forms of the polymer were placed into the PTFE device sitting on a piece of filter paper.

To try and mimic the pressure exerted on the polymer by a baby, experiments were

also carried out placing a weight on top of the polymer. The pressure to be exerted was 0.7 psi and this was calculated to be equal to a weight of 65.38 g.

The weight was constructed using a metre length of wood of the correct diameter to fit into the PTFE device. The end that was to sit on top of the sample of polymer was given a PTFE tip and a brass weight fitted on the other end, making up the remainder of the weight.

Condition Employed	Value of condition
Field of view	15 mm
Slice thickness	2 mm
Bandwidth	900 Hz
Number of experiments	16
Time of the echo	13.15 ms
Repetition time	1020 ms
Total acquisition time	34 minutes 49 seconds
90° pulse	52 μs
180° pulse	4000 μs
Relaxation delay	1 s
Dwell time	20 μs

Table 2.1. Typical parameters for MRI experiments.

Synthesis of homogenous pellets for MRI

0.07% crosslinker

This gel was synthesised in a similar fashion to DMRD1, stopping after the gel was

cooled. Four gels were synthesised differing in the depth of the monomer solution transferred to the dish for polymerisation (4,6,8 and 9 mm). Pellets of gel were made using cork borers of different diameters (17,18,22,23,25,26,28 mm) to ensure the resulting dry pellet would be of the required dimensions. The pellets were dried in a desiccator to ensure even drying. Once the pellet was dry it was then filed to the correct dimensions using sandpaper.

0.05% crosslinker

Gel was also synthesised with a lower crosslinker level than normal. In this case 0.289 g crosslinker was added. Only two depths of gel were synthesised (6 and 9 mm), again cutting out pellets with the same diameters as above. The gel pellets were then dried in an desiccator to ensure even drying.

To calibrate the images produced from the above experiments, a new PTFE device was constructed (see figure 2.2.). Water was placed in a second compartment surrounding the sample. Calibrations were carried out using granules (0.30 g) and a pellet (0.50 g) both with 4 ml water.

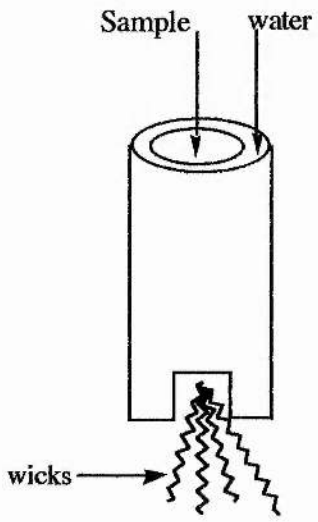

Figure 2.2. Second PTFE device used in NMR imaging.

Polymer State	Weight of polymer (g)	Weight used (0.7 psi)	Volume liquid (ml)	Crosslinker level %
granules	0.50	no	4 H_2O	
granules	0.50	yes	4 H_2O	
pellet (KBr)	0.48	no	4 H_2O	
pellet (KBr)	0.47	yes	4 H_2O	
pellet (KBr)	0.49	no	4 NaCl	
pellet (KBr)	0.50	yes	4 NaCl	
pellet	0.75	no	4 H_2O	0.05
pellet	1.01	no	4 H_2O	0.07
pellet	0.74	yes	4 H_2O	0.07
pellet	0.70	yes	4 H_2O	0.05

Table 2.2. Imaging Experiments.

The data was worked up using a Bruker X32 stand alone workstation using the Bruker UXNMR package of programmes.

Swelling of polymer samples for sodium relaxation measurements and NMR of Hydrogels.

Polymer samples were swollen to different degrees of hydration where 1 g polymer in 1 g water is equivalent to 100 % hydration. The samples were usually left swelling in sealed sample vials for approximately twelve hours.

Sodium relaxation measurements

Sodium T_1 relaxation measurements were carried out using a saturation recovery pulse

sequence. Typical conditions employed were recycle delay 500 ms, 90° pulse 3.3 μs, 180° pulse 6.6 μs and various delays ranging from 1 μs to 500 ms. Fifty pulses were used to saturate the system. Measurements were carried out on various hydrated samples ranging from dry polymer to 10000 % hydrated. Samples of polymer with different degrees of neutralisation were also investigated dry and hydrated.

Off-resonance Decoupling

This experiment was carried out to ensure structural details seen in the spectra of superabsorbent polymer hydrogels were not artefacts. Off-resonance decoupling is a partial decoupling technique that uses a strong RF field in the ^{1}H NMR region with a frequency that is just off the resonance signal irradiated. A proton spectrum was run where the on-resonance decoupler frequency was found to be 8232.701 Hz. ^{13}C spectra were carried out with decoupler frequencies of 7000 Hz and 9000 Hz. This allowed any line splittings that were still present in the hydrogel spectra to be observed.

Extraction of Soluble Polymers

Extraction of the soluble polymers from superabsorbent polymers involved carrying out the extractables experiment. For this experiment 1 g polymer was placed into a beaker and 185 g 0.9 % NaCl (9 g in 1000 g water) was added. The resulting gel solution was stirred at 300 rpm for 16 hours at room temperature, after which time it was filtered. This results in a solution which contains the soluble polymers. To isolate the soluble polymers from this solution the water was driven off using a rotary evaporator, leaving a dusty white solid of low density. To ensure no further crosslinking had been introduced from heating, the white solid was redissolved in water, from which it was assumed no further crosslinking had been introduced. To check if the properties of the polymer without the soluble components were any

different from the regular polymer an equal amount of water was added to 1 g of each.

Absorption under load testing

This test involved placing 0.16 g polymer into a cylindrical vessel uniformly over a piece of mesh-wire across the bottom. The weight of the vessel containing the polymer was noted and the vessel was placed in a petri dish containing 0.9 % saline while subjecting the polymer to loadings of 0.28 and 0.7 psi for one hour. After this time the vessel containing the swollen polymer was weighed and the difference between the weights of the dry and swollen polymer was used to work out the absorption under load which is reported in grams of liquid absorbed per gram of polymer.

Gel Volume testing

This test involves placing 0.2 g polymer into a beaker and adding 20 g of a solution of 0.3 gdm^{-3} blue dextran in 1.0 % saline. The resulting solutions were stirred at 100 rpm at room temperature for forty five minutes. The final blue dextran concentration was measured using UV/visible spectroscopy at 617 nm against the starting solution.

Chapter Three

Generations Of Superabsorbent Polymer

Chemdal has manufactured many different generations of superabsorbent polymer, each one serving different purposes and performing better than the previous one. Six different generations of superabsorbent polymer were investigated using solid state ^{13}C NMR in an attempt to observe any differences in structure between the different generations.

The first two generations of superabsorbent polymer 1000 and 1100 are synthesised by modified bulk polymerisation (MBP). This polymerisation involves using a high monomer concentration and high initiator levels to achieve a very rapid rate of reaction. This causes the water in the system to boil off leaving the polymer in a solid state with minimal or no extra drying. This process is rarely used in industry due to its major disadvantages. The increase in viscosity with polymerisation which prevents the dissipation of heat causes charring or even degradation of the product. Also as a result of the limited solubility of sodium acrylate at high monomer concentrations, the degree of neutralisation is typically lower than optimal, say 50-60 % rather than the preferred 70-75 %.

The remaining generations of superabsorbent polymer 2000, 2300, DMRD1 and DMRD2 are synthesised by gel polymerisation where a lower monomer concentration and a slower rate of polymerisation produces gentler reaction conditions leading to a gelled product. The resulting gel must be dried by application of energy but this is compensated for by the improvement in product performance . ASAP 2000 and 2300 are pre-neutralised polymers whereas DMRD1 and DMRD2 are post-neutralised polymers. The newer generations of superabsorbent polymer have improved performance over the older generations through lower extractable levels and higher gel volumes.

NMR of Superabsorbent Polymers

A typical ^{13}C solid state NMR spectrum of a superabsorbent polymer contains two fairly broad peaks (see figure 3.1). The first peak found at approximately 184 ppm corresponds to the carbonyl group from the backbone of the polymer. As the crosslinking in personal care products is very low, the carbonyl group from the crosslinker is not observed. At higher levels of crosslinking the carbonyl group of the crosslinker would be observed as a shoulder to the right of the main carbonyl peak. The other peak, found at approximately 40 ppm corresponds to the aliphatic carbons of the polymer. Unfortunately it is impossible to observe the individual resonances of the $\underline{C}H$ and $\underline{C}H_2$ carbons as in most synthetic polymers they overlap forming a broad peak. Heating of the polymer above its glass temperature can result in the splitting of the individual resonances and give more information on the structure of the polymer. In crystalline organic materials ^{13}C linewidths obtained on the MSL 500 spectrometer are typically 50-100 Hz. The linewidths here which are approximately 2000 Hz are indicative of a disordered structure for the polymer. The range of different environments found for each site is reflected in the range of chemical shifts found in the broad lines. Spinning side bands of the carbonyl resonance are also found in the spectrum at the spinning speed away from the centre band.

Comparing the NMR spectrum of each different polymer generation no obvious differences can be seen (see figures 3.1, 3.2 and 3.3). All generations show the same two broad peaks at approximately the same chemical shifts. The only observable difference between the different spectra is the change of width at half height of the aliphatic peak, although the change is not consistent with the improved performance of the newer generations of superabsorbent polymer. The polymers were also investigated after being hydrated and redried. Again no differences were observed between the different generations of superabsorbent polymers although there were small changes in the width of the aliphatic peak at half height again not connected with

the different generations of superabsorbent polymer.

As cross polarisation spectra were showing no obvious differences a single pulse high power decoupled pulse sequence was also used. These spectra also failed to produce any differences between the different generations of superabsorbent polymer or any differences from the cross polarisation spectra.

Soluble polymers

As a result of the free-radical process used to synthesise superabsorbent polymers a distribution of chain lengths and crosslinker concentrations occur during the polymerisation due to the monomer and initiator concentration varying with conversion. Low molecular weight chains have a lower probability of being incorporated into the network and when not incorporated become the soluble fraction of the polymer.[1] These uncrosslinked chains can be solvated and contribute to the swelling if retained in the gel phase. When the soluble fraction is retained in the gel phase the chemical potential of the water in the gel is lowered, resulting in an increased difference in the chemical potential of water in the gel phase and the external phase. This difference in chemical potential is the driving force for swelling and hence an increased difference results in increased swelling.[1] The soluble fraction can easily be extracted from the polymer when the polymer is swollen in excess liquid and hence are often termed 'extractables'.[2]

As the structure of the soluble fraction of the commercial superabsorbent polymers manufactured by Chemdal had never been determined, they were extracted from the polymer. This was achieved by carrying out the extractables experiment (see experimental page 56) which resulted in a solution containing the soluble polymers. To isolate the soluble polymers from this solution, the water was driven off using a rotary evaporator leaving a dusty white solid of low density. To check for further

crosslinking which may have been introduced from heating, the white solid was redissolved in water, from which it was assumed that no further crosslinking had taken place. A solid-state ^{13}C CPMAS spectrum was used to investigate the structure of the soluble fraction of the polymer. From looking at the ^{13}C CPMAS spectrum of the soluble fraction, two peaks similar to those in the spectrum of the polymer containing the soluble fraction were observed. Again these peaks were found at approximately 40 ppm and 185 ppm corresponding to the aliphatic carbons and a carbonyl group respectively. The linewidths of the peaks found in the spectrum of the soluble fraction are similar to those in the spectrum of the polymer still containing the soluble fraction. This suggests that the soluble polymers have the structure of a linear polyacrylate (see figure 3.4). From the chemical shift of the carbonyl group it is thought that the soluble fraction exists as sodium polyacrylate. A single pulse high power decoupled spectrum was also carried but appears to contain no further information on the structure of the soluble fraction. The portion of the superabsorbent polymer that no longer contained the soluble polymers was also isolated and dried. Solid-state ^{13}C CPMAS and single pulse high power decoupled spectra were carried out and again no further information was observed. The properties of the polymer without the soluble fraction were investigated to observe any differences from the polymer containing the soluble fraction. This was achieved by adding an equal amount of water to a 1 g sample of each. The polymer without the soluble fraction absorbed less of the water remaining wet, showing that the soluble fraction is important in the absorption properties of the superabsorbent polymer. A solution spectrum of the soluble fraction was run overnight using D_2O as the solvent, to compare with the solid state spectrum. Unfortunately nothing was seen in this spectrum as the soluble fraction is a large molecule which tumbles slowly in solution and has a short T_1 relaxation time.

Competitor Samples

Samples from Dow Chemicals, Stockhausen, Atochem, Hoechst Celanese Co-operation and Camelot were also investigated using solid state ^{13}C CPMAS to compare with samples from Chemdal. The above companies are the main manufacturers of superabsorbent polymers both in granular and fibrous form. The solid-state ^{13}C NMR spectra of all samples excluding Camelot contained two similar broad peaks to that of Chemdal's superabsorbent polymers. These samples like Chemdal's are all in the granular form. The peaks present in these spectra are also found at approximately 40 ppm and 184 ppm and correspond to the aliphatic carbons and a carbonyl group respectively. No crosslinker is seen as a shoulder on the carbonyl peak suggesting that the level of crosslinker in the competitor samples is also very low or that the crosslinker does not contain a carbonyl group. The Camelot superabsorbent fibre sample on the other hand shows a very different solid state ^{13}C NMR spectrum (see figure 3.5). This spectrum contains many more narrower peaks suggesting that the sample is more crystalline than the others. Superabsorbent fibres manufactured by Camelot are co-polymers of maleic anhydride and isobutylene usually crosslinked with a crosslinker from the group of alkanolamines e.g. tris(hydroxymethyl)aminomethane or polyhydroxylic compounds such as poly(alkyne glycol).[3] The solid-state ^{13}C NMR spectrum contains two carbonyl peaks found at approximately 180 and 184 ppm which could be attributed to the two carbonyl groups from the maleic anhydride. Two peaks are also found at 65 and 59 ppm which are believed to relate to the $\underline{C}$-N carbon from the crosslinker. The other peaks present in the spectrum are due to the aliphatic carbons within the polymer. The peaks found at 41 and 37 ppm are assumed to be due to the two $\underline{C}H$ resonances, the peak at 28 ppm the $\underline{C}H_2$ resonance and the small peak at 21 ppm the $\underline{C}H_3$ resonance. This interpretation of the NMR spectrum is not conclusive as the structure is not fully known.

Conclusion

Solid-state NMR is a good reliable method for looking at the structure of these insoluble compounds. Little detail is seen in the solid-state ^{13}C NMR spectra of superabsorbent polymers as a result of the overlapping of broad peaks, however, it has been shown that no major structural differences can be seen between the different generations of superabsorbent polymers. The structure of the soluble fraction was also observed using solid-state ^{13}C NMR and was found to be a polyacrylate. It has also been shown through the use of solid-state ^{13}C NMR that the superabsorbent polymers manufactured by the major competitors of Chemdal have similar structures to the polymers manufactured by Chemdal with one exception.

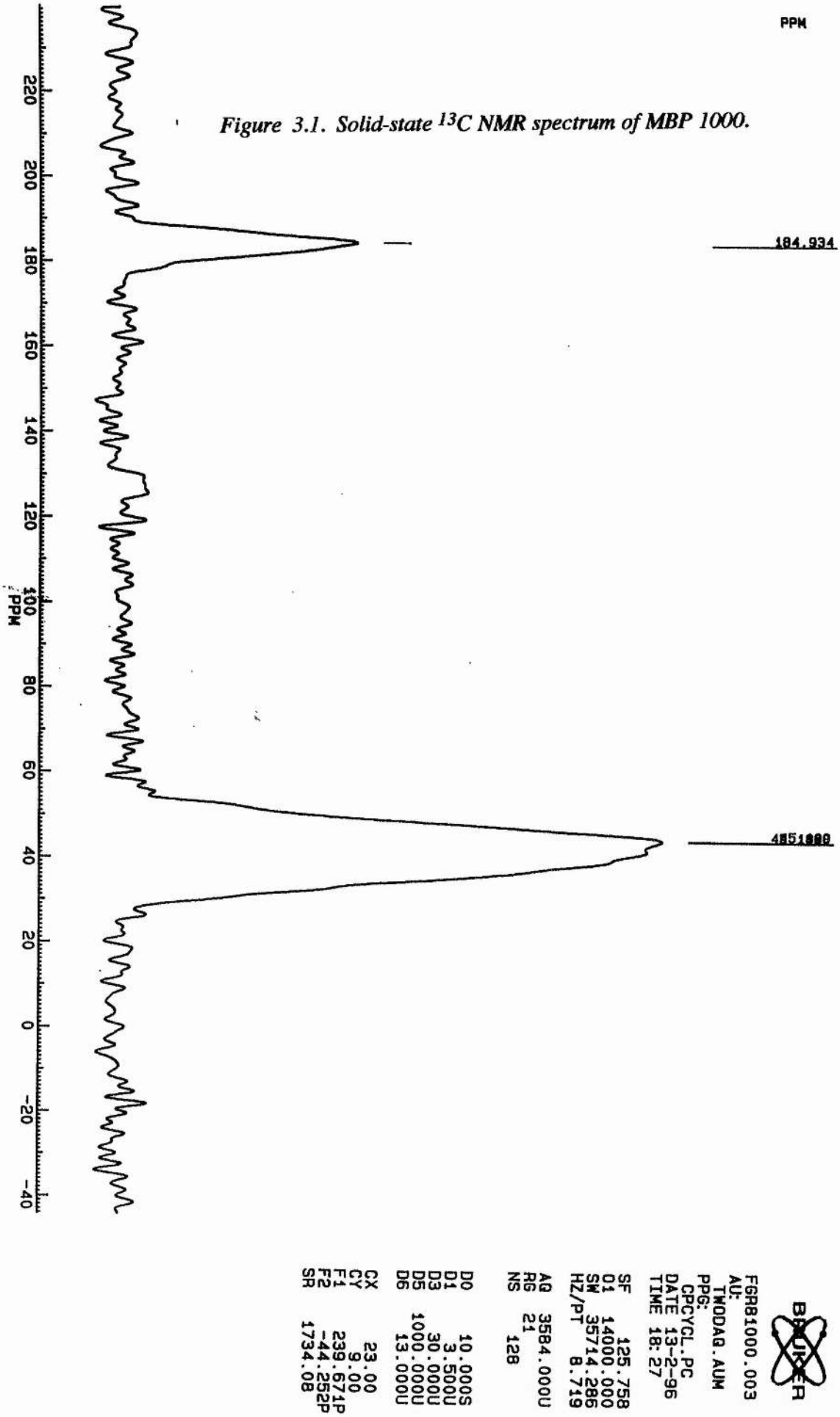

Figure 3.1. Solid-state ^{13}C NMR spectrum of MBP 1000.

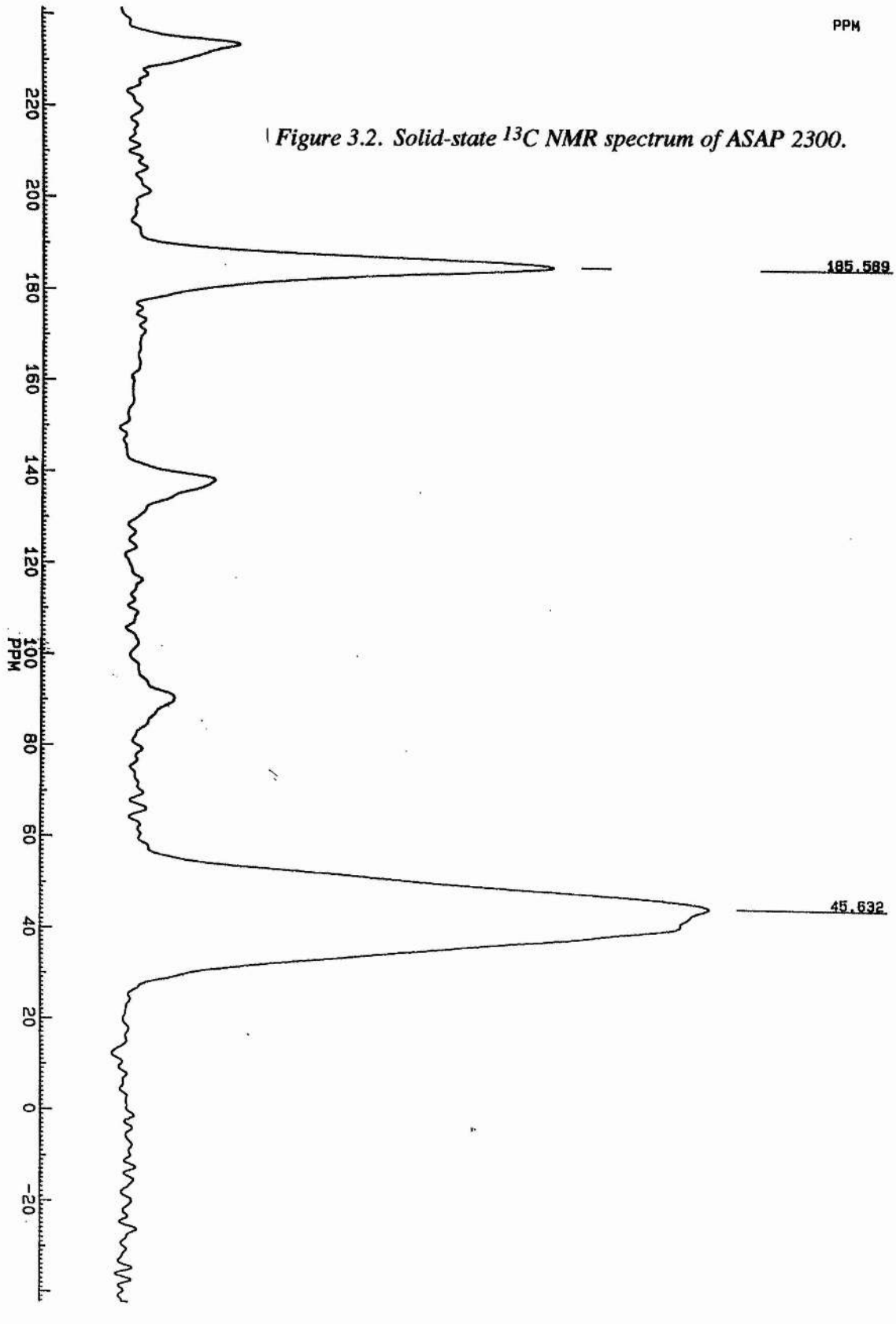

Figure 3.2. Solid-state ^{13}C NMR spectrum of ASAP 2300.

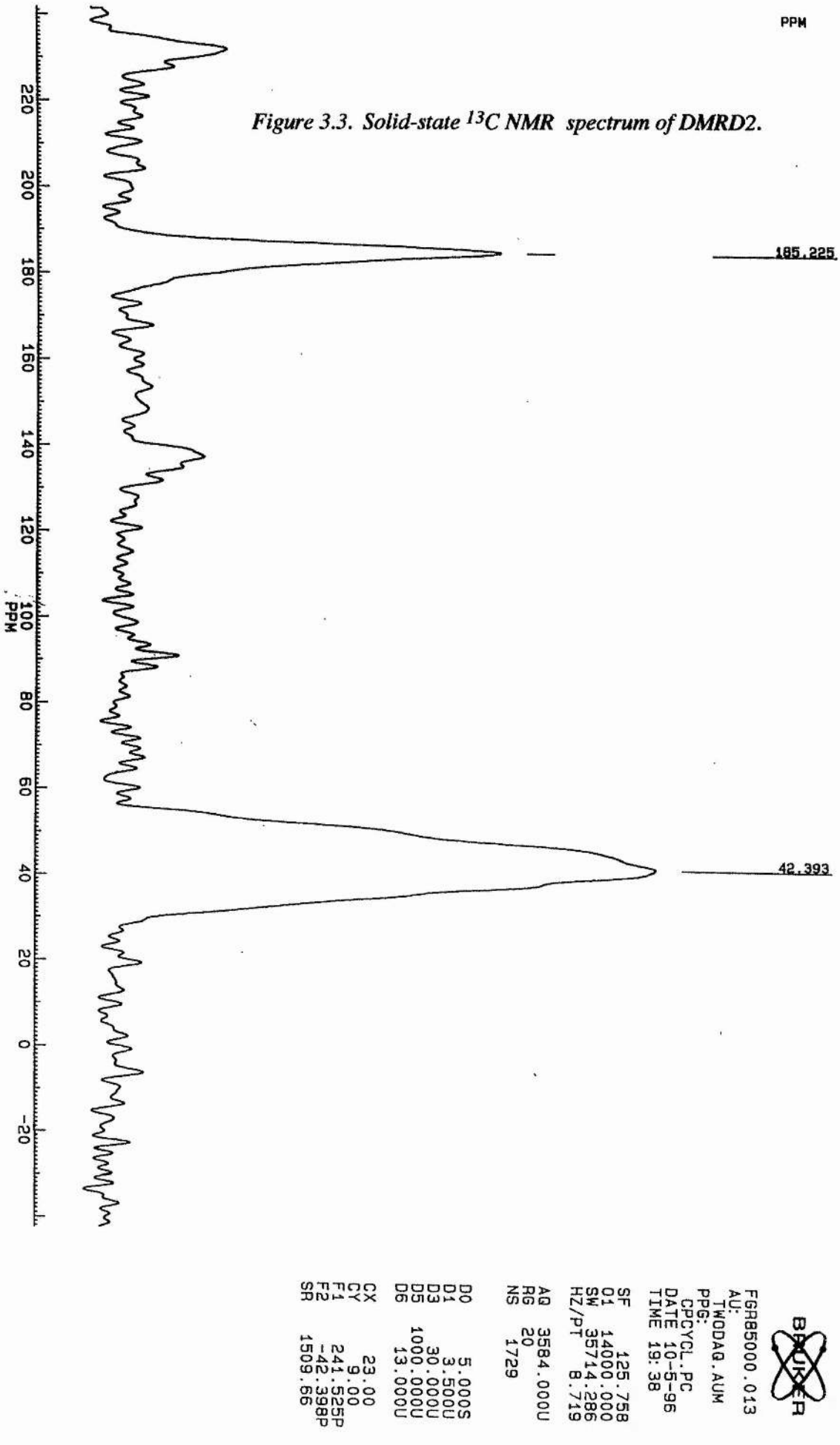

Figure 3.3. Solid-state ^{13}C NMR spectrum of DMRD2.

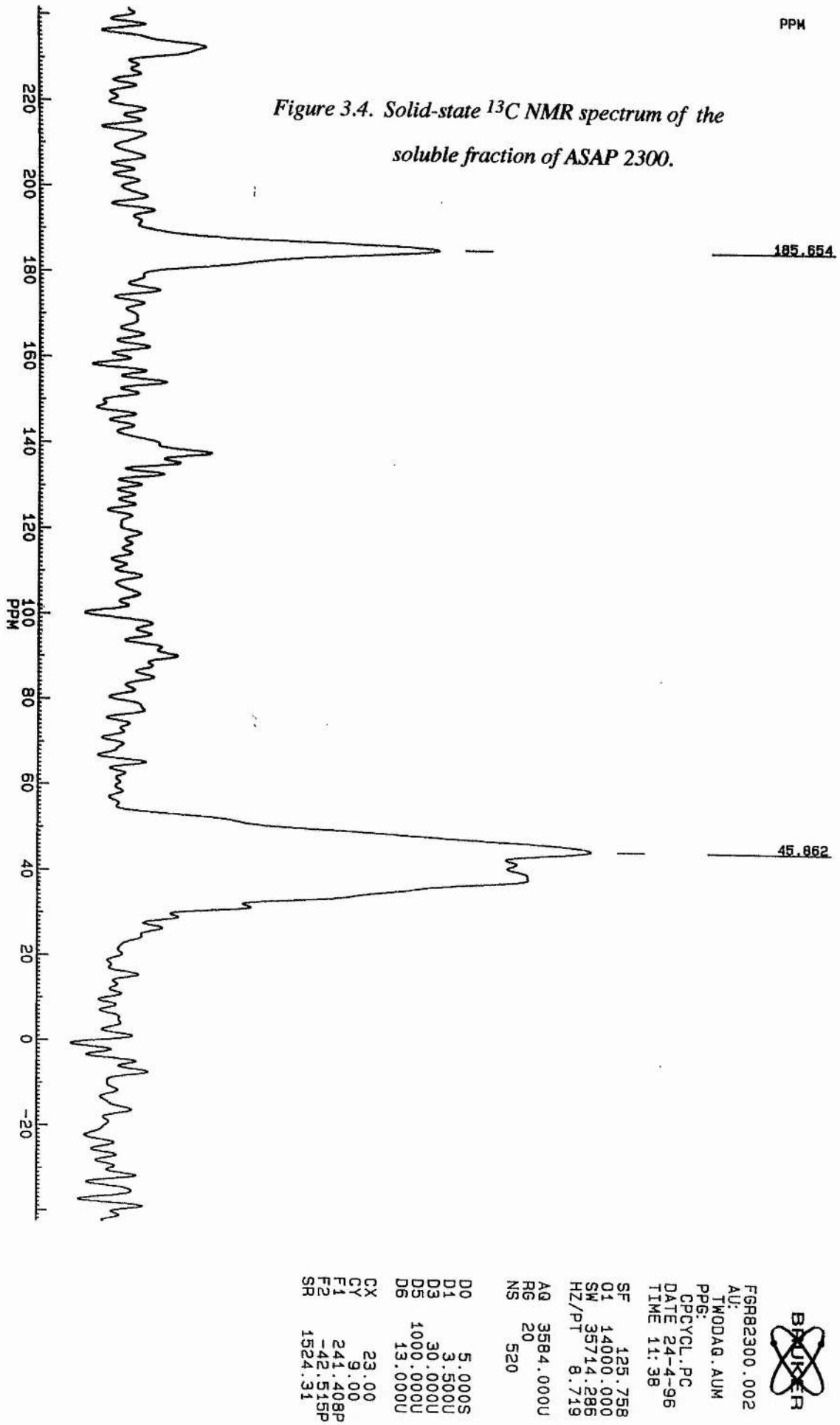

Figure 3.4. Solid-state ^{13}C NMR spectrum of the soluble fraction of ASAP 2300.

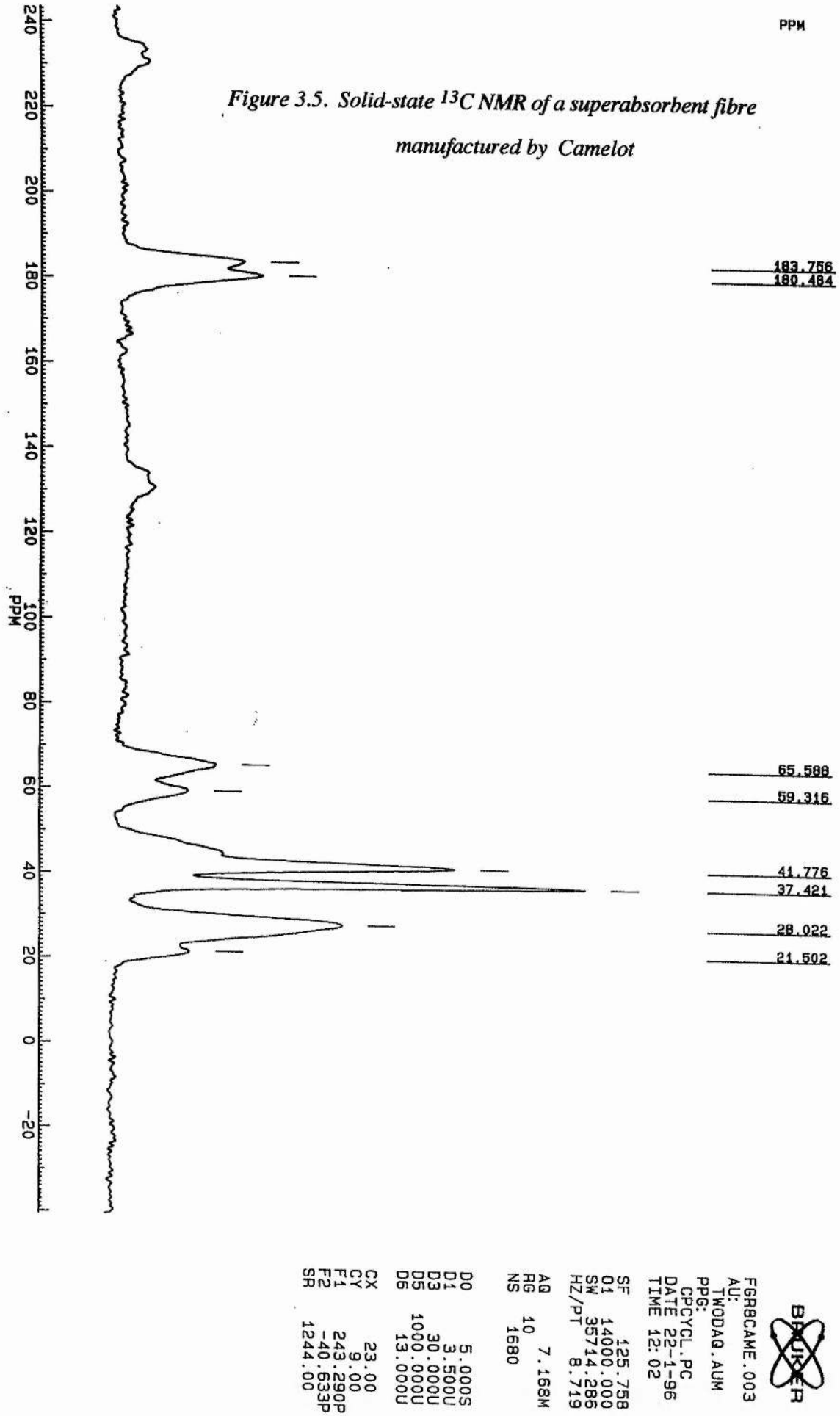

Figure 3.5. Solid-state ^{13}C NMR of a superabsorbent fibre manufactured by Camelot

References

1. F. L. Buchholz, A. T. Graham; Modern Superabsorbent Polymer Technology; John Wiley & Sons, New York, NY, 1998, Chapter 5
2. F. Engelhardt, G. Ebert, R. Funk; *Advanced Materials*, (1992), **4**, 227-230.
3. F. L. Buchholz, A. T. Graham; Modern Superabsorbent Polymer Technology; John Wiley & Sons, New York, NY, 1998, Chapter 6.

Chapter Four

Osmotic ion exclusion membrane

Superabsorbent Polymers granules tend to clump or "gel block" (liquid cannot flow readily through the gel) when aqueous liquids are added to them. The surface of the massed particles swell rapidly to form a soft deformable layer. The resulting particle deformation and interparticle adhesion reduces interparticle porosity and limits the swelling rate of the polymer mass to the diffusion rate of liquid through the partially swollen mass. The first attempts to overcome this problem used multivalent cations to form a crosslinked surface layer that was more rigid than the original core polymer.[1] To produce products with improved dispersibilty and absorption rate the surface of crosslinked polyacrylate particles was reacted with a variety of multifunctional organic compounds.[2] From the swelling capacity data as a function of particle size it is demonstrated that a shell of appreciable thickness is formed around the superabsorbent particle by surface crosslinking. This shell with higher crosslink density provides a more rigid surface layer during swelling and prevents "gel blocking" that would otherwise occur early in the swelling. As a result liquid can flow through the bed of the particles to each particle permanently assuring the effective surface area available for swelling increasing the swelling rate. The polymer particles now contain a discontinuous network.

Commercial superabsorbent polymers are coated after they have been synthesised to the desired particle size to enhance their water absorptive and retention properties.[3,4] Surface crosslinking is done using compounds which can react with two or more groups on the polymer backbone such as polyvalent metal ion salts, multi-functional organic crosslinkers, free radical initiators or monomer coatings that are then polymerised. In superabsorbent polymers the surface crosslinking reagents need to be able to react with the carboxylic acid or carboxylate moieties on separate adjacent chains. A heating step is normally required for the reaction of the surface crosslinking agents with the partially neutralised poly(acrylic acid) backbone.[5]

Discussion

There has been some discussion within Chemdal as to whether or not the coating on superabsorbent polymers provides the polymer with an osmotic ion-exclusion membrane. The coated sample was coated with a solution of EGDGE (ethyleneglycoldiglycidyl ether) where the two epoxide rings open to form ether linkages with pendant polymeric chains at the surface of the polymer particle. To test if such a membrane exists a sodium ion-selective electrode was used. The ion-selective electrode allowed the measurement of $[Na^+]$ in a solution of NaCl before and after the addition of the superabsorbent polymer. This enabled consequent changes in $[Na^+]$ to be detected, allowing us to tell if the polymer and external solution are exchanging cations. A scaled down gel volume test will be carried out to swell the polymer in 1 % NaCl.

Before any experiments were carried out a calibration curve was set up using solutions of various concentrations of NaCl. A graph was drawn of the voltage of the solution versus the log of the concentration (see table 4.1 and figure 4.1).

Na Concentration (M)	Voltage of solution (mV)
$1x10^{-4}$	-187.0
$1x10^{-3}$	-141.0
$1x10^{-2}$	-85.0
$5x10^{-2}$	-45.0
$1x10^{-1}$	-27.0
$5x10^{-1}$	+14.0
1	+34.0

Table 4.1. Calibration Curve set-up.

The voltage reading for the solution of 1 % (0.17112 M) NaCl before any polymer was added was found to be -125.0 mV which also lies on the calibration curve. The experiment was carried out under the same conditions using six different generations of superabsorbent polymer 1000, 1100, 2000, 2300 and DMRD1 (see table 4.2 for quantities used). Both coated and uncoated samples of DMRD1 were tested. After the resulting gels had been filtered, readings were taken of the supernatant fluid (see table 4.3).

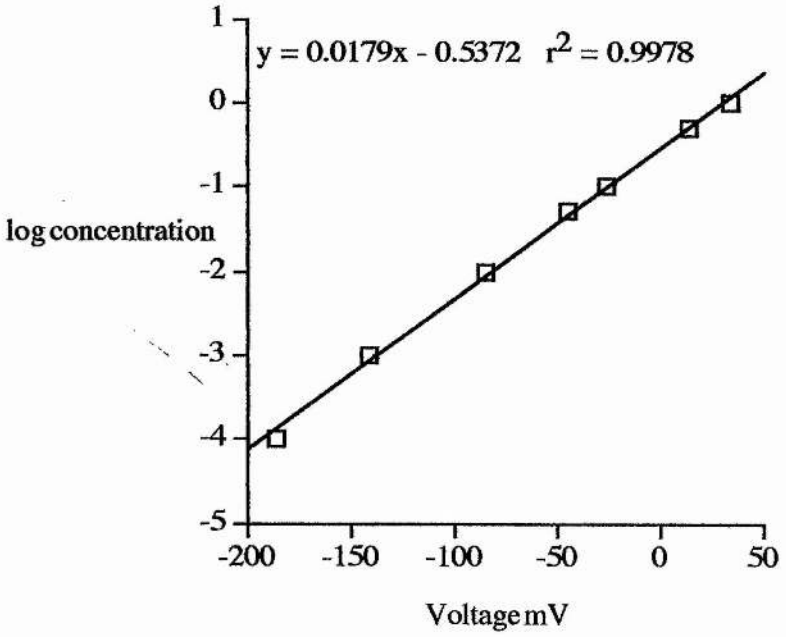

Figure 4.1. Calibration Curve.

The corresponding concentration of the supernatant solutions were found from the calibration curve. Several calculations were then used to work out the percentage exclusion of sodium ions by the superabsorbent polymer (see table 4.3 for results).

Sample	Weight of polymer	Weight of saline	Weight of gel
1000	0.20g	20.00g	3.78g
1100	0.21g	20.00g	2.85g
2000	0.21g	20.01g	2.82g
2300	0.20g	20.01g	3.02g
DMRD1 c*	0.21g	20.00g	3.95g
DMRD1 uc+	0.21g	20.00g	3.11g

Table 4.2. Quantities used in the experiment.

Calculation

Weight of liquid absorbed by the polymer = Wt

Wt = Wgel - Wsap (Wgel = weight of the dry polymer)

(Wgel = weight of the gel)

Weight of the excess supernatant = Wx

Wx = Wo - Wt (Wo = weight of saline used)

If all the sodium ions were excluded from the gel, the molarity of the solution would increase to **M100% exclusion = Mo x (Wo/Wx)**

(Mo = Molarity of original saline)

The percentage exclusion (efficiency of ion exclusion) is obtained from the actual molarity by: **% exclusion = (Mt/M100%) x 100**

(Mt = Actual molarity)

* Coated superabsorbent polymer

+ Uncoated superabsorbent polymer

As can be seen from table 4.3 a change in voltage from the starting 1 % NaCl solution is observed for each different polymer generation. This indicates a change in the sodium ion concentration of the solution after the superabsorbent polymer has been added. Also observed from the table is that each polymer generation has a relatively high percentage exclusion of sodium ions. No obvious pattern is seen in the percentage ion-exclusion connecting the different generations of superabsorbent polymer to their performance. We can therefore conclude that the polymer does contain an osmotic ion-exclusion membrane although it is not provided by the coating on the polymer. This is evident from the uncoated material also excluding sodium ions.

Sample	Voltage (mV)	Molarity (M)	Wt	Wx	Molarity if 100%	% exclusion
1000	-123.0	0.00183	3.58	16.42	0.00208	88.0
1100	-128.0	0.00149	2.64	17.36	0.00197	75.6
2000	-126.0	0.00163	2.61	17.40	0.00197	82.7
2300	-129.0	0.00143	2.82	17.19	0.00199	71.9
dmrd1 (c)	-129.0	0.00143	3.74	16.26	0.00201	71.1
dmrd1(uc)	-127.0	0.00155	2.90	17.10	0.00200	77.5

Table 4.3. Results from various different generations of polymer.

After discussion it was thought that perhaps the change in voltage of the solution may be caused by the leaching of the soluble linear polymers present in superabsorbent polymers.

Washed Superabsorbent Polymers

To check whether or not the soluble polymers were leaching into the external NaCl

solution it was decided to repeat the whole experiment first washing the same polymers as above three times to remove the soluble components. The sodium ion concentration of the washings were measured and found to be typically less than $5x10^{-4}$ M. The whole experiment was repeated three times using the washed samples (see tables 4.4, 4.5 and 4.6).

Sample	Polymer weight	Saline weight	Gel weight
1000	0.21g	19.99g	3.91g
1100	0.20g	20.01g	1.79g
2000	0.21g	20.01g	2.26g
2300	0.20g	20.03g	2.70g
DMRD1 c	0.20g	19.99g	1.94g
DMRD1 uc	0.20g	20.00g	2.86g

Table 4.4. Quantities used in second experiment.

Sample	Voltage (mV)	Molarity (M)	Wt (g)	Wx (g)	Molarity if 100%	% exclusion
1000	-127.0	0.00155	3.70	16.2	0.00211	73.5
1100	-125.0	0.00168	1.59	18.41	0.00186	90.3
2000	-125.0	0.00168	2.06	17.94	0.00191	88.0
2300	-129.0	0.00143	2.50	17.53	0.00196	73.0
dmrd1 c	-127.0	0.00155	1.74	18.25	0.00187	82.9
dmrd1uc	-123.0	0.00182	2.66	17.34	0.00198	92.0

Table 4.5. Results after washing of polymers..

By using the calibration curve already set up the corresponding sodium concentration for the measured voltages could be found. Using the above calculation the efficiency of the ion-exclusion could be worked out. Only one set of values were used to work out the efficiency of the ion-exclusion although repetition of the experiments shows that the method is fairly reliable.

Sample	Weight Dry Polymer (g)	Weight Saline (g)	Gel Weight (g)	Voltage (mV)
1000	0.20	20.00	3.71	-127.0
1000	0.20	20.00	3.06	-127.0
1100	0.20	19.99	2.31	-123.0
1100	0.20	19.99	2.09	-124.0
2000	0.20	19.99	2.50	-124.0
2000	0.20	20.00	2.34	-124.0
2300	0.19	20.01	2.50	-129.0
2300	0.19	20.00	2.26	-129.0
dmrd1 uc	0.21	20.00	2.45	-124.0
dmrd1 uc	0.20	20.00	2.04	-124.0
dmrd1 c	0.20	20.00	2.40	-125.0
dmrd1 c	0.20	20.00	2.78	-127.0

Table 4.6. Results from repeated experiments using washed polymer.

As can be seen from table 4.5 a change in voltage occurs for all solutions after the washed polymer has been added. This change in voltage again indicates that a change in the sodium ion concentration of the solution is occurring. This change in sodium ion concentration is again seen for all superabsorbent polymer generations including the uncoated material. It was found that all superabsorbent polymer generations had a

high efficiency of ion-exclusion including the uncoated material. This shows us that the polymer does indeed contain an ion-exclusion membrane although it is not provided by the coating of the polymer. These results also show that removing the soluble polymers does not greatly affect the efficiency of the ion-exclusion although an increase is seen for all generations excluding MBP 1000. Simultaneously, a decrease in the amount of liquid absorbed by the polymers is observed which is consistent with the test carried out in chapter 3 on polymers with the soluble component removed.

Therefore, it can be concluded that superabsorbent polymers do contain an osmotic ion-exclusion membrane which excludes the majority of the sodium ions. However, this ion-exclusion membrane is not provided by the coating on the polymer as the same results are seen for uncoated material.

From the results obtained it is presumed that no sodium ions migrate from the polymer to the external NaCl solution whereas small percentage of the sodium ions from the NaCl solution migrate into the polymer gel.

Neutralisation increases the swelling capacity by increasing the concentration of ions in the gel. As an electrolyte gel is increasingly neutralised more salt present in the swelling liquid is excluded from the gel phase during swelling.[6] This exclusion of salt from the polyelectrolyte gel phase is known as Donnan exclusion. A Donnan equilibrium is set up when two coexisting phases are subjected to the condition that one or several of the ionic components cannot migrate from one phase to the other.[7] The principle of the Donnan membrane equilibrium allows a better understanding of the effects of the macro-ions of the polyacrylate network and how they interact with the ions of simple salts that are present in swelling liquids such as urine. The existence of a Donnan potential means that the ions present in the external liquid phase will be excluded from the gel depending on the relative concentrations of salt in the

external solution and the fixed charges in the polyelectrolyte phase. Under these circumstances the gel can be viewed as acting as both a polymer solution and a membrane whereby the gel behaves as if a nonelastic gel substance is contained by an elastic ionised membrane.[6] As a result of the magnitude of the salt exclusion depending on the concentration of the fixed charges of the polyelectrolyte in the gel, salt exclusion depends on the extent of swelling. As the gel swells, the concentration of the fixed charges decrease along with the Donnan potential, resulting in the exclusion of salt from the swelling gel decreasing as the gel swells. The Donnan potential is greatest and therefore more co-ions excluded when the concentration difference between the gel phase and the external solution is large. Therefore, a high exchange capacity, high crosslinking and increasing dilution are favourable for a higher exclusion of salt from the gel.[7] In this study measurements were carried out at 100 fold dilution which is favourable for a higher exclusion of sodium ions from the gel. The superabsorbent polymers used in this study are neutralised to approximately 75 % which will also increase the exclusion of sodium ions from the gel.

Soluble polymers present in superabsorbent polymers can affect the rate of swelling.[6] The molecular mass of soluble polymer relative to the molecular mass between the crosslinks in the network determines whether the soluble polymer will diffuse from the gel and how rapidly they will be extracted. However, once extracted from the gel, the soluble polymer can depress the swelling by reducing the chemical potential of the water in the external solution and may even slow the flow of liquid through the mass of particles by increasing the viscosity of the external solution. As seen from table 4.5 once the soluble polymers have been removed from the superabsorbent polymers the amount of solution taken up by the polymer is decreased. The percentage exclusion is also increased after the extraction of the soluble polymer.

Conclusion

From this work on superabsorbent polymers it can be assumed from the change observed in the voltage of the solution that an osmotic ion-exclusion membrane does exist. However, this membrane is not provided by the coating on the polymer as the uncoated material shows the same results as the coated material. After the removal of the soluble fraction from the polymer the osmotic ion-exclusion membrane still exists for all samples of superabsorbent polymers. A high efficiency of ion-exclusion is seen for all samples as a result of using diluted solutions to obtain a higher accuracy in the measurements and using samples with a high degree of neutralisation. From these results new applications for superabsorbent polymers could be suggested, including ion-exchange materials.

References

1. S. H. Ganslaw, H. G. Katz; US Patent, 4,043,952, (1977).
2. T. Tsubakimoto, T. Shimomura, Y. Irie; US Patent,4,666,983, (1987).
3. H. Nagorski; ACS Symposium Series, (1994), **573**, Chapter 8.
4. F. L. Buchholz; ACS Symposium Series, (1994), **573**, Chapter 2.
5. F. L. Buchholz, A. T. Graham; Modern Superabsorbent Polymer Technology; John Wiley & Sons Ltd.: New York, NY, 1998, Chapter 3.
6. F. L. Buchholz, A. T. Graham; Modern Superabsorbent Polymer Technology; John Wiley & Sons Ltd.: New York, NY, 1998, Chapter 5.
7. C. E. Harland; Ion Exchange Theory and Practice; Royal Society of Chemistry: Cambridge, 1994, 2nd Edition, Chapter 5.

Chapter Five

Nuclear Magnetic resonance imaging (MRI)

MRI is a recent technique in NMR, first discovered in 1973 by Lauterbur.[1,2] MRI is a non-destructive and non-invasive technique for the study of molecular dynamics, chemical environments and *in vivo* and *vitro* biochemical processes. The word nuclear has been removed to make a name that will not frighten the public.

MRI is most widely used in medical applications as a diagnostic aid in clinical practice to produce images from inside the human body. MRI can detect many clinical diseases such as hydrocephalus, tumours, aneurysms and meningitis observing morphological changes in the tissue. Due to the brain having very little movement, good contrast resolution, a long T_2 relaxation time improving the signal to noise ratio and the absence of signal from the bone, MRI is mostly used to detect cerebral conditions. MRI has provided the physician with clear pictures of the interior of the human body from any angle without using any hazardous radiation. The most widely used nucleus for imaging is the proton due to its high abundance in the human body (mainly from water and fat) and having the highest magnetic moment among stable nuclei. There has also been some interest in imaging nuclei such as ^{2}H, ^{7}Li, ^{19}F, ^{23}Na and also the imaging of unpaired electrons.[2]

Other applications of MRI have been much slower to develop than those of a medical nature. Many problems have been encountered with the imaging of solids due to short T_2 relaxation times and the restriction of atomic motion. Solids give broad lines causing problems for MRI but this can be overcome using the same techniques as for conventional solid-state NMR.[3,4,5]

The use of MRI in polymers has recently received great attention with many new applications being found. These new applications include the study of physical ageing of elastomers such as rubber, where MRI provides a method of monitoring various

changes in the material's properties without destruction of the sample.[6] As the NMR spectra of elastomers contain narrow lines they are good materials for using with MRI. Elastomers also have a high molecular mobility as a result of their glass transition temperature being well below the temperature of use[7] and are rich in protons. Rubber samples consisting of three pieces of rubber with different crosslink density have been identified using parameter selective MRI.[8]

MRI has also been used to obtain spatial information on the propagation of the strain induced by stress in a crosslinked poly(methacrylic) water gel.[9] During these experiments ^1H spin density and T_2 enhanced NMR imaging patterns for water in the gel under stress were observed. Spatial distributions of ^1H spin density and molecular motion of water molecules in the gel are changed by altering the strength of the stress. It was found that in the compressed region, the molecular motion of water was slower and the ^1H spin density lower compared with the surrounding uncompressed region. ^1H NMR imaging patterns have also been produced to provide information on the spatial distribution of the ^1H spin density and the ^1H T_2 relaxation times of a crosslinked poly(methacrylic) gel[10] using the results to clarify translational behaviour of water molecules in a gel under a shrinkage process brought on by the application of an electric field. It was found that after applying an electric field a cylindrical gel shrank to the shape of a wine stopper during a long elapsed time period. At the positive electrode side the ^1H spin densities were high and the mobility of water was low compared with the negative electrode (low ^1H spin densities and high water mobility).

It is also possible to study the adsorption and diffusion of various liquids into polymeric materials using MRI. The main advantage of using MRI for this application is the visual presentation of the data in the form of images, allowing the concentration and location of the liquid to be viewed directly.[11,12] The diffusion of methanol into poly(methacrylic) gel was followed by MRI allowing the diffusion coefficient to be

calculated by measuring the thickness of the adsorbed layer as a function of time. The dynamics of sorption and diffusion can also be measured using MRI. The solvent attack on the polymer is an important mechanism in the degradation of the polymer by both diffusion and liquid entering the voids reducing the tensile strength. Polymerisation reactions can be followed *in situ* using MRI giving quantitative data on monomer concentration and the rate of polymerisation.[13] The polymerisation of both acrylamide gels[14] and methylmethacrylate have been followed using imaging techniques. MRI can also be of great economic importance allowing casting defects in ceramics to be found before firing takes place.[7]

In conventional NMR the applied magnetic field is made constant over the sample volume with shimming where the NMR frequencies are identical for each volume element of the sample. In a MRI experiment a spatial map of the concentration of the nucleus under observation is obtained. Lauterbur pointed out that if a field gradient is applied to a structured object then each nucleus will respond with its own NMR frequency determined by its position. Therefore, the NMR frequency becomes a function of the position in space[1] and the amplitude encodes the material density.[5] The NMR spectrum is a 1-dimensional projection of the nuclear density along the gradient direction. The production of images requires the spatial encoding of the proton signals by field gradients accomplished by applying three separate orthogonal gradients at appropriate points in the pulse sequence. Gradients are generated by gradient coils mounted within the probehead.

A gradient spin-echo pulse sequence is normally employed to obtain ^1H NMR images (see figure 5.1). An advantage of this pulse sequence is the introduction of T_2 dependence to the signal helping to identify many tissues and pathologies which have similar T_1 values but different T_2 values.[15] In the spin-echo pulse sequence a hard 90° RF pulse is applied exciting all protons within the sample. Transverse magnetisation created by the RF pulse, dephases immediately after the pulse due to T_2

and field inhomogeneities. This is refocused using a Gaussian 180° refocusing pulse after a time equal to TE/2 (TE is the time delay between the RF excitation and the measurement of the signal), creating a spin echo at time TE that is corrected for field inhomogeneities.[1,15,16]

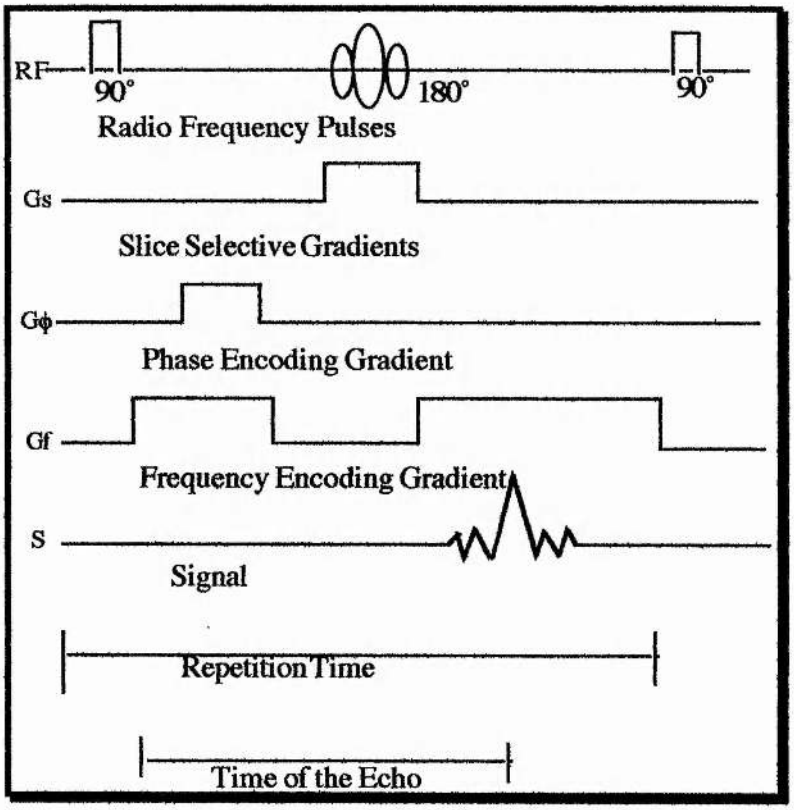

Figure 5.1. Spin-echo gradient timing diagram.

The soft 180° pulse is applied in conjuction with a slice selective gradient (G_S) allowing selected spins in a plane through the sample to be irradiated. The gradient is first applied across the sample resulting in a particular frequency corresponding to a plane of constant frequency perpendicular to the direction of the gradient. The 180° pulse applied converts the z magnetisation of the slice into transverse magnetisation

The duration of the RF pulse is chosen so that its spectrum is a narrow block of frequencies. The region of the sample with nuclei who resonate at the frequencies

within the RF pulse will be excited, while the rest of the sample will not. The thickness and position of the slice depend on the RF pulse and the strength of the gradient, changing the position of the plane by simply changing the frequency of the RF pulse.

A phase encoding gradient ($G\phi$) is applied between the 90° and 180° slice selective pulses. This causes the spins to dephase at a rate directly proportional to the magnitude of the gradient. During the time when the phase encoding gradient is switched on each transverse magnetisation vector precesses at its own Larmor frequency. After the gradient has been turned off, although each vector experiences the same magnetic field and have identical Larmor frequencies, the phase angle ϕ for each vector is different (the phase angle is the angle between a reference axis and the magnetisation vector at the time the phase encoding gradient has been turned off). After the 180° pulse and during the time the echo is collected, the frequency encoding gradient (G_f) is applied.[1,15,16] As a result of each spin experiencing a different magnetic field the NMR spectrum contains many signals where the amplitude of the signal is proportional to the number of spins in a plane perpendicular to the gradient. Frequency encoding causes the resonance frequency to be proportional to the position in the RF coil of the spin and is responsible for the formation of an echo. An additional gradient is applied between the 90° and 180° pulses in the same direction as the frequency encoding gradient. This gradient dephases the spins so that they will rephase by the centre of the echo.[1,15,16] The sequence of pulses is usually repeated 128 or 256 times to collect all the data necessary to produce an image where the time between the repetitions of the sequence is called the repetition time (TR). The phase encoding gradient is varied in equal steps between $G\phi$ and $-G\phi$ with each repetition of the pulse sequence.

Discussion

The purpose of MRI in this project was to try and investigate what happens during the absorption of water by superabsorbent polymers. As already mentioned superabsorbent polymers can absorb and retain several hundred times their own weight in water. As the liquid is absorbed into the polymer it swells forming a gel, resulting in an increase in volume which can be observed using the naked eye. The change in volume is a result of the water diffusing into the polymer causing the polymer chains to relax and diffuse outwardly into the liquid. MRI will allow the absorption of liquid to be observed as an image from inside the polymer without invasion or destruction. From the images produced it is hoped to be able to tell something about the mechanism of the absorption of liquid into the polymer.

Before any imaging experiments could be carried out the ^1H T_2 relaxation time of the protons in the superabsorbent polymer gel had to be measured. This was to ensure that the ^1H relaxation times were not too fast for imaging to be carried out. ^1H T_2 relaxation times were measured using a CPMG pulse sequence of four superabsorbent polymer gels of DMRD1 at various degrees of hydration. Graphs were plotted of ln(Ao-At) versus delay (where Ao is the infinity intensity value and At the intensity at time t) calculating the relaxation time for each gel from 1/slope of the graph (see table 5.1 for relaxation times). One graph has been included as a representative of all samples (see figure 5.2).

The results in table 5.1 show that the T_2 relaxation time of the protons in the superabsorbent polymer gel decreases with increasing hydration until 2000 % hydration is reached (1 g polymer in 20 g water). The T_2 relaxation time of the protons was slow enough to enable imaging of the absorption of liquids by superabsorbent polymers to be carried out.

Sample	T_2 value from slope of graph
1g polymer in 2g water	25.40 milliseconds
1g polymer in 5g water	24.15 milliseconds
1g polymer in 10g water	22.82 milliseconds
1g polymer in 20g water	26.70 milliseconds

Table 5.1. T_2 Relaxation times of DMRD1 hydrated to various degrees.

Ten different samples of DMRD1 were imaged absorbing liquid, varying a different parameter in each experiment. From the images produced it was hoped to be able to carry out volumetric and gravimetric analysis of the absorption process and produce a model of the system.

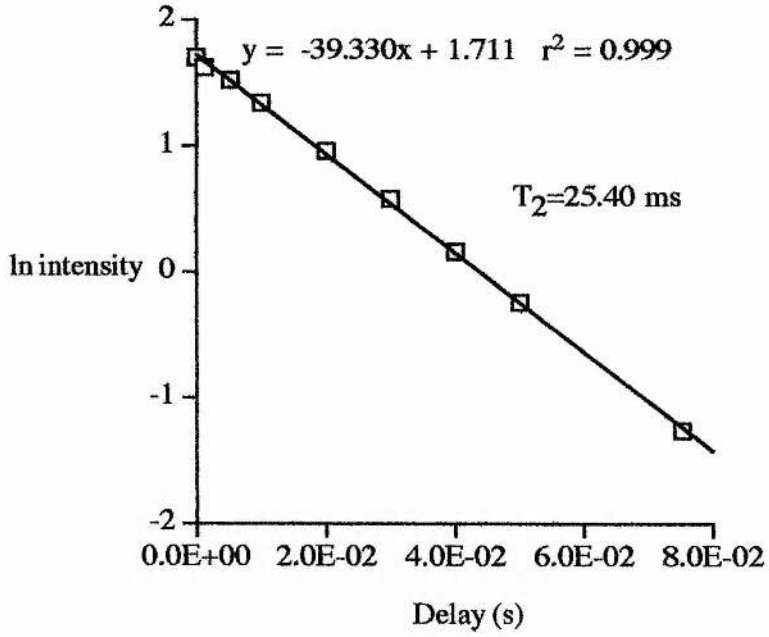

Figure 5.2. Graph of ln intensity versus delay for 1g polymer in 2g water.

A teflon device was specially designed (see figure 5.3) to allow the absorption of water into the superabsorbent polymer to be imaged. Superabsorbent polymers

absorb water very quickly but for images to be produced it was required to feed the water to the polymer fairly slowly. This problem was solved by attaching seven wicks to the bottom of the teflon device which would feed the water slowly to the polymer sample. To make sure the water was distributed evenly to the polymer sample a piece of filter paper was placed on top of the wicks and under the polymer sample which was present as a flat disc or loose granules. Discs were made either by compressing particles of the superabsorbent polymer together or by obtaining the whole disc from a single homogeneous polymerisation experiment. The teflon device was designed to fit into a 25 mm NMR tube which contained an amount of water at the bottom.

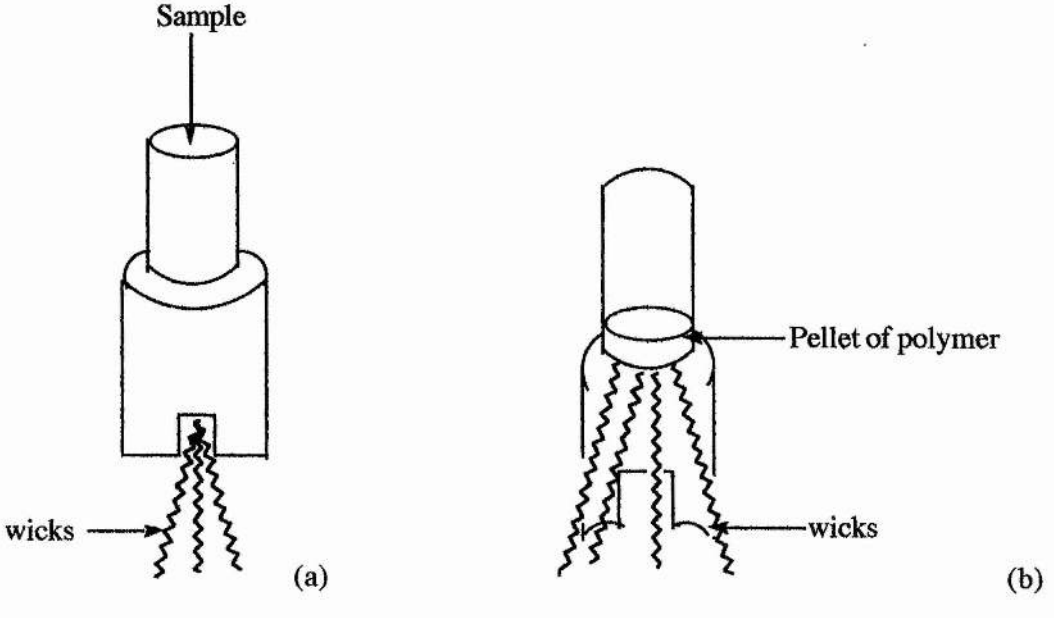

Figure 5.3. Teflon device used in imaging (a). Diagram showing a section through the teflon device (b).

Imaging was first carried out using a spin-echo pulse sequence on loose

superabsorbent polymer granules and pellets made using a KBr press, absorbing water. This would hopefully show any differences in the rate and mechanism of absorption between loose and compressed polymer.

To try and mimic what happens when a load is placed on top of the swelling superabsorbent polymer (i.e. when a baby sits down on its nappy), imaging experiments of both granules and pellets absorbing water were also carried out with a weight (0.7 psi) resting on top of the dry polymer. This would help to observe any differences in swelling when the polymer has a load pressing down on it. Polymer pellets were also imaged absorbing, with and without the weight, 1 % (0.17112 M) NaCl. This was to put the experiment under similar conditions as experiments carried out in the laboratory and when the polymer is absorbing urine in babies nappies and adult incontinence pads. The absorption of NaCl should hopefully show differences in the images from the absorption of water due to the polymer swelling less in the salt solution.

Each individual polymer particle has a built in memory and when compressed into a pellet each particle retains its memory and behaves as an individual particle. Therefore, as the water diffuses into the pellet it will go in the spaces between the individual particles with a capillary action. It was thought that this would cause problems with the analytical analysis of the images and to overcome this problem homogeneous superabsorbent polymer gel pellets were synthesised. To observe the effects of crosslinking on the swelling homogeneous pellets were synthesised with two different crosslinker levels 0.07 % and 0.05 % (standard level). The higher the crosslinker level in the superabsorbent polymer the less will be the swelling. Pellets with both levels of crosslinker were imaged absorbing water with and without the weight on top of the polymer sample.

A sequence of seventy ^{1}H T_1 and T_2 weighted images of a 2 mm vertical slice through

the sample was produced for each different experiment showing clearly the swelling of the superabsorbent polymer from inside (see figure 5.4). The first image in the sequence of each different experiment shows little detail as the polymer has not swollen very much. As the polymer begins to swell grey regions begin to appear at the bottom of the images. From further images it can be seen that the polymer swells evenly across the sample until a certain point where the middle of the sample begins to swell more quickly producing a dome shaped image. With further swelling of the polymer the dome shape proceeds to increase in size with the contrast throughout the grey area becoming less homogeneous. This suggests that the polymer is not absorbing the water evenly as different intensities are seen throughout the image. A white region begins to appear at the top of the image showing a region higher in intensity than the region behind it. Therefore, as a concentration difference is seen in the image it can be concluded that the superabsorbent polymer is not absorbing the water evenly throughout the sample. Bright white spots seen in the images are caused by the wicks folding back into the image (this is a feature of the experiment and is unable to be removed). The first image in figure 5.4 (top left image) is also the first image of the sequence with the next two images (bottom left and top right images) coming from the middle of the sequence and the final image (bottom right image) being the final image in the sequence. When looking at the images of the absorption of NaCl less inhomogeneity is seen throughout the grey region due to the polymer swelling less in the salt solution. The images produced from all experiments are seen to be fairly similar using the naked eye and require analysis to show any differences between them.

A calibration experiment was carried out to determine if the brighter parts in the images represented regions of high water content. Water was placed in a separate compartment surrounding the polymer sample in a redesigned teflon device to give an indication of the brightness of a high water content region. A homogeneous pellet was imaged absorbing water surrounded by the compartment containing the water.

So that no other software can be used Bruker systems store images as binary files and differ the contrast levels in each image of the sequence making it very difficult to compare images. Therefore, to enable analytical work to be carried out on the images and comparisons to be made they first had to be converted to ASCII files. This resulted in two columns of numbers which were then reformatted to give a square of numbers 128 by 128. The numbers were then fed into Excel where 3-dimensional plots of the intensity for each individual image were produced. The breaking of the Bruker code was carried out by Dr Mary-Jane Tremayne and I wish to thank her for carrying out this work. Figure 5.5 shows the plots of four images from a sequence as an example again from the same positions in the image sequence as figure 5.4. From these pictures the change in volume and relative intensity can be seen. Unfortunately these pictures cannot be compared with each other due to the problem of differing contrast caused by the Bruker software. Figure 5.6 shows the plots of 4 images from the calibration experiment, again at the same positions from the image sequence. From these pictures it is very difficult to determine if the brighter region within the images is a high water region as again these pictures cannot be compared with one another.

Homogeneous pellets were synthesised to prevent the diffusion of water into the spaces between the individual particles to simplify the analysis of the images. As a result of the pellet swelling more in the horizontal direction than the vertical one shown in figure 5.7 (also dries faster in the horizontal direction than the vertical one) it was discovered that the pellet had twisted during the experiment. This twisting also occurred when a weight was placed on top of the pellet. This is a function of the non-uniform swelling of the gel pellet typically swelling more quickly at the outer surfaces initially. For a large piece of gel this results initially in a smooth piece of gel swelling to look like a brain covered in lots of corrugations and contours, although equilibrium restores the original smooth surface of the gel. This phenomenon may be causing the

pellet to twist while absorbing liquid but causing slight differences due to the smaller piece of gel used in the imaging study. Therefore, it was extremely difficult to carry out any analytical work on the absorption of liquid into the polymer and to produce a model of the system. Future work would be to investigate ways of redesigning the teflon device in order to prevent the pellet from twisting while it is absorbing the liquid. This could be achieved by placing extra bits of teflon inside the device preventing any swelling in the horizontal direction. A rectangular piece of gel could then be cut from the pellet and placed inside the device for further imaging studies to be carried out (see figure 5.8).

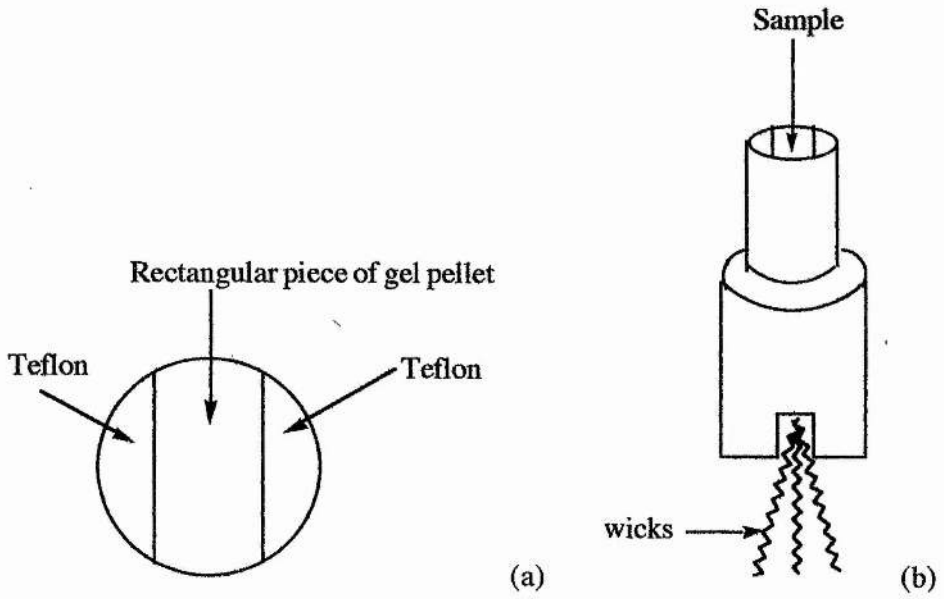

Figure 5.8. Redesigned teflon device for further imaging work. Diagram (a) view from above, diagram (b) side view.

Conclusion

It has been shown from this work that the absorption of liquids by superabsorbent polymers can be visualised using magnetic resonance imaging. It has also been shown that the absorption is not even throughout the polymer as seen through a

contrast difference within the image. Further work is required to carry out volumetric and gravimetric analysis of the images to try and understand the mechanism of absorption of liquids into superabsorbent polymers. Standardisation of the contrast within each image would have to be carried out allowing the images and pictures to be compared with each other. This would then give a better picture of the increase in intensity as the polymer swells and whether the brighter region is a region of higher water content. If the brighter region of the image was a region of high water content it could be assumed that a solvent front was present inside the polymer with less water behind the front.

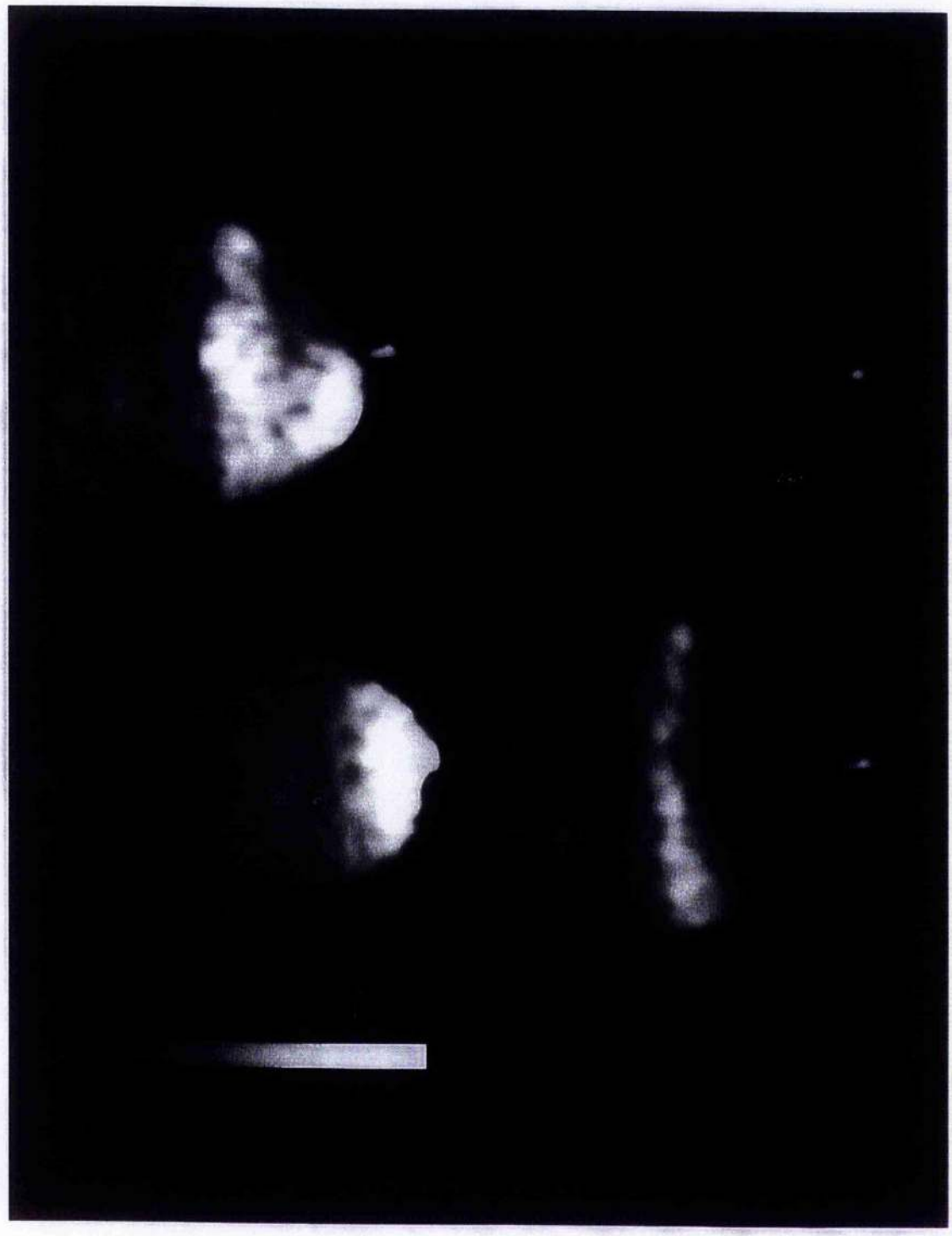

Figure 5.4. Selected images from a typical imaging sequence.

Figure 5.5. Pictures representing selected images from a typical imaging sequence.

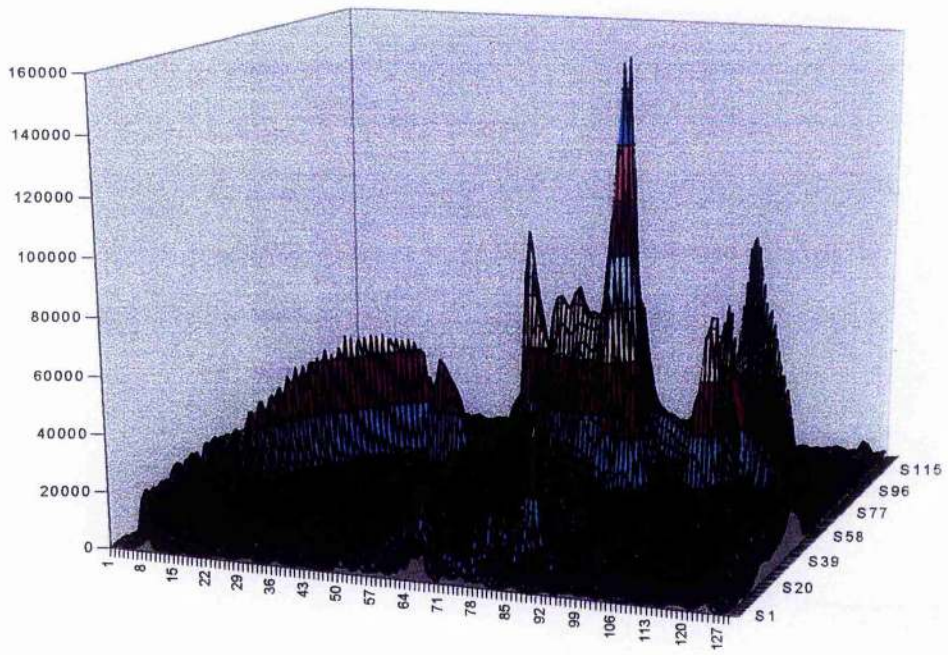

Image 1

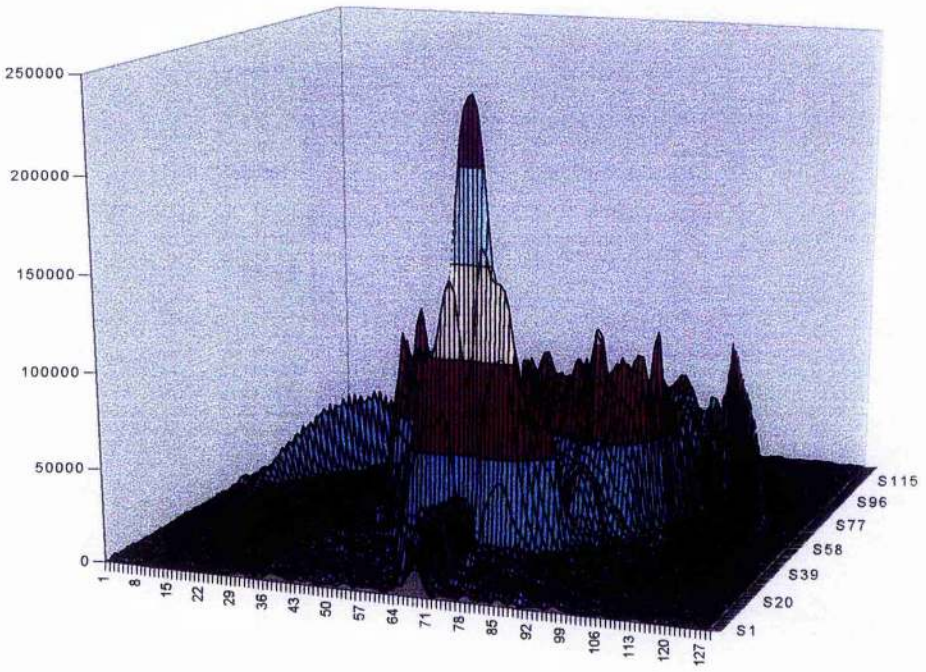

Image 2

Figure 5.5. Pictures representing selected images from a typical imaging sequence.

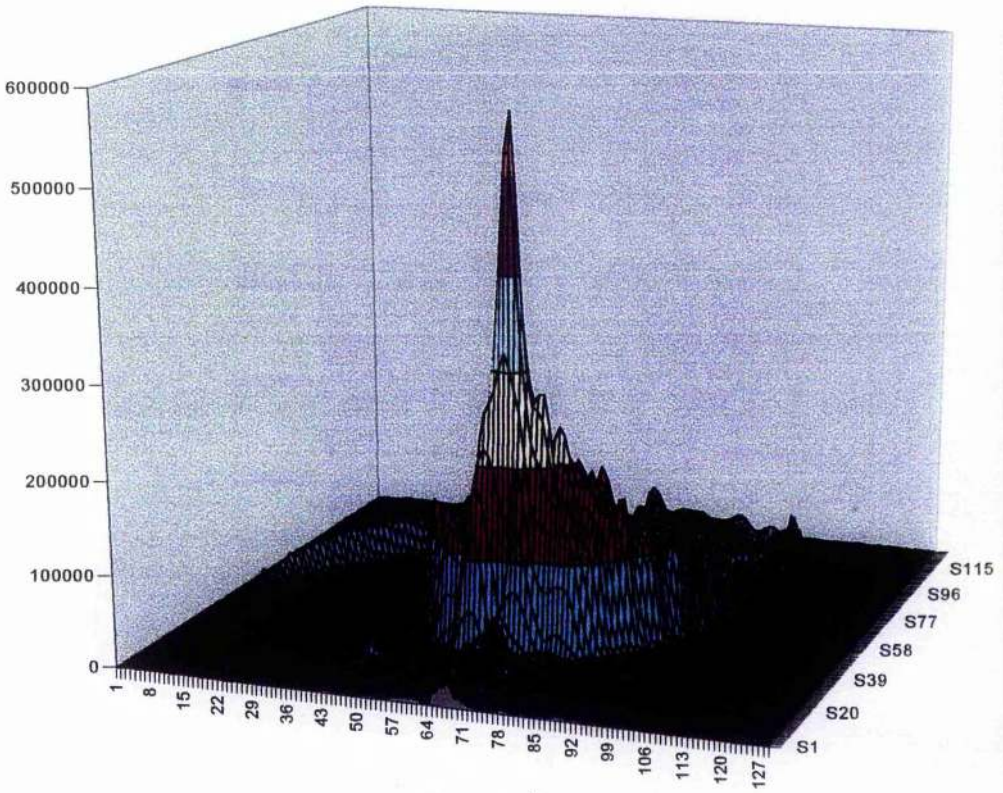

Image 3

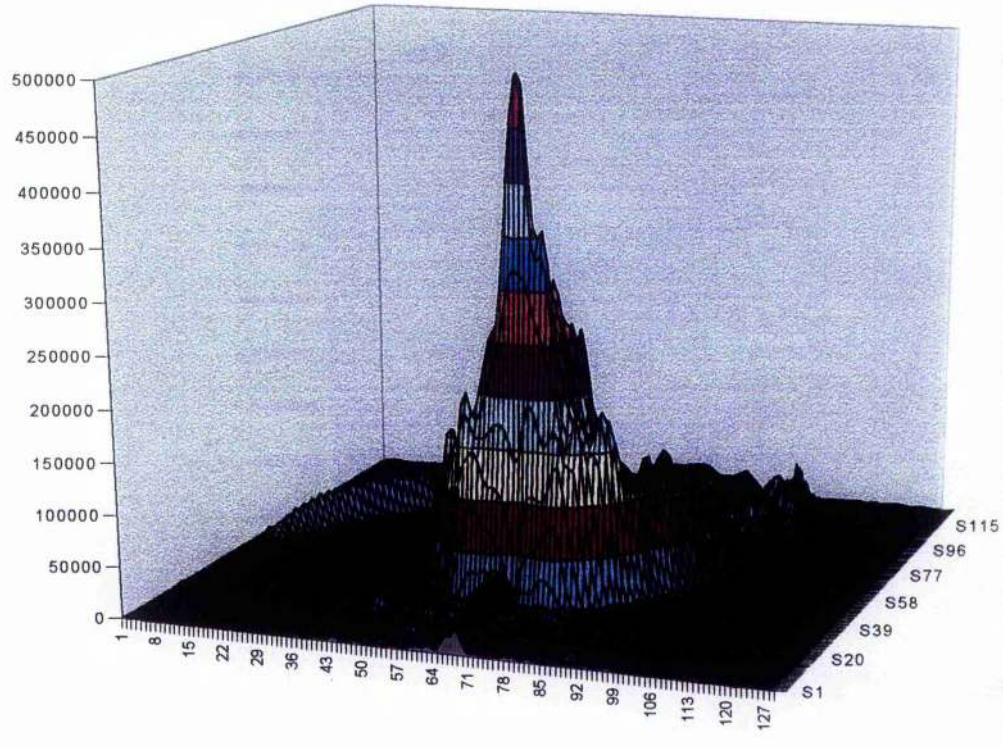

Image 4

Picture 5.6. Pictures representing images from calibration experiment.

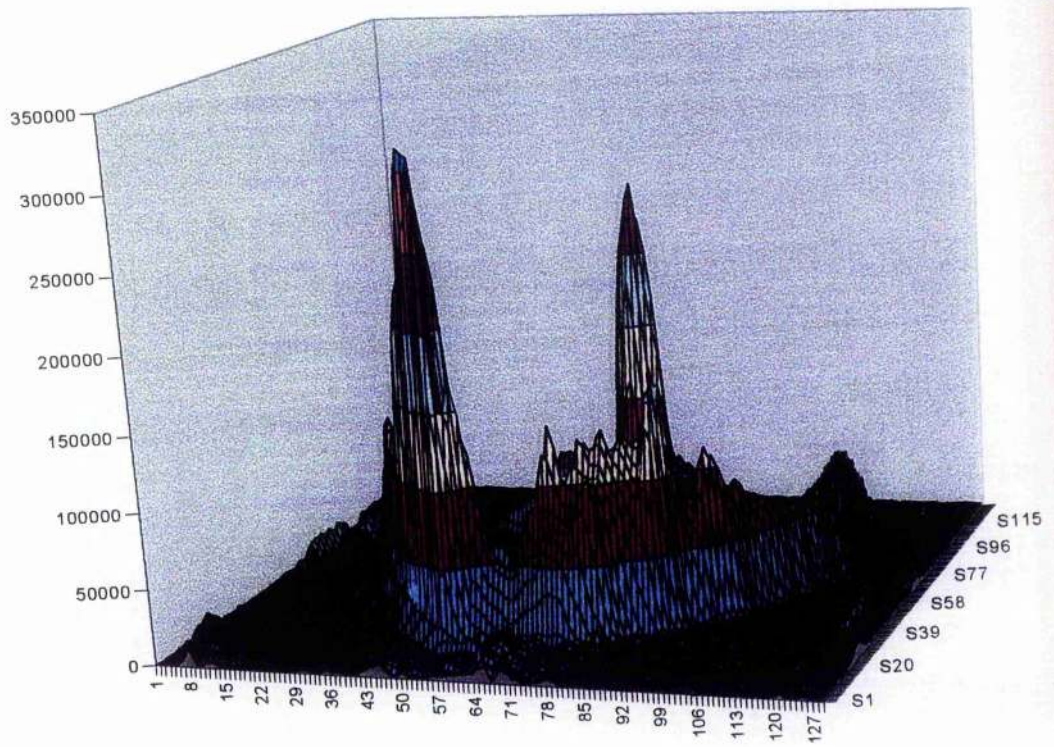

Image 1

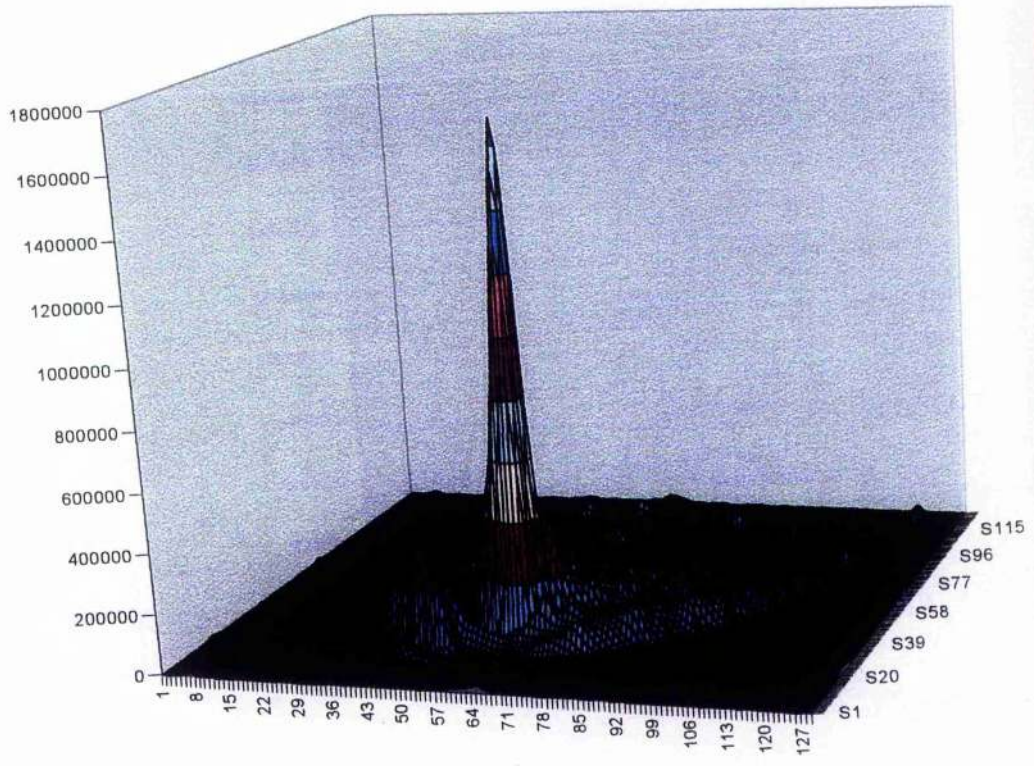

Image 2

Picture 5.6. Pictures representing images from calibration experiment.

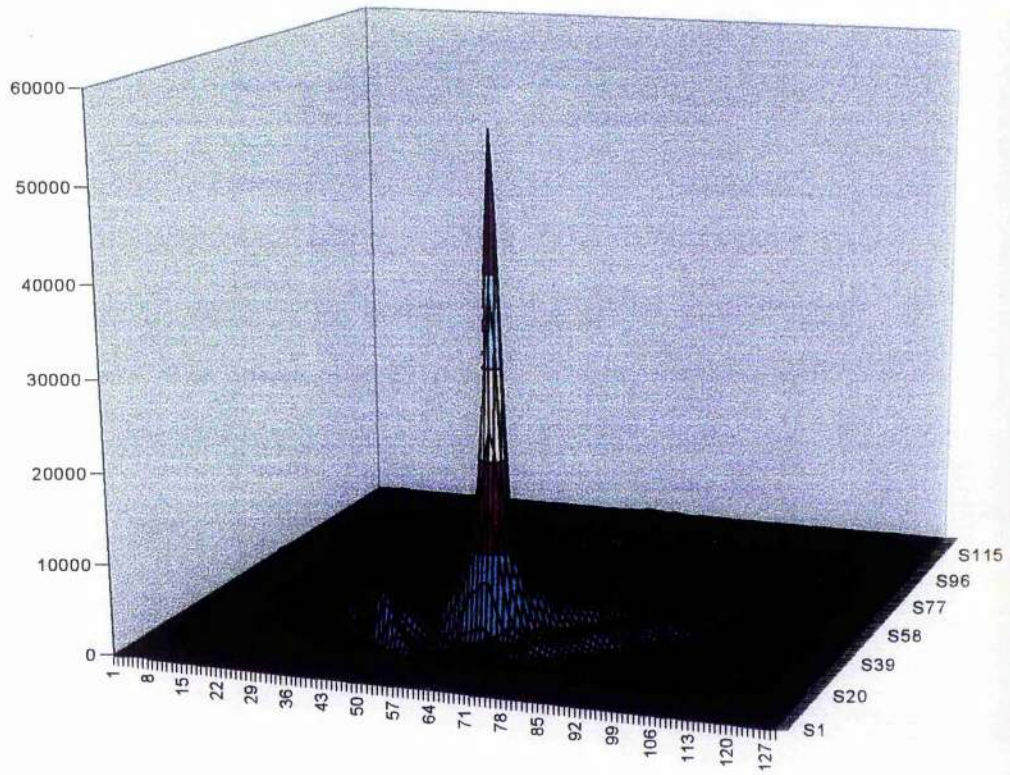

Image 3

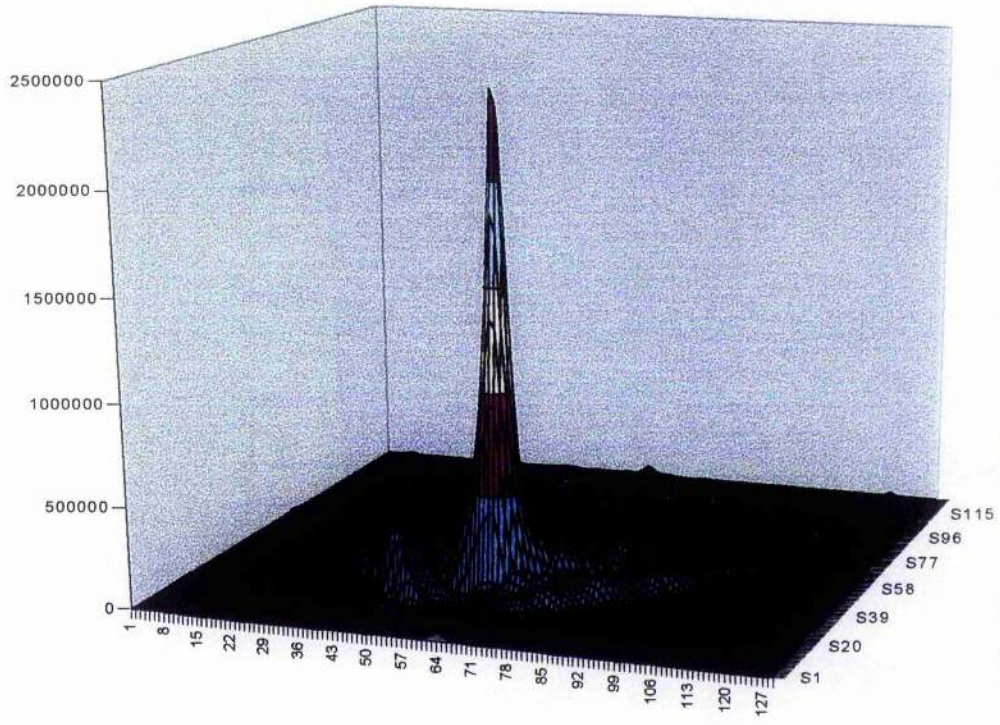

Image 4

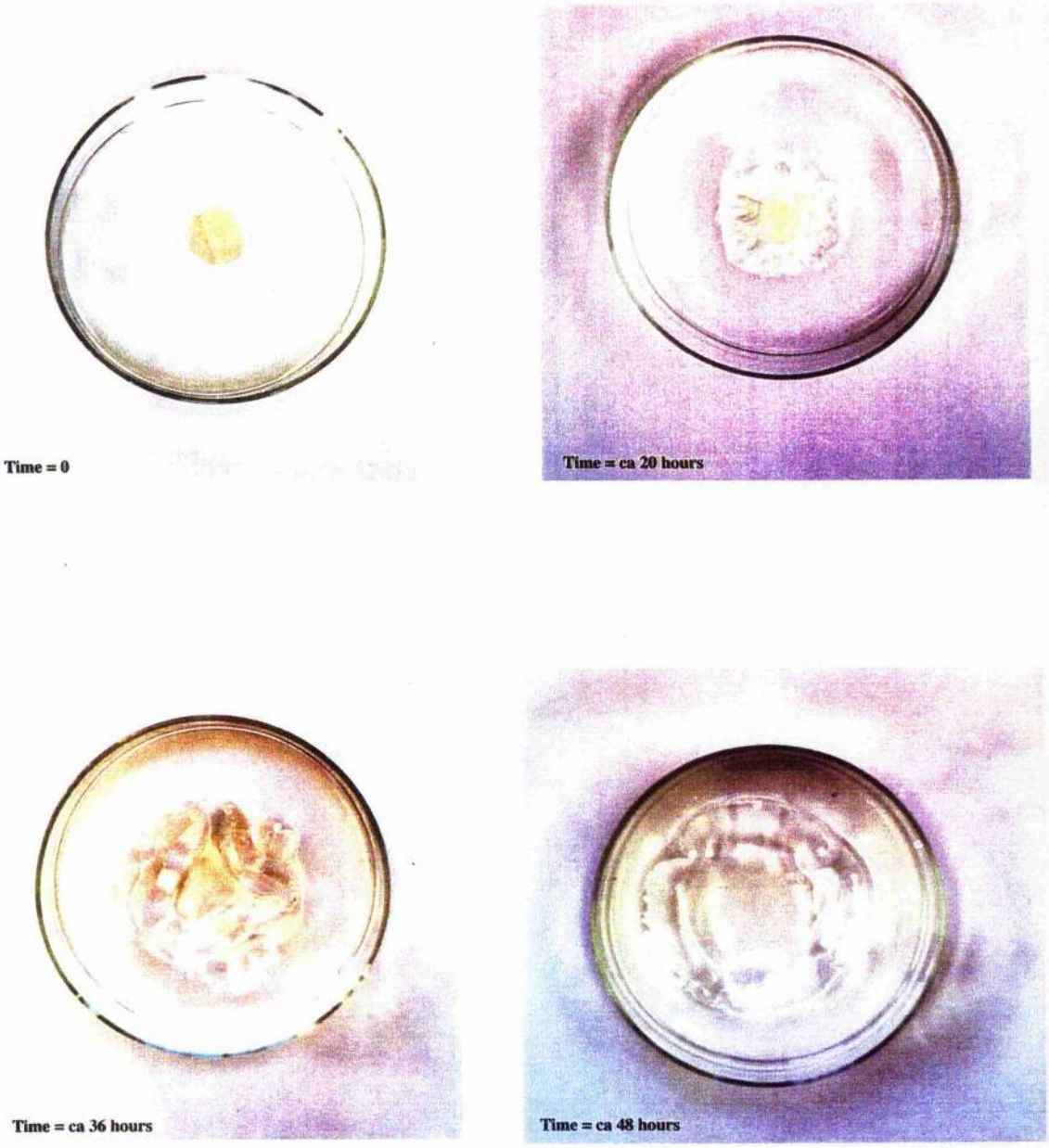

Figure 5.7. Homogeneous pellet swelling in water.

References

1. W. Kuhn; *Angewandte Chemise Int. Eng. Ed.*, (1990), **29**,1-19.
2. E. R. Andrew; Encyclopaedia of NMR, (1996), 2462-2471.
3. B. Blumich, P. Blumler, E. Gunther, G. Schauss, H. W. Spiess; *Makromol. Chem., Macromol. Symp.*, (1991), **44**, 37-45.
4. F. Weigand, D. E. Demco, B. Blumich, H. W. Spiess; *Solid State Nuclear Magnetic Resonance*, (1996), **6**, 357-365.
5. P. J. McDonald; *Spectroscopy Europe*, (1995), **7**, 25-30.
6. B. Blumich, P. Blumler; *Makromol. Chem.*, (1993), **194**, 2133-2161.
7. A. N. Garroway, Encyclopaedia of NMR, (1996), 3683-3692.
8. W. Kuhn, P. Barth, S. Hafner, G. Simon, H. Schneider; *Macromolecules*, (1994), **27**, 5773-5779.
9. H. Yasunaga, H. Kurosu, I. Ando; *Macromolecules*, (1992), **25**, 6505-6509.
10. T. Shibuya, H. Yasunaga, H. Kurosu, I. Ando; *Macromolecules*, (1995), **28**, 4377-4382.
11. J. L. Koenig; Polymer Spectroscopy, John Wiley & Sons, New York, NY, (1996) Chapter 6.
12. J. Grasselli; *European Spectroscopy News*, (1988), **80**, 36-39.
13. P. Jezzard, C. J. Wiggins, T. A. Carpenter, L. D. Hall, P. Jackson, N. J. Clayden, N. J. Walton; *Advanced Materials*, (1992), **4**, 82-90.
14. S. Ahuja, S. L. Dieckman, N. Gopalsami, A. C. Raptis; *Macromolecules*, (1996), **29**, 5356-5360.
15. C. A. Fyfe, L. H. Randall, N. E. Burlinson; *Journal of Polymer Science: Part A: Polymer Chemistry*, (1993), **31**, 159-168.
16. L. E. Crooks; Encyclopaedia of NMR, (1996), 2439-2454.

Chapter Six

Neutralisation Domains

As already mentioned in the introduction, an important factor in the manufacture of polyacrylate superabsorbent polymers is the degree of neutralisation. The monomers and crosslinker are dissolved in water before polymerisation at a desired concentration, usually 10-70%. The acrylic acid is usually partially neutralised before the polymerisation is initiated, but the crosslinked polymer can also be neutralised after the polymerisation is complete. Inexpensive bases such as sodium hydroxide and sodium carbonate are normally used as neutralising agents. The superabsorbent polymers manufactured commercially by Chemdal are pre-neutralised using sodium hydroxide and post-neutralised using sodium carbonate.

To observe any differences in the behaviour of microdistribution between pre- and post-neutralised superabsorbent polymers the solid-state ^{13}C NMR spectra were measured. In this case microdistribution will correspond to different domains of the polymer which contain only carboxylic acid groups or sodium carboxylate groups. By looking at the carbonyl region of the ^{13}C NMR spectrum the individual regions will be able to be detected as NMR is a very powerful tool for polymer structure characterisation. Typically the carbonyl shift of $\underline{C}O_2H$ is 180 ppm and in $\underline{C}O_2^-$ is 186 ppm. Thus, domains containing substantially only one form of the acid and not the other should be distinguishable. Mixed domains in which H^+ is not exchanging would give rise to a broad peak whereas mixed domains with rapid exchange of H^+ would give rise to a relatively sharp peak between the two extremes of chemical shift. Solid state ^{13}C CPMAS spectra should be capable of giving valuable information on the domain structure in partially neutralised superabsorbent polymers.

Isolated domains containing $\underline{C}O_2H$ or $\underline{C}O_2^-$ should give rise to two peaks at around 180 and 186 ppm. In practice given the linewidth normally observed in these systems this could be observed as an unresolved or partly resolved peak and shoulder.

Discussion

Two different generations of superabsorbent polymer were synthesised, ASAP 2300 pre-neutralised with sodium hydroxide and DMRD1 post-neutralised with sodium carbonate. ASAP 2300 was also synthesised using sodium carbonate as the neutralising agent, to observe any differences in structure caused by using a different neutralising agent. Each polymer generation was synthesised with degrees of neutralisation 0, 25, 50 75 and 100%. During the polymerisation the temperature of the solution was noted at 30 second time intervals and graphs drawn of time versus temperature (see figures 6.1. and 6.2.).

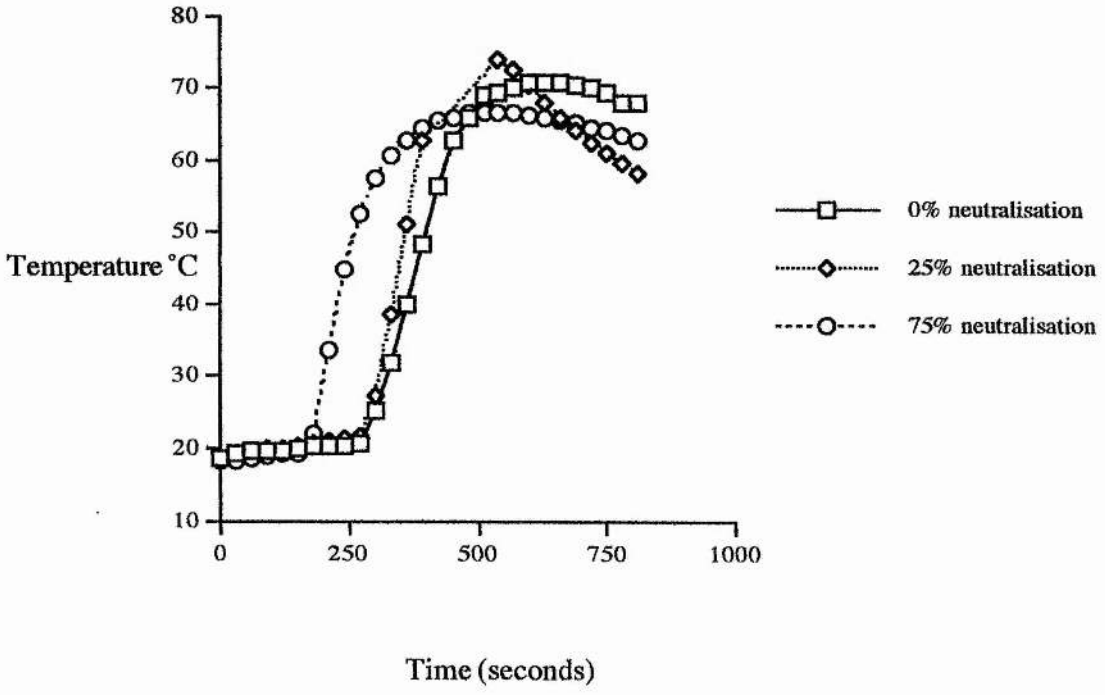

Figure 6.1. Isotherms for pre-neutralisation with sodium hydroxide.

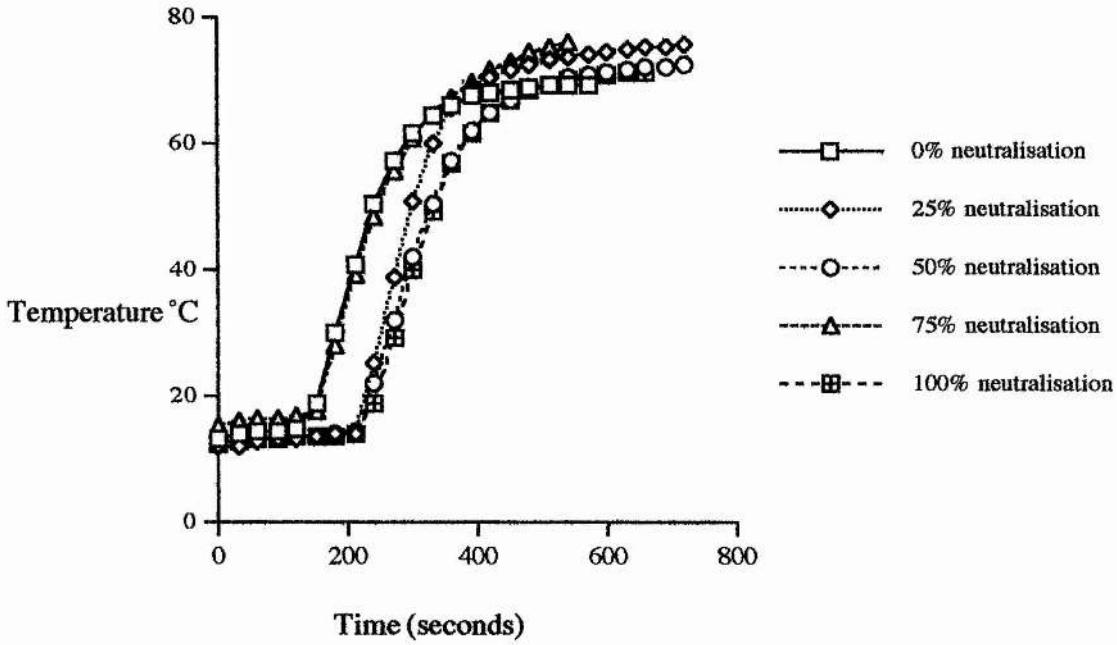

Figure 6.2. Isotherms for post-neutralisation.

Once synthesised the polymers were tested using the gel volume and absorption under load tests (see page 57 for method). Results were varied showing that some polymers' performance were quite good and others were not (see table 6.1). This however was not important to the investigation of the domain structure by NMR.

ASAP 2300 Pre-neutralised with NaOH

The solid state ^{13}C NMR spectra showed the two standard peaks observed in a solid state ^{13}C NMR spectrum of a superabsorbent polymer. The two peaks correspond to a single carbonyl peak which shifts between 180 and 186 ppm as the degree of neutralisation increases, and the aliphatic peak at approximately 40 ppm. The spectra also contain spinning side bands at approximately 136 and 226 ppm. The carbonyl

peak for 0 % neutralisation is found at 180 ppm which corresponds to the normal position for $\underline{C}O_2H$, while for 100 % neutralisation it is found at 186 ppm, corresponding to the normal position for $\underline{C}O_2Na$.

Polymer used	Gel volume result g/g	AUL result g/g
ASAP 2300 DN=0%	5.4	9.04
ASAP 2300 DN=25%	19.0	19.63
ASAP 2300 DN=50%	41.4	22.46
ASAP 2300 DN=75%	43.8	22.71
ASAP 2300 DN=100%	26.7	9.94
DMRD1 DN=0%	6.5	9.25
DMRD1 DN=25%	10.8	10.55
DMRD1 DN=50%	20.8	16.85
DMRD1 DN=75%	34.5	19.22
DMRD1 DN=100%	46.2	12.34
2300 DN=25% Na_2CO_3	27.7	20.88
2300 DN=50% Na_2CO_3	37.8	21.67
2300 DN=75% Na_2CO_3	38.2	26.58
2300 DN=100% Na_2CO_3	28.9	10.13

Table 6.1. Results of testing of synthesised polymers.

The data for the ^{13}C chemical shifts of $\underline{C}O_2H$ are obtained using either neat liquids or concentrated solutions and the observed shift for the free acid is that of the dimeric form rather than the monomeric form. The carbonyl oxygen will therefore be strongly hydrogen-bonded which gives the carbonyl carbon substantial deshielding.[1] It is therefore, reasonable to suggest this is the main factor giving rise to the chemical shift

difference between the carboxyl carbon of the acid and the corresponding salt. The ionic form of the acid group $\underline{C}O_2^-$ is found to be less electronegative than the acid itself and this would also be expected to be moved to a lower frequency.[2] In actual fact, the reverse happens and $\underline{C}O_2^-$ is shifted to a higher frequency. A chemical shift difference of approximately +6 ppm is seen for the salt relative to the carboxylic acid.

The single carbonyl peak of the polymers with intermediate degrees of neutralisation shifts between 180 and 186 ppm in approximately 1 ppm steps. This indicates that there are no distinct regions within the polymer which contain only CO_2H or CO_2Na (see figure 6.3).

Also observed from the spectra is an increase in the width at half height of the aliphatic peak with increasing neutralisation. It is impossible to differentiate between the chemical shifts for CH and CH_2 as they are both contained within the aliphatic peak. Unfortunately, the overlapping of peaks is seen in the NMR spectra of most polymers. The increase in width of the aliphatic peak can be accounted for by an increasing difference between the chemical shifts of the CH and CH_2 groups within the polymer, caused by an increase in the number of carboxylic acid groups being converted to carboxylate groups. The carbonyl peak also becomes sharper as the degree of neutralisation increases.

In order to ensure that spectra were obtained from a polymer with randomly neutralised acid groups the polymers were hydrated with water and redried. The ^{13}C solid state NMR spectra were measured and again the same characteristic single carbonyl signal shifting between the position for $\underline{C}O_2H$ and $\underline{C}O_2Na$ as a function of neutralisation was seen. The width of the aliphatic peak at half height is not seen to vary much with increasing neutralisation although the chemical shifts for the CH and CH_2 groups shift high frequency (see figure 6.3). In order to check the position of the un-neutralised $\underline{C}O_2H$ resonance in these polymers, the polymer was washed with

0.1 M HCl and then redried. This produced dramatic changes in the ^{13}C solid state NMR spectra. The carbonyl peak for each different degree of neutralisation has shifted to approximately 180 ppm, the position of the carbonyl peak in the un-neutralised polymer. The carbonyl peak in these spectra are found to be fairly symmetrical. The width at half height of the aliphatic peak is observed as being similar for each washed polymer sample with no change in chemical shift. This also shows that in the fully acid form the CO_2H groups are present as hydrogen bonded dimers. It seems that the pre-neutralised polymer has no domain structure and has a randomly mixed array of CO_2H and CO_2^- groups. The line widths suggest, but do not prove that there is not a rapid exchange of H^+ (see figure 6.4).

DMRD1 Post-neutralised with Na_2CO_3

The ^{13}C solid state NMR for the post-neutralised polymer showed the two standard peaks found in a ^{13}C solid state NMR spectrum of a superabsorbent polymer. Again, these two peaks correspond to a carbonyl peak which shifts between 180 and 186 ppm as the degree of neutralisation increases, and the aliphatic peak at approximately 40 ppm. The spectra also contain spinning side bands at approximately 136 and 206 ppm. A single carbonyl peak is observed at 180 ppm for 0 % neutralisation and 186 ppm for 100 % neutralisation, again corresponding to the positions for $\underline{C}O_2H$ and $\underline{C}O_2Na$ respectively. However, major differences are seen in the carbonyl region for intermediate degrees of neutralisation where a twin carbonyl signal consisting of a peak and a pronounced shoulder is seen (see figure 6.5). This suggests that there are distinct domains within the post-neutralised polymer which do not exchange within the NMR timescale. Also observed from the spectra is the increase in the width at half height of the aliphatic peak with increasing neutralisation. This is again caused by the increase in the number of CO_2H groups being converted into CO_2Na groups causing the difference between chemical shifts of the CH and CH_2 groups to be increased.

After hydration with water and redrying, the ^{13}C solid state NMR spectra again showed major differences from the unhydrated polymer. Instead of seeing a twin carbonyl signal for intermediate degrees of neutralisation, this time only a single signal is observed. This peak is found at 180 ppm for 0 % neutralisation and 186 ppm for 100 % neutralisation with the intermediate degrees of neutralisation, shifting between the two extremes with steps of approximately 1 ppm. The single carbonyl signal now seen for the intermediate degrees of neutralisation is positioned at an intermediate chemical shift between the two chemical shifts extremes. The difference seen in the carbonyl region between the dry and rehydrated polymer is most probably caused by hydration allowing reorganisation of the neutralisation from a domain structure to a random array as was seen in the pre-neutralised polymers (see figure 6.6).

Washing the polymer with 0.1 M HCl and redrying produces the same effects as seen for ASAP 2300. The carbonyl signal shifts to 180 ppm for each different degree of neutralisation, the position for the carbonyl group in the un-neutralised polymer. The width at half height of the aliphatic peak does not change after the polymers have been washed (see figure 6.7).

ASAP 2300 Pre-neutralised with Na_2CO_3

Pre-neutralising with a different neutralising agent is shown to have no effect on the structure of the polymer. The ^{13}C solid state NMR spectra are almost all identical to those of ASAP 2300 pre-neutralised with sodium hydroxide. Therefore, the differences seen between pre- and post- neutralised are not attributed to the difference in neutralising agent, but to the time when neutralisation takes place.

Summary

Major differences are seen between the spectra of pre- and post-neutralised

superabsorbent polymers. In the spectra of pre-neutralised polymer no distinct domains of CO_2H and CO_2Na are seen. There is a single carbonyl peak which moves between the chemical shifts for 0 % and 100 % neutralisation. In contrast, the spectra of the post-neutralised polymer does contain distinct domains. A twin carbonyl signal which does not exchange within the NMR timescale, is observed. Hydration of the individual polymers again shows differences between the pre- and post-neutralised polymers. For the pre-neutralised polymer no differences are seen in the spectra of the hydrated polymer from the spectra of the unhydrated polymer. Again, differences appear in the spectra of the post-neutralised polymer where a signal carbonyl signal is observed in contrast to the twin carbonyl signal. An explanation for this difference could be that hydration has caused the individual domains within the polymer to reorganise, becoming indistinct as in the pre-neutralised polymer. Washing both the pre- and post-neutralised polymers with HCl produces the same effect. The carbonyl peak for each degree of neutralisation shifts to 180 ppm, the position of the carbonyl peak in the un-neutralised polymer. The use of a different neutralising agent for pre-neutralisation of the polymer is seen to produce no difference in the structure of the polymer. This shows us that the difference in the structure between pre- and post-neutralised polymer cannot be attributed to the use of a different neutralising agent but is in fact brought about at the time at which the polymer is neutralised.

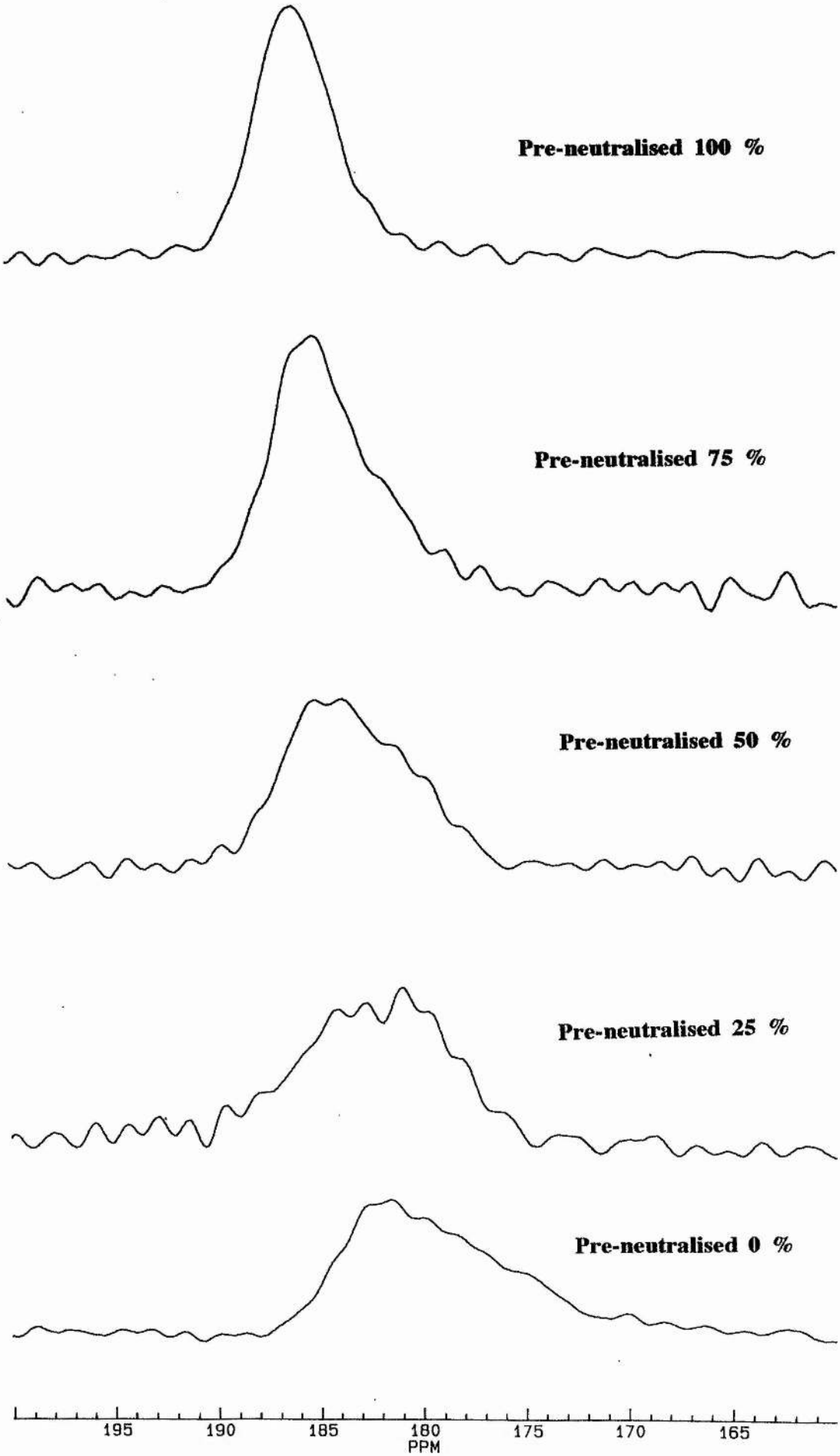

Figure 6.3. Carbonyl region of dry ASAP 2300 with increasing neutralisation.

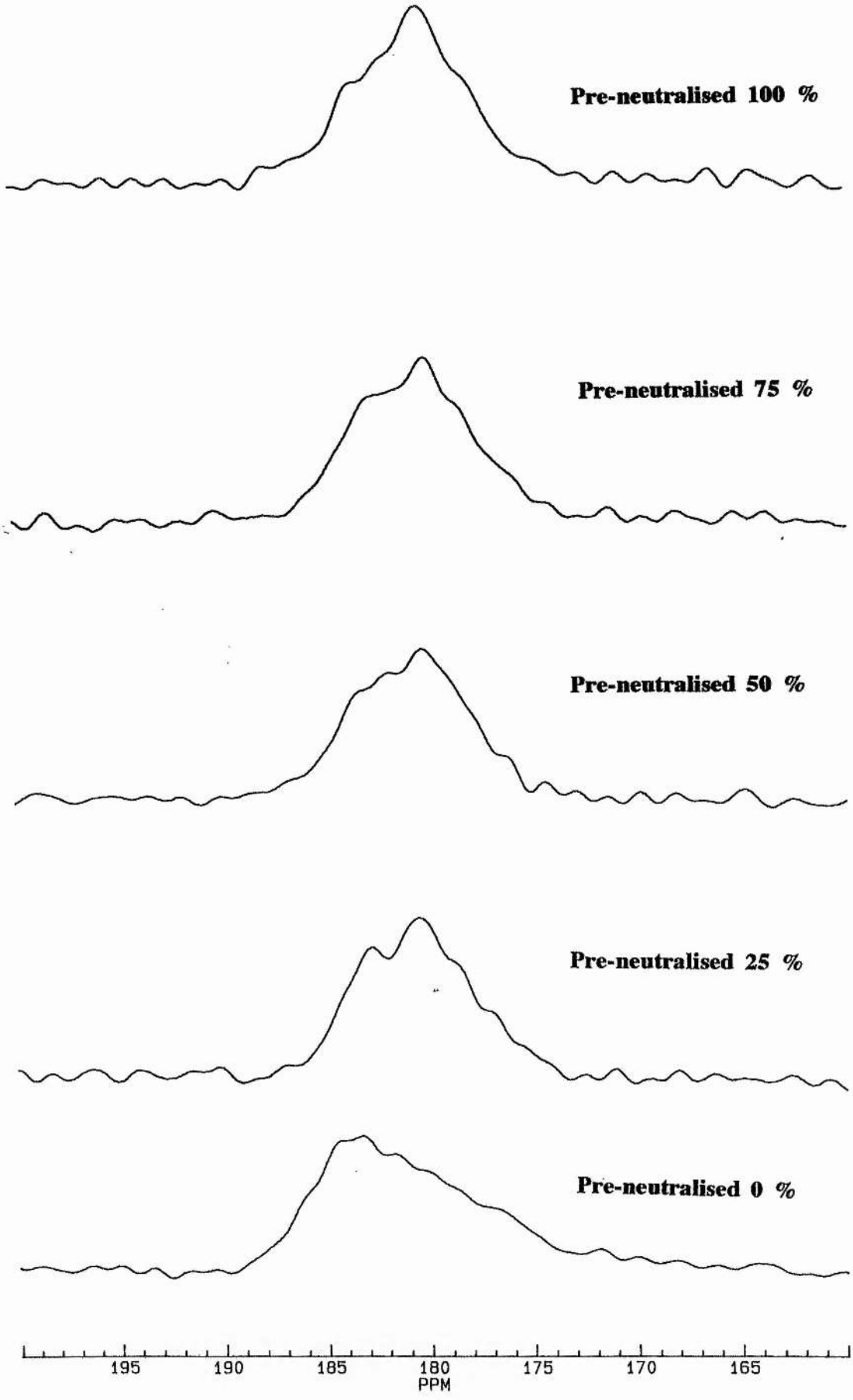

Figure 6.4. Carbonyl region of ASAP 2300 washed with HCl.

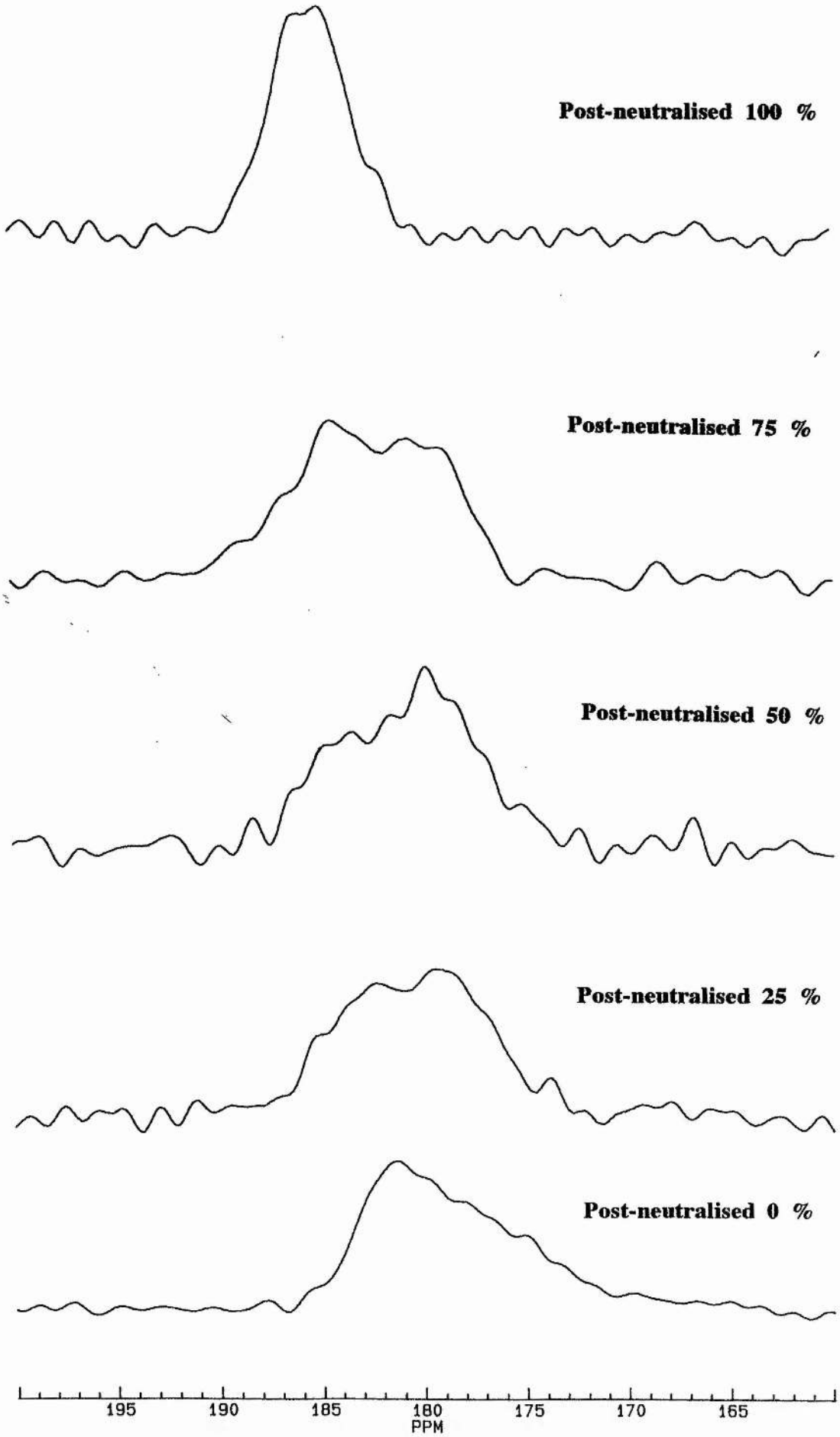

Figure 6.5. Carbonyl region of dry DMRD1 with increasing neutralisation.

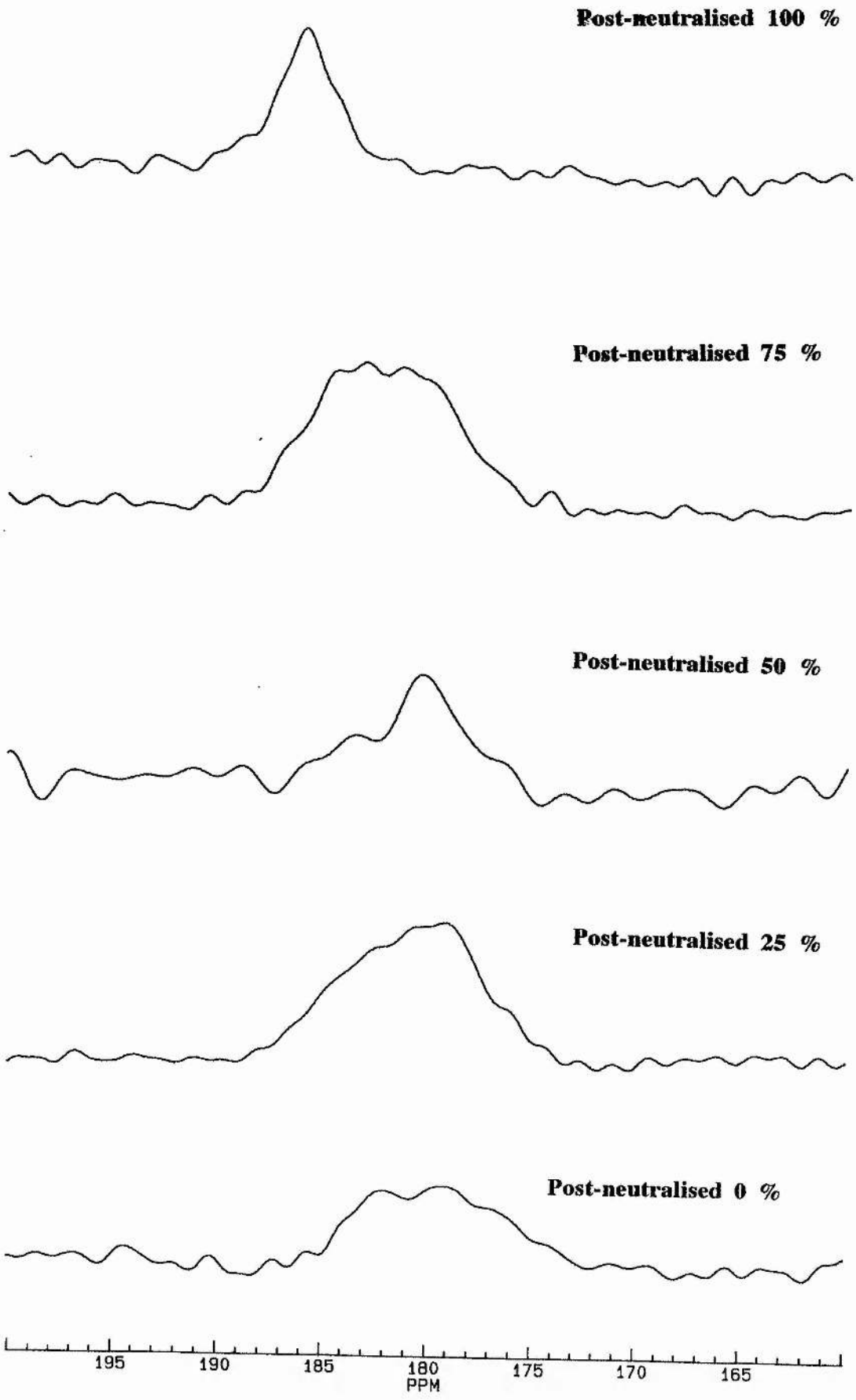

Figure 6.6. Carbonyl region of DMRD1 hydrated and redried.

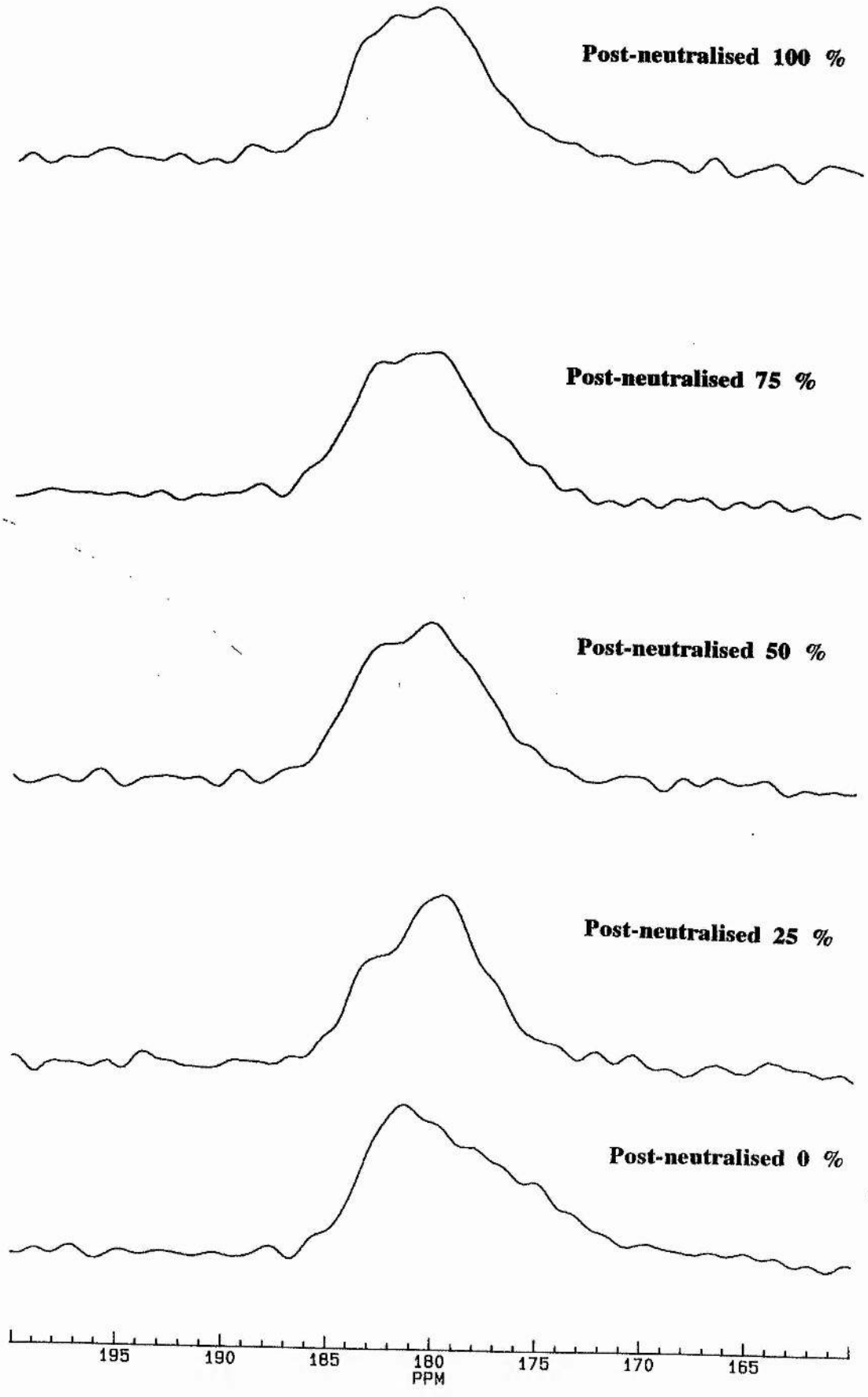

Figure 6.7. Carbonyl region of DMRD1 washed with HCl.

References

1. J. B. Stothers, P. C. Lauterbur; *Canadian Journal of Chemistry*, (1964), **42**, 1563-1576.
2. R. Hagen, J. D. Roberts; *J. Am. Chem. Soc.*, (1969), **91**, 4504-4606.

Chapter Seven

Hydrogels of Superabsorbent Polymers

Hydrogels are three-dimensionally crosslinked hydrophilic polymers which are capable of swelling in water or solvents and retaining large amounts of liquid in the swollen state.[1] Hydrogels can be regarded as a three-dimensional membrane which is readily permeable to solvents but cannot swell indefinitely because of the crosslinks.[2] Limited swelling is caused by the osmotic pressure due to counter-ions in the bulk of the gel. Hydrogels are mainly used as material for optical elements such as contact lenses. Highly swollen hydrogels only differ slightly from water in their optical characteristics, as with a large degree of swelling the concentration of the polymer becomes very low. This means that the highly swollen gel has a high refractive index and a low absorption in the visible spectral range.[2] There are many other useful applications of hydrogels due to their high sensitivity to small changes in environmental conditions allowing them to be used as "intelligent materials". This property makes them useful material for semiconductor components and stabilisers for optically active media in high capacity tuneable dye lasers.[2]

NMR studies on hydrogels have been limited to date. Most NMR investigations on crosslinked polymers are done using dry polymer which results in broad lines due to the crosslinking reducing the mobility of the polymer leading to longer correlation times and shorter relaxation times. High resolution ^{1}H NMR has been found to be of little use for the characterisation of crosslinked hydrogels due to the overlapping of very broad peaks.[3] Initial ^{13}C NMR studies of crosslinked polymers were not performed on hydrogels, but on hydrophobic gels swollen with non polar solvents. These studies demonstrated that the linewidths may be dramatically reduced by swelling the crosslinked polymer in an appropriate solvent.[3,4] This is caused by the increased segmental chain motions within the gel becoming significant enough to eliminate much of the dipolar interaction.[5] Schafer was the first to demonstrate that ^{1}H NMR spectra provided no usable information on poly(vinyl chloride) hydrogels

due to spectral line broadening arising from strong dipolar coupling.[3] ^{13}C NMR spectra, on the other hand were resolved enough to reveal details about the polymer microstructure including tacticity. Many different crosslinked polymer networks have been investigated in this way including poly(methylmethacrylate), poly(2-hydroxyethylmethacrylate) and poly(N-vinylpyrrolidone). It was also shown by several researchers that swelling polystyrene networks in chloroform greatly improved the resolution in the ^{13}C NMR spectra.[3]

Nefal *et al.* used high resolution ^{13}C NMR to study crosslinked poly(sodium acrylate) networks swollen with water.[3] This application was concerned with the dependence of the linewidths on the degree of crosslinking and attributed the dependence to unresolved chemical shift structure due to multiplicity of chemical environments introduced by crosslinking. Looking at superabsorbent polymers in their swollen state allows them to be investigated in the same physical state into which they turn after absorbing particular fluids. From further studies on solid crosslinked polyacrylates as hydrogels it was found that if the degree of crosslinking was low enough, highly swollen samples provided well resolved ^{13}C spectra that could be used to determine tacticity.[3]

Discussion

The aim of this investigation was to look at hydrogels of superabsorbent polymers by solid state ^{13}C NMR to observe any structural differences between the dry and swollen polymer. ASAP 2300 was used entirely in this investigation, swollen to various degrees using distilled water. Superabsorbent polymers used in the personal care industry have very low levels of crosslinker so it was hoped the ^{13}C NMR spectra of the hydrogels would be sufficiently well resolved to provide structural details unable to be seen in the spectrum of dry polymer. Samples of ASAP 2300 with various degrees of neutralisation were also investigated in the swollen state to

observe the effects of neutralisation on swelling.

Fourteen different hydrogels were made from commercial ASAP 2300 (75 % neutralised) with amounts of water ranging from 0.25 g to 50 g. The chemical shifts of all peaks present within the ^{13}C NMR spectra were noted (see table 7.1.).

Amount of water in hydrogel (g)	Chemical Shift of CO group ppm	Chemical Shift of CH group	Chemical Shift of CH_2 (RHS) ppm	Chemical Shift of CH_2 (LHS) ppm
0.25	185.022	45.853	38.809	
0.50	184.279	45.567	38.000	
0.75	184.413	45.381	37.039	
1.00	184.328	45.606	36.872	
1.50	184.234	45.518	36.822	
2.00	184.123	45.601	36.908	38.133
3.50	184.132	45.609	36.934	38.077
5.00	184.156	45.590	36.875	38.099
7.50	184.151	45.591	36.847	38.076
10.00	184.141	45.621	37.049	38.160
20.00	183.965	45.558	36.870	38.000
30.00	184.108	45.517	37.013	38.344
40.00	184.205	45.438	36.849	38.000
50.00	184.163	45.593	37.007	38.200

Table 7.1. Chemical Shifts of carbon atoms found in spectra of hydrogels.

The NMR investigation of hydrogels began using CPMAS, the pulse sequence that had been used with the dry polymer. After looking at the first sample of polymer (1 g

in 0.25 g water) it was no longer possible to use CPMAS for further samples as no signal was observed. It was believed this was due to the chains of polymer being too mobile in the gel state, so a single pulse high power decoupling sequence was used instead. The high chain mobility is also evident from the lack of side-bands in the high power decoupled spectra. For the samples of hydrogel with degrees of hydration less than 100 % (1 g polymer in 1 g water), similar spectra to those of the dry superabsorbent polymer are seen. A carbonyl peak is seen at approximately 184 ppm and an aliphatic peak around 40 ppm. This time however, the aliphatic peak is split into two parts corresponding to the CH and CH_2 groups. The part found at approximately 45 ppm is found to correspond to the CH group and the part at approximately 38 ppm, the CH_2 group. Although more structural details can be observed from these spectra the peaks are still broad. The chemical shift difference between these two aliphatic peaks becomes larger the more hydrated the polymer gets (see figure 7.1).

In the spectrum of ASAP 2300 100 % hydrated, major differences are observed from the above reported spectra. Again a carbonyl peak is observed at approximately 184 ppm, whereas this time the aliphatic peak has split into two distinct peaks which are found at 45.606 and 36.872 ppm and correspond to the CH and CH_2 groups, respectively. When the polymer is further hydrated to 150 % a small peak is seen on the left of the CH_2 peak. From this we can tell that further structural details are able to be observed the more hydrated the polymer becomes. Further narrowing of the peaks is also observed with the carbonyl peak again being found at approximately 184 ppm. A slight change in the chemical shift of both the CH and CH_2 peaks is seen.

Further structural details are observed in the spectrum of ASAP 2300, 200% hydrated. This time the CH_2 peak has further split into two parts, the left hand side (LHS) part appearing at 38.133 ppm and the right hand side (RHS) part appearing at 36.908 ppm. The two parts are found to be unequal in intensity, the RHS part being

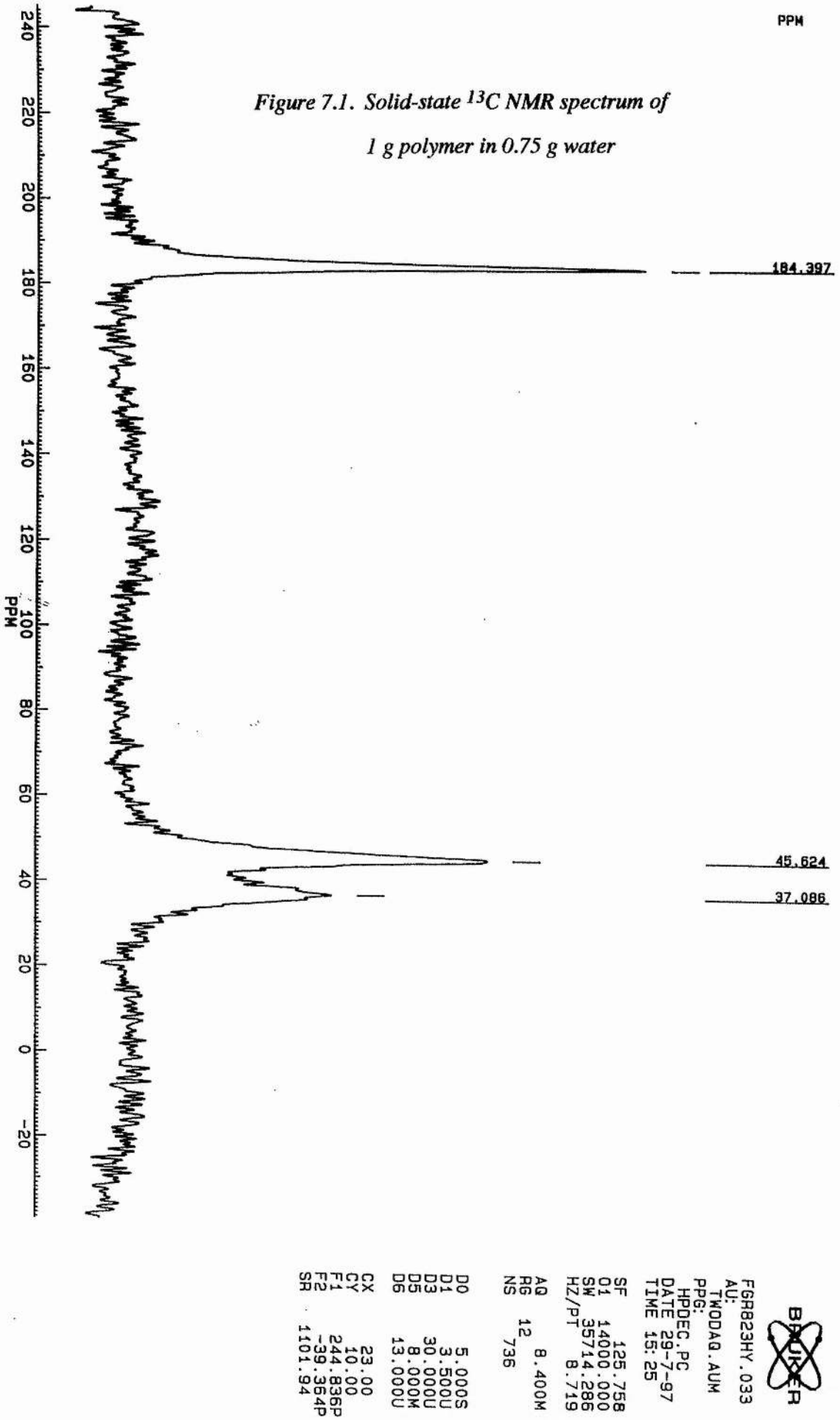

Figure 7.1. Solid-state ^{13}C NMR spectrum of 1 g polymer in 0.75 g water

higher in intensity than the left. The CH peak has experienced a slight shift to the left, however the carbonyl peak is still present at 184 ppm. A very slight narrowing of the peaks is observed with further hydration. For further hydrogels with degrees of hydration 350 % and 500 % no further differences are seen although the CH and CH_2 peaks experience slight shifts in their chemical shifts. When the polymer is hydrated to 750 % the intensities of the two CH_2 peaks almost become equal, but with further hydration the intensities again become unequal with the RHS peak being higher in intensity than the LHS peak (see figure 7.2). With further hydration no real differences are seen. The signal to noise ratio decreases with increasing hydration although it is still good enough to observe structural features within the spectra. The chemical shift of each peak was noted for each degree of hydration and graphs drawn of amount of water in hydrogel versus chemical shift (see figures 7.3., 7.4., 7.5. and 7.6.).

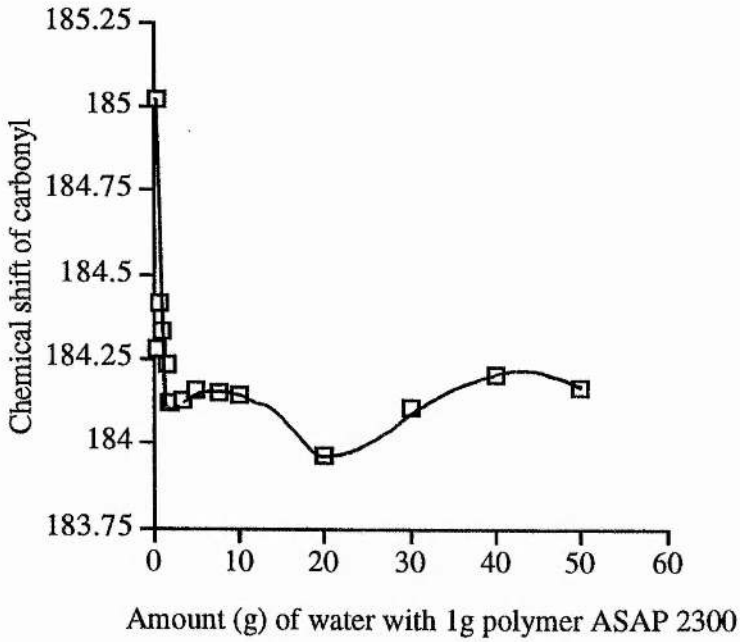

Figure 7.3. Chemical shift of carbonyl group with varying degrees of hydration.

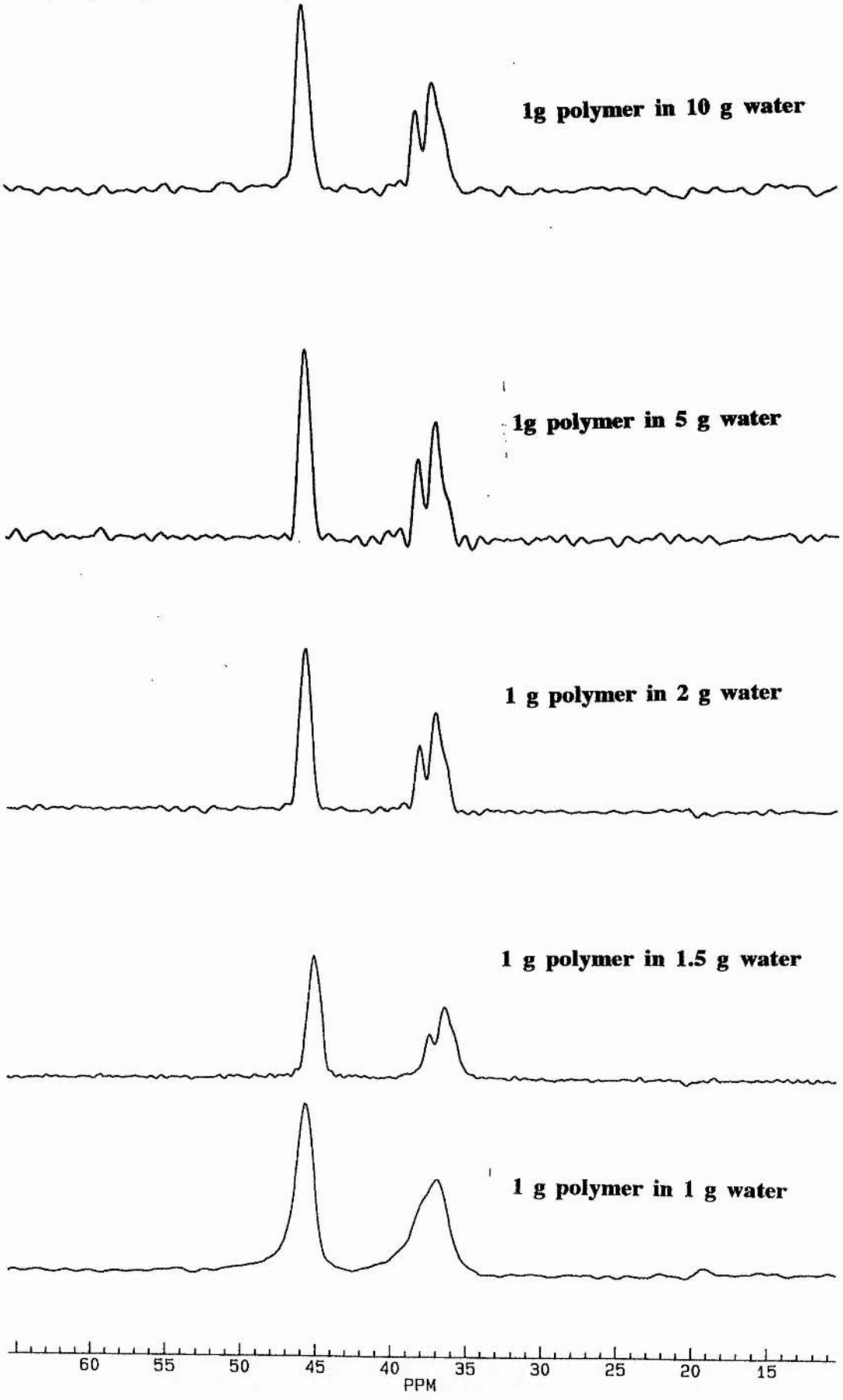

Figure 7.2. Aliphatic region of solid-state ^{13}C NMR spectra of hydrogels.

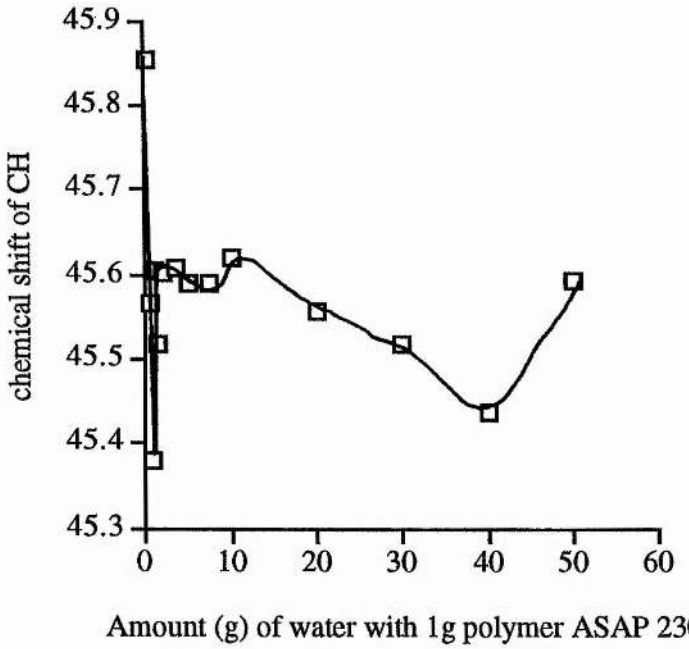

Figure 7.4. Chemical shift of CH group with varying degrees of hydration.

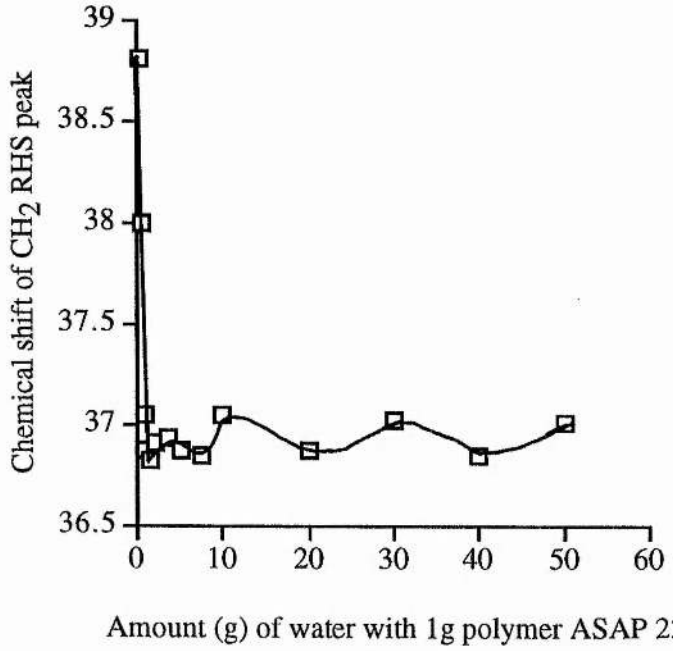

Figure 7.5. Chemical shift of RHS CH_2 group with varying degrees of hydration.

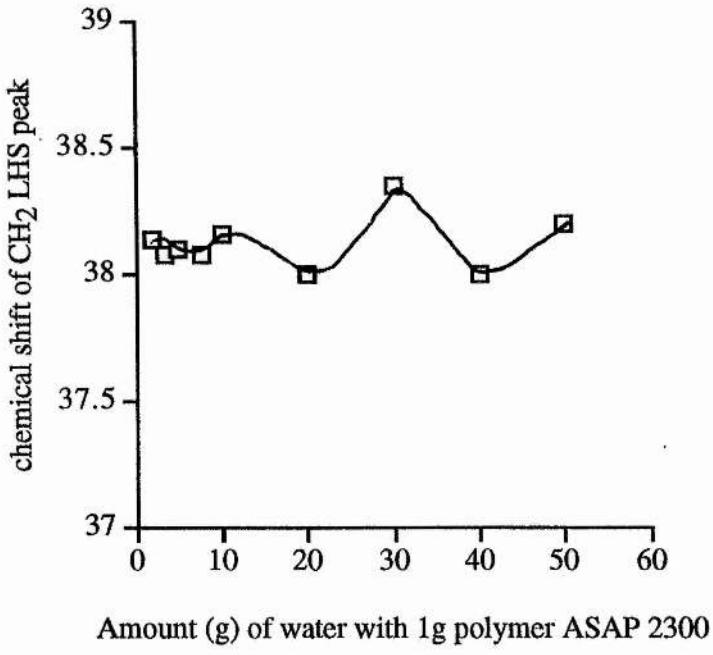

Figure 7.6. Chemical Shift of LHS CH_2 group with varying degrees of hydration.

To ensure the structural details observed in these spectra were not artefacts an off-resonance decoupling experiment was carried out. ^{13}C NMR spectra carried out with decoupler frequencies off-resonance were still seen to contain the same structural details, indicating that they are not artifacts.

The major chemical shift differences occur in the initial 0 % to 200 % water region beyond which there is virtually no change. This indicates that the major structural changes in the polymer on hydration occur within this region.

Hydrogel of ASAP 2300 at various degrees of neutralisation

Samples of ASAP 2300 with varying degrees of neutralisation were also investigated using solid state ^{13}C NMR, in the swollen state. This time the partially neutralised

samples were all swollen to just one degree of hydration so that the effects of neutralisation on swelling could be observed. The samples with 0, 25, 50, 75 and 100 % neutralisation were all swollen to 200 % hydration (1 g polymer in 2 g water).

Looking at the spectrum of the 200 % hydrogel that is un-neutralised 3 sharp peaks are seen. The carbonyl peak is found at 180 ppm and the CH and CH_2 peaks are found at 42.557 and 35.276 ppm, respectively. The spectrum of the hydrogel 200 % neutralised to 25 % is almost similar to that of 0 % neutralisation. A slight shift high frequency is seen for all three peaks where the carbonyl peak is now found at 181.217 ppm. This is consistent with the shift seen for the carbonyl peak in the work done on neutralisation domains. Small splitting in the CH_2 peak is observed for the 50 % neutralised hydrogel with a carbonyl shift to 182.517 ppm, again consistent with the carbonyl shift seen when investigating domains within the polymer. When we look at the 75 % neutralised hydrogel, differences begin to appear in the spectrum. This time the CH_2 peak has split into two parts with the LHS part being lower in intensity than the RHS part. A high frequency shift is seen for all peaks within the spectrum. The hydrogel that is 100 % neutralised has almost the same spectrum as that of 75 % neutralised where the intensities of the two parts of the CH_2 peak have become closer to each other (see figure 7.7). The chemical shifts of each peak were noted (see table 7.2.) and graphs drawn for each peak (see figures 7.8, 7.9, 7.10 and 7.11).

A high resolution ^{13}C NMR spectrum was also obtained of a hydrogel of ASAP 2300 (70% neutralised) swollen in D_2O to 8000 %. This spectrum also shows three sharp peaks which correspond to the carbonyl, CH and CH_2 groups. The peak corresponding to the CH_2 group is split into two parts showing structural detail (see figure 7.12).

The structural detail seen within the spectra of the CH_2 groups of superabsorbent polymer hydrogels is believed to be attributed to the different tacticities of the

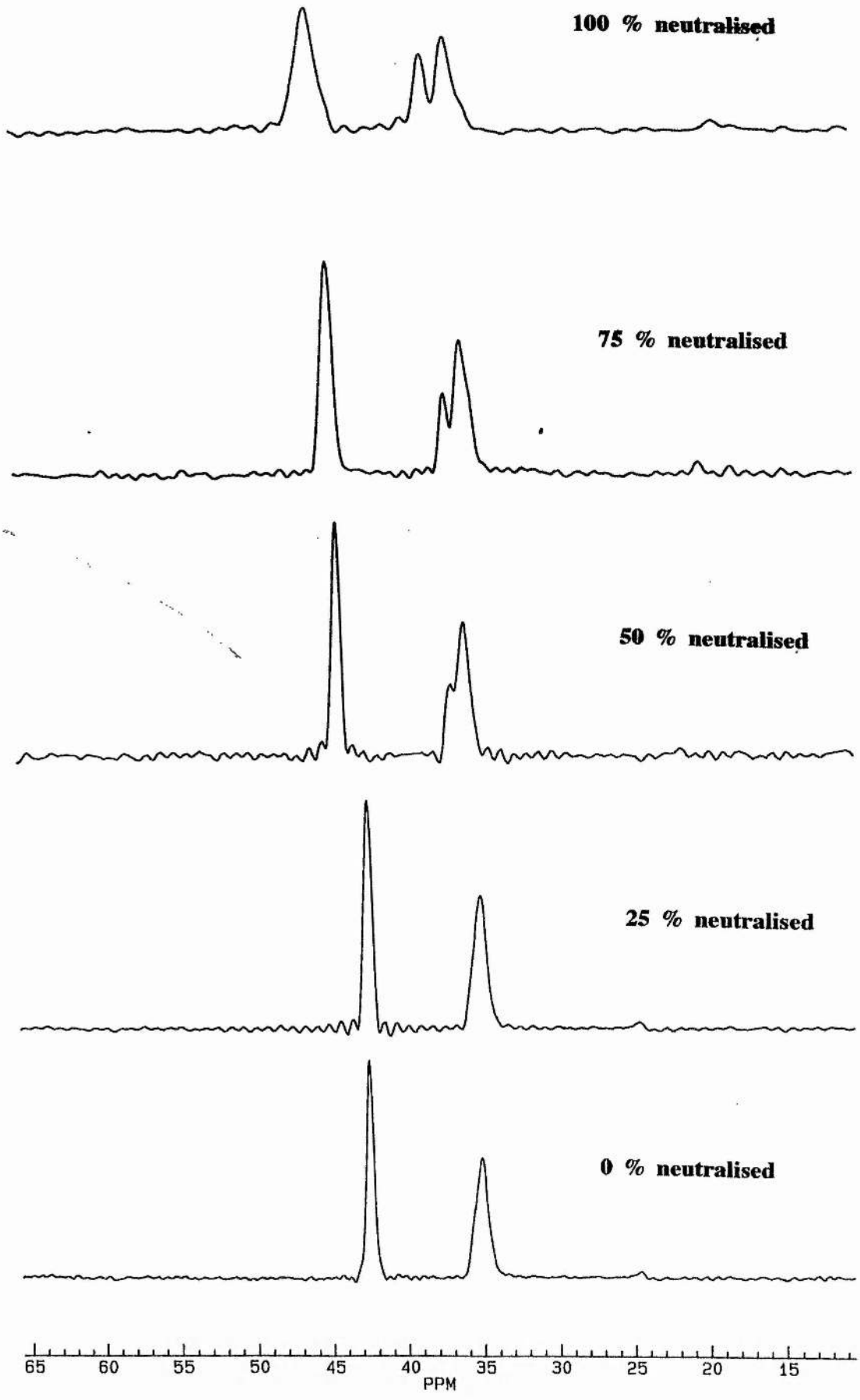

Figure 7.7. Aliphatic region of hydrogels with increasing neutralisation.

polymer. See introduction page 40.

Degree of Neutralisation %	Chemical Shift of CO group ppm	Chemical Shift of CH group ppm	Chemical Shift of CH_2 (RHS) ppm	Chemical shift of CH_2 (LHS) ppm
0	179.704	42.2557	35.276	
25	181.217	43.523	35.697	
50	182.517	44.492	36.176	
75	183.628	45.034	36.303	36.303
100	184.917	46.082	37.033	38.548

Table 7.2. Chemical Shifts of carbon atoms of ASAP 2300 200 % hydrated as a function of the degree of neutralisation.

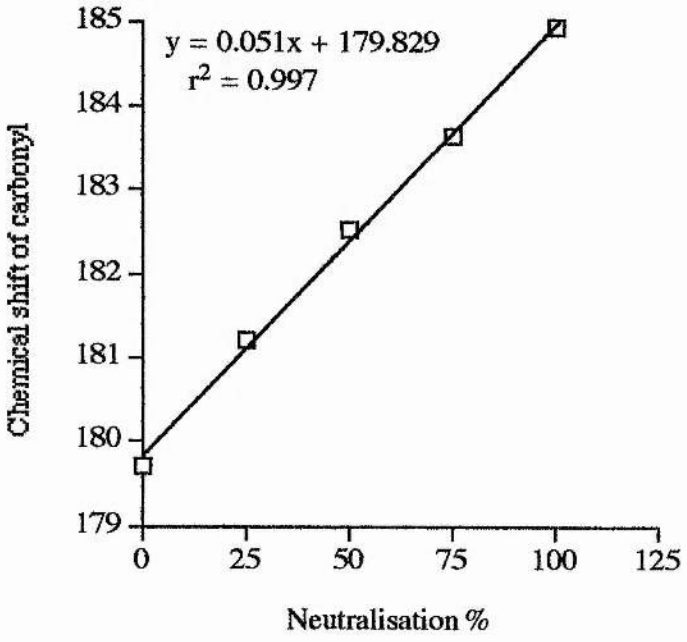

Figure 7.8. Chemical shifts of carbonyl group with increasing neutralisation .

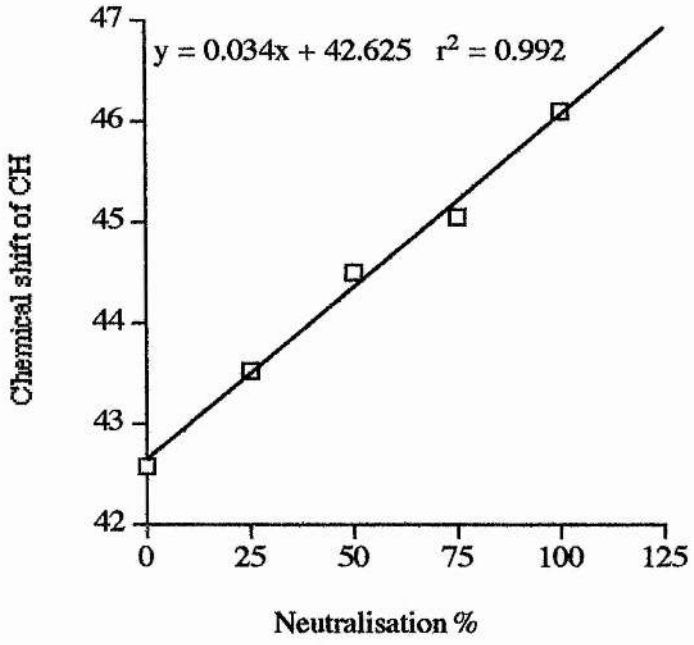

Figure 7.9. Chemical shift of CH group with increasing neutralisation.

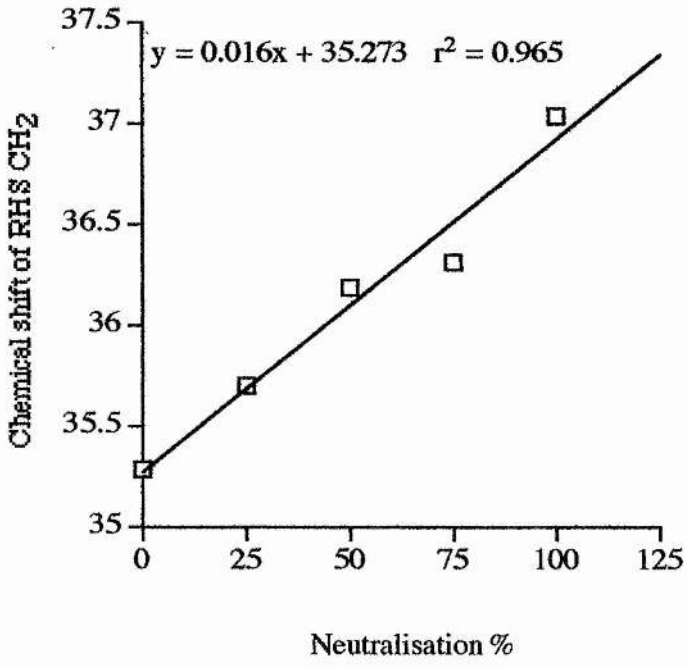

Figure 7.10. Chemical shifts of RHS CH_2 group with increasing neutralisation.

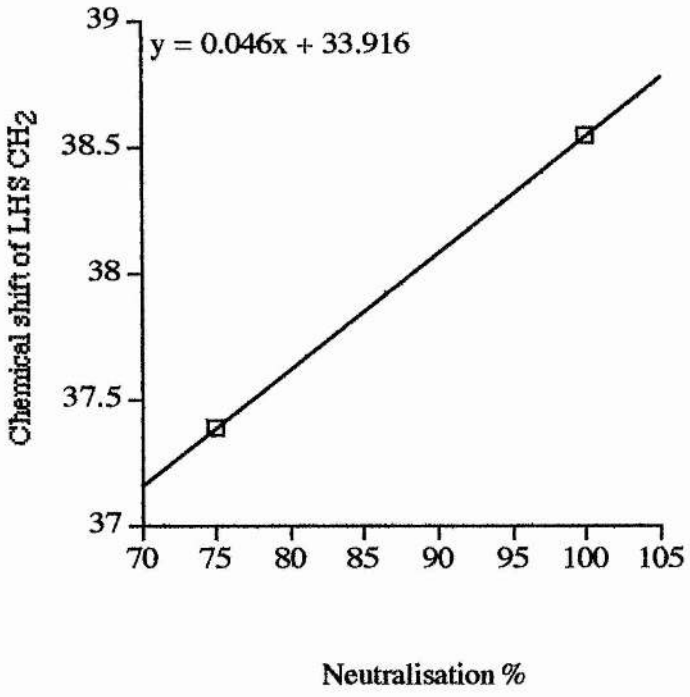

Figure 7.11. Chemical shifts of LHS CH_2 group with increasing neutralisation.

The microstructure of a solution of a highly swollen linear poly(sodium acrylate) in D_2O has been investigated using ^{13}C NMR.[6] From the NMR spectrum it can be seen that the carbonyl region is insensitive to tacticity whereas the methine and methylene resonances tend to split according to odd (triad or even pentad) and even (hexad) monomer sequence lengths respectively.[6] This is the case for other homopolymers such as polyacrylamide.[7] The splitting for the methine region was described in terms of triad resolution by Trong *et al.*[8] where the description of Lancaster and O'Connor was adopted. This description stated that at triad level the lowest and highest field peaks correspond to the syndiotactic (mm) and isotatic (rr) sequences respectively.[6] In the spectrum of highly swollen linear poly(sodium acrylate) the highest field methine peak is attributed to an isotatic sequence and the central two methine peaks which overlap, to heterotactic sequences. The methylene resonance presented a complex envelope and analysis was not attempted. A ^{13}C NMR tacticity study was

also carried out using highly swollen poly(acrylic acid) where the resonance peaks of the three carbons appear at lower field than for the neutralised polymer and are less split.[8,9] The splitting increases in the order carbonyl, methine and methylene. The ^{13}C NMR spectrum of poly(vinylchloride) in chlorobenzene was obtained by Schaefer and was well resolved enough to reveal details of the microstructure of the polymer chain.[5,10] The methine carbon resonance appears at low field and is split into three lines attributed to iso-, hetero- and syndiotatic triads. The three lines are in the intensity ratio 1:2:1 which is consistent with the approximate random steric configuration of poly(vinylchloride). The methylene carbon resonance appears at a higher field and is split into two equal intensity lines, attributed to iso- and syndiotatic dyads. The solid-state ^{13}C NMR of poly(vinylchloride) has also been measured and shows subtleties that can be encountered in the solid state.[11] The solid-state spectrum suggest a similar interpretation for the three methine lines although the shifts are much larger and the resolutions different. This is due to the intra- and intermolecular hydrogen bonding discriminating between the different triads, amplifying the shifts and changing the relative intensities. The methine carbons at the centre of a mm triad can form two intermolecular hydrogen bonds, although not all do because of other constraints in the crystalline solid and the possibility of intermolecular hydrogen bonds. The intensity of the mm signal in solution is distributed amongst three peaks in the solid-state spectrum.

The microstructure of many other polymers has been determined using ^{13}C NMR. These include polymers such as polypropylene poly(vinylfluoride) and poly(methylmethacrylate).[10]

No previous reports of a tacticity study on crosslinked poly(sodium acrylate) have been found. From the spectra obtained from hydrogels of superabsorbent polymers it can be seen that structural detail appears at the methylene carbon resonance after the polymer has been hydrated to 150 %. There is no structural detail seen at the carbonyl

resonance which is typical for a homopolymer. In the earlier tacticity studies of linear poly(sodium acrylate) structural detail is seen at the methine carbon resonance, however, this is not seen in the spectra of swollen superabsorbent polymers. The lack of detail may be attributed to the crosslinking within the polymer causing the peaks to overlap. The exact tacticity of the superabsorbent polymer cannot be determined due to a lack of structural detail within the methine carbon resonance. However, it may be possible from earlier tacticity studies to assign the peaks of the methylene carbon resonances to iso- and syndiotactic dyads. It is also evident from looking at the spectra of swollen superabsorbent polymers with varying degrees of neutralisation, that structural detail is also only observed after the polymer has been neutralised to 75 %.

Figure 7.12. High resolution spectrum of hydrogel of ASAP 2300.

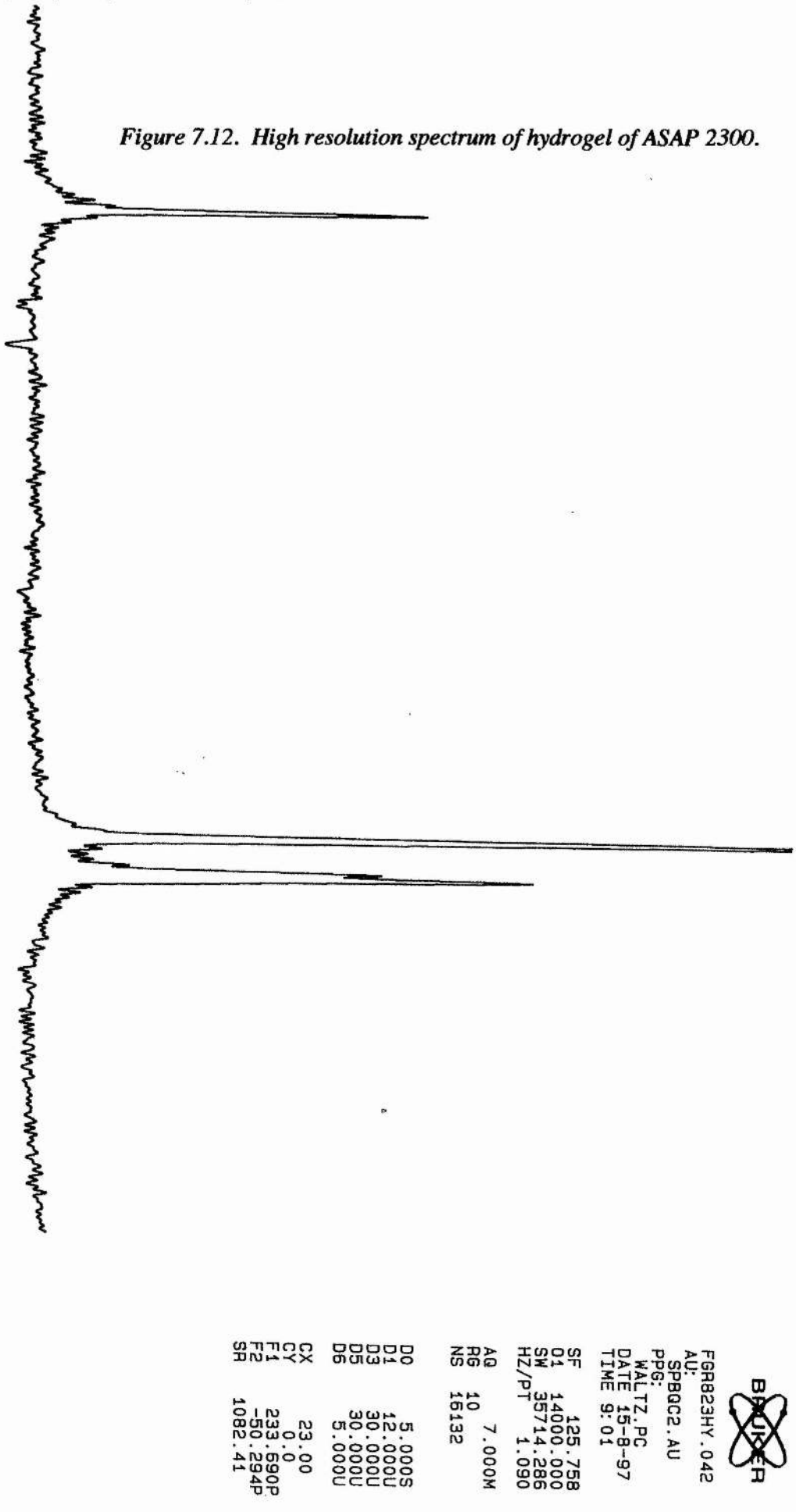

References

1. K. S. Kazanskii, S. A. Dubrovskii; *Advances in Polymer Science*, (1992), **104**, 97-133.
2. T. V. Budtova, I. E. Suleimenov, S. Ya Frenkel; *Russian Journal of Applied Chemistry*, (1997), **70**, 507-516.
3. A. M. Mathur, A. B. Scranton; *Biomaterials*, (1996), **17**, 547-557.
4. A. D. Bain, D. R. Eaton, A. E. Hamielec, M. Mlekuz, B. G. Sayer; *Macromolecules*, (1989), **22**, 3561-3564.
5. J. Schaefer; *Macromolecules*, (1971), **4**, 110-112.
6. A. Neppal, D. R. Eaton, D. Hunkeler, A. E. Hamielec; *Polymer*, (1988), **29**, 1383-1343.
7. N. D. Truong, J. C. Galin, J. Francois, Q. T. Pham; *Polymer*, (1986), **27**, 467-475.
8. N. D. Truong, J. C. Galin, J. Francois, Q. T. Pham; *Polymer*, (1986), **27**, 459-466.
9. J. Schaefer; *Macromolecules*, (1971), **4**, 98-104.
10. A. E. Tonelli, F. C. Schilling; *Acc. Chem. Res.*, (1981), **14**, 233-238.
11. V. J. McBrierty, K. J. Packer; Nuclear Magnetic Resonance in Solid Polymers; Cambridge University Press: Cambridge, UK, 1993, Chapter 5.

Chapter Eight

Sodium Relaxation of Superabsorbent Polymers

Sodium is a quadrupolar nucleus with spin $I=\frac{3}{2}$ which as a result of having an asymmetric spherical charge distribution, possesses an electric quadrupole moment. This quadrupole moment couples with an electric field gradient (efg) experienced by the nucleus giving rise to quadrupolar relaxation.[1,2,3] Spin $I=\frac{3}{2}$ gives rise to four (2I+1) energy levels which can be characterised by the magnetic quantum numbers $m_I = -\frac{3}{2}, -\frac{1}{2}, +\frac{1}{2}$ and $+\frac{3}{2}$. The transitions between the energy states are degenerate in the absence of an electric field gradient at the nucleus. The degeneracy is lifted by the quadrupolar interaction (see figure 8.1).

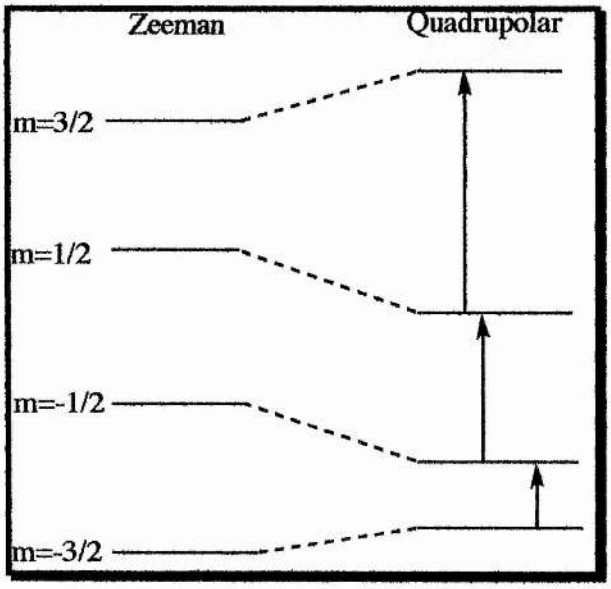

Figure 8.1. Schematic diagram of the energy states for spin 3/2 nucleus in the absence (left) and in the presence (right) of a quadrupolar interaction.

Usually the quadrupolar interaction is stronger than other interactions such as chemical shift and dipole-dipole couplings and dominates the spectra of quadrupolar nuclei in solid materials.[3,4] Liquid state NMR spectra of free quadrupolar ions are not affected

to a comparable extent as the fast isotropic tumbling of the molecules diminishes the impact of the quadrupolar interaction.[3] It has been demonstrated that in the case where relaxation is dominated by quadrupolar relaxation, the time dependence of the magnetisation cannot, in general, be described by a single exponential for the transverse and longitudinal magnetisation. Generally the relaxation of spin $I=\frac{3}{2}$ nuclei is biexponential and gives rise to two NMR lines having different widths and slightly different absorption frequencies.[5]

In polyelectrolyte solutions such as poly(acrylic acid) the quadrupolar relaxation of sodium is completely dominated by the interaction of its quadrupole moment with the electric field gradients brought about by the polymer.[5] It has been demonstrated that there is a significant increase in the biexponential character of the relaxation when the solution is diluted. The ^{23}Na longitudinal relaxation rates for aqueous solutions of poly(acrylic acid) at various degrees of neutralisation have been studied.[1,6]

The chemical shift of resonance of ^{23}Na is caused by perturbations of the electrons of the Na atoms and is expected to be sensitive to the immediate environment only. The sodium resonance of $^{23}Na^+$ in aqueous solutions gives a single symmetrical peak which can be as narrow as 10 Hz at half height, in spite of the large quadrupole moment.[5] This resonance is broadened in an asymmetrical environment. Chemical shift changes of ^{23}Na are dominated by changes in the paramagnetic shielding term.[7] The sodium ion is not easily polarised and the chemical shifts are fairly small, typically a few parts per million.[7] It is well known that ^{23}Na chemical shift measurements have an unambiguous meaning and it should be possible to decide which compounds or ions are in contact with the Na^+ ion (sodium ions interacting with carboxylic groups have a negative chemical shift). It has also been shown that the chemical shift of ^{23}Na is solvent dependent which is thought to be contradictory as Na^+ has no unpaired electrons in its p-orbitals and therefore should have a vanishing contribution to nuclear shielding. In order to account for the solvent shifts it is

necessary to assume that electrons are donated by the solvent into a 3p orbital of the sodium atom.[2] A high frequency movement of the chemical shift is observed as the solvent becomes a better donor but it has been calculated that only small degrees of electron transfer occur for instance in the interaction of Na^+ with water molecules where only the first water molecule co-ordinated to the Na^+ by its oxygen atoms has a bond that is not purely ionic.[2]

Sodium NMR relaxational studies have been carried out on synthetic amphoteric copolymer hydrogels containing both acidic and basic groups, under a variety of water contents. Alkali metal and halide NMR are sensitive to the immediate chemical environment and the mobility of ions and or water in aqueous solution.[5] This work was pioneered to gain an basis for interpreting the fundamental modes of ionic interactions occurring in polyelectrolyte systems. It was found for a 1:1 sodium methacrylate-co-(*N*,*N*-dimethylamino)ethyl methacrylate hydrogel that as the amount of water is decreased at a constant temperature, the linewidths reached 10 kHz at 2 % water content.[5] Therefore, the linewidths depend on the number of water molecules per sodium ion. Simultaneously the resonance shifts approximately 20 ppm to a lower frequency. From this study it was found that ^{23}Na linewidths and chemical shifts, where the largest changes occurred were in the range of 1-5 water molecules per sodium ion with the chemical shift moving over a range of 20 ppm. There is strong evidence for the formation of contact ion pairs with the polyions in this range due to the chemical shift moving to a lower frequency. The linewidths decrease rapidly with an increasing water content. These results indicate the presence of 5 or 6 water molecules in the first hydration sphere of the sodium ion. In this range the water molecules are expected to participate in the first hydration sphere of the Na^+ ion or interact with the COO^- group. Here the hydrogen bonding between the COO^- group and the water of a hydrated counter-ion plays an important role.

Moving from 6 to 15 water molecules per sodium ion the ^{23}Na linewidths slowly

decrease with the chemical shift moving to a higher frequency. A reasonable explanation for this would be in terms of the hydrogen bonding between the water molecules in Na^+ hydration spheres and the CO_2^- moieties. As the water molecule is filled with the first hydration sphere around Na^+ ions, the formation of contact pairs is broken and the hydrogen bonding becomes important. Although it is difficult to assign a particular molecular motion from the correlation times, a few mechanisms were considered. The rate of exchange of a sodium ion between a free and bound state is correlated to values within a few nanoseconds indicating that the overall motion of the polymer chains is too slow to affect the correlation time which remains constant throughout this range. If the ^{23}Na ion motions mainly depend on atmospheric condensation (loose ion pairs), the bound state is taken to comprise those Na^+ ions that reside a certain distance from the polymer surface where the distance is usually chosen approximately as the diameter of a hydrated Na^+ ion.

From this study is was also shown that decreasing relaxation rates are observed in this range as the water content is increased.[5]

Discussion

Sodium relaxational studies were carried out on dry and swollen superabsorbent polymers to investigate the changes in the sodium environment as the polymer became further hydrated. Spin-lattice relaxation times were measured using a saturation pulse sequence with relaxation delays of between 1 μs and 500 ms as appropriate and a suitable recycling delay. Twenty four samples of DMRD1 (75% neutralised) with hydration levels ranging from 0-10,000 % were investigated (see table 8.1). A single symmetrical peak was present in the spectra for all samples of superabsorbent polymer (see figure 8.2) and the chemical shift was noted for each relative to the peak in a spectrum of solid sodium chloride occurring at 0.00 ppm. For each delay the intensity of the peak was noted and a graph drawn of ln(Ao-At) versus time for each sample

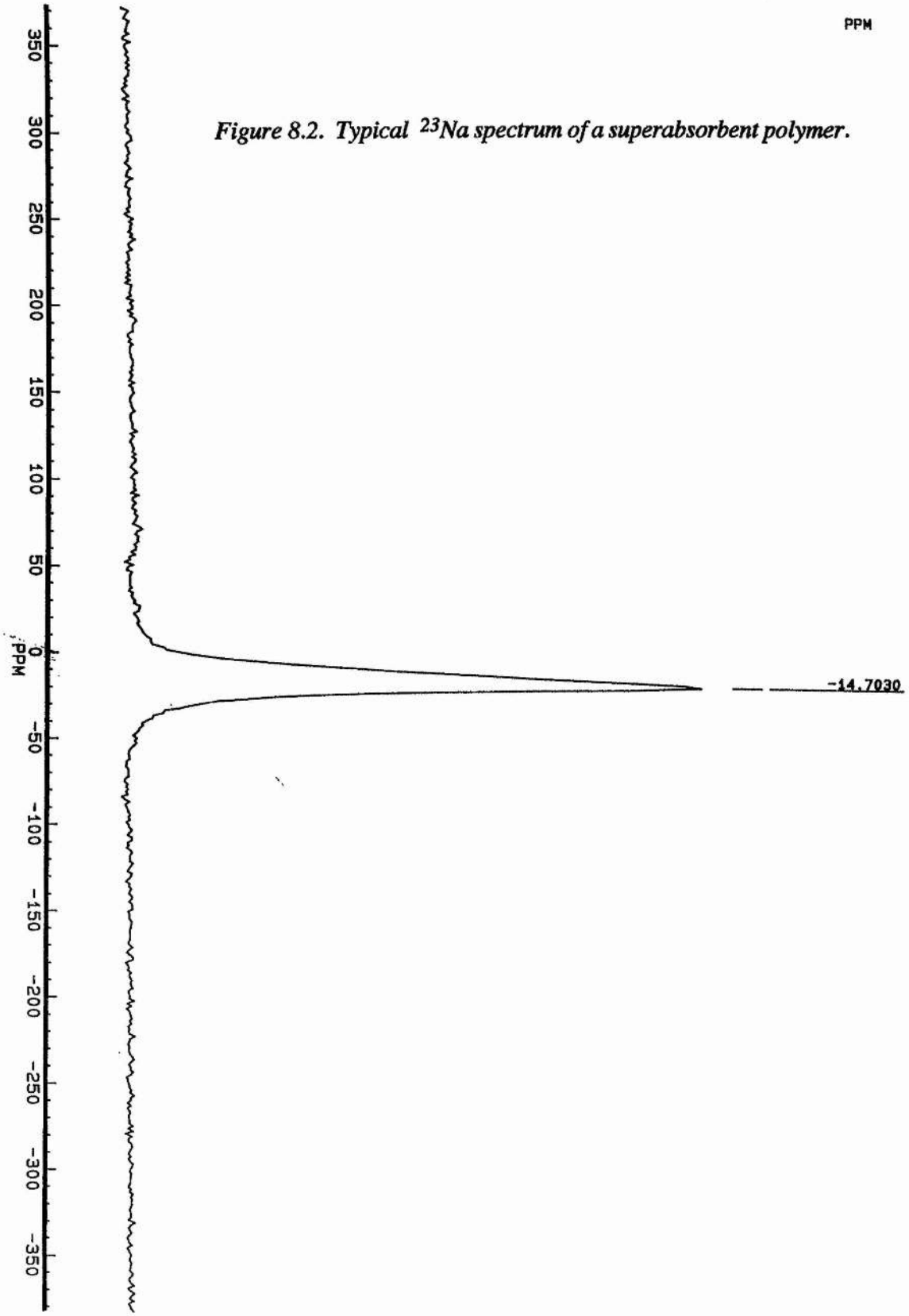

Figure 8.2. Typical ^{23}Na spectrum of a superabsorbent polymer.

(where Ao is the infinity intensity value and At the intensity at time t). The relaxation times are calculated from 1/slope of the graphs. Two T_1 graphs have been added to show a representation of all the samples (see figure 8.3 and 8.4).

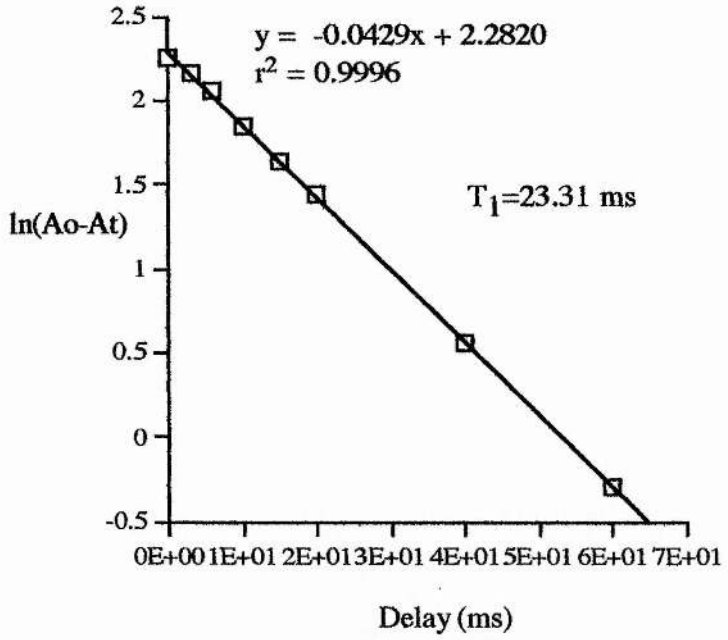

Figure 8.3. ^{23}Na T_1 Relaxation of DMRD1 6000% hydrated.

A further graph was drawn of all the T_1 relaxation times against the percentage hydration to show what happens as the amount of water is increased (see figures 8.5 and 8.6). From the table and the graph it can be seen that between 0 and 25 % hydration there is a decrease in the relaxation time of the Na^+ within the superabsorbent polymer. With further hydration the relaxation time of the sodium ions gradually increases and starts to level off as 10,000 % hydration is reached. The relaxation time minimum is found at 25 % hydration.

% Hydration	T_1 (ms)	Chemical shift (ppm)
0	6.54	-13.66
5	3.55	-12.18
10	2.16	-12.18
25	0.57	-9.23
50	0.65	-6.27
60	1.10	-7.01
75	1.44	-7.01
100	2.42	-7.01
150	7.62	-7.01
200	10.64	-7.19
250	13.33	-7.19
300	14.71	-7.19
400	15.06	-7.19
500	14.86	-7.38
600	17.86	-7.38
1000	21.01	-7.38
2000	22.08	-7.38
3000	19.19	-7.38
4000	20.60	-7.38
5000	20.90	-7.38
6000	23.31	-7.38
7000	23.09	-7.38
8000	23.53	-7.38
10000	24.70	-7.38

Table 8.1. Relaxation times and chemical shifts of superabsorbent polymers.

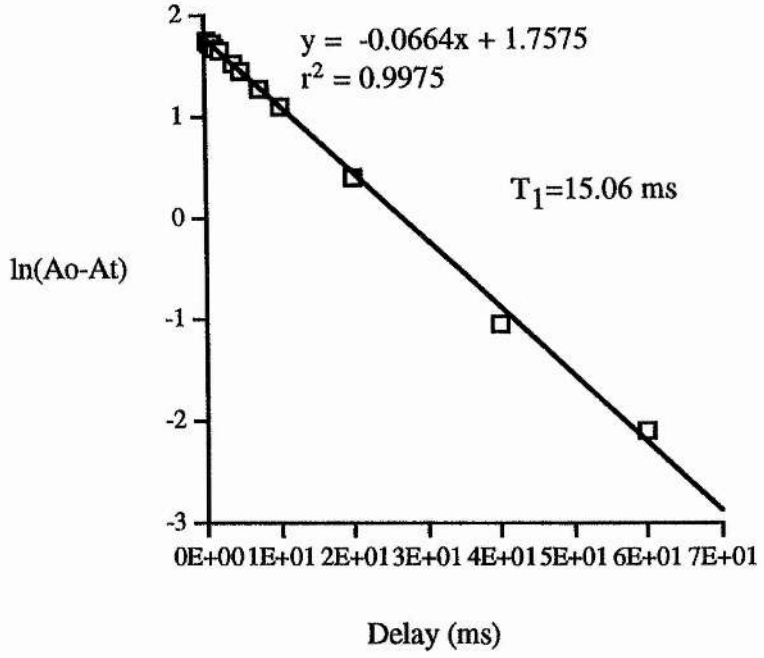

Figure 8.4. ^{23}Na T_1 Relaxation of DMRD1 400% hydrated.

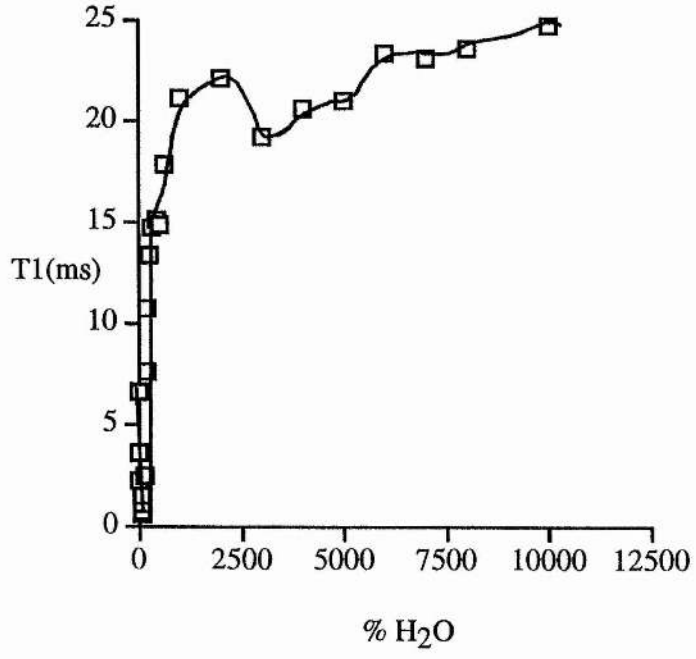

Figure 8.5. ^{23}Na T_1 Relaxation of DMRD1 at various degrees of hydration.

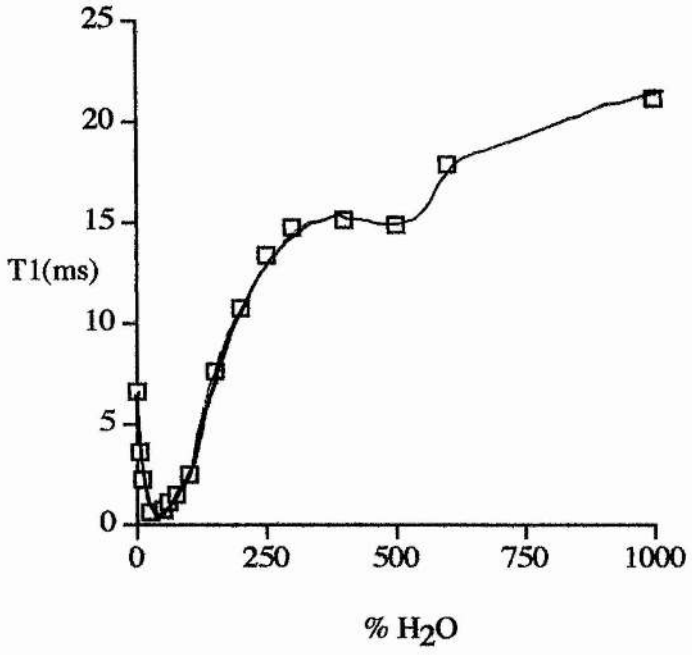

Figure 8.6. Section of ^{23}Na T_1 graph for DMRD1 at various degrees of hydration.

A graph was also drawn of the chemical shift of the Na peak against the percentage hydration for each sample (see figures 8.7 and 8.8).

From the graph and the table it can be seen that between 0 and 50 % hydration the chemical shift of the Na peak moves approximately 7 ppm to higher frequency. With further hydration of the superabsorbent polymer the chemical shift of the peak moves slowly to low frequency approximately 1 ppm. The range in which the biggest change in chemical shift is observed is almost consistent with the range in which the decrease in relaxation time is seen.

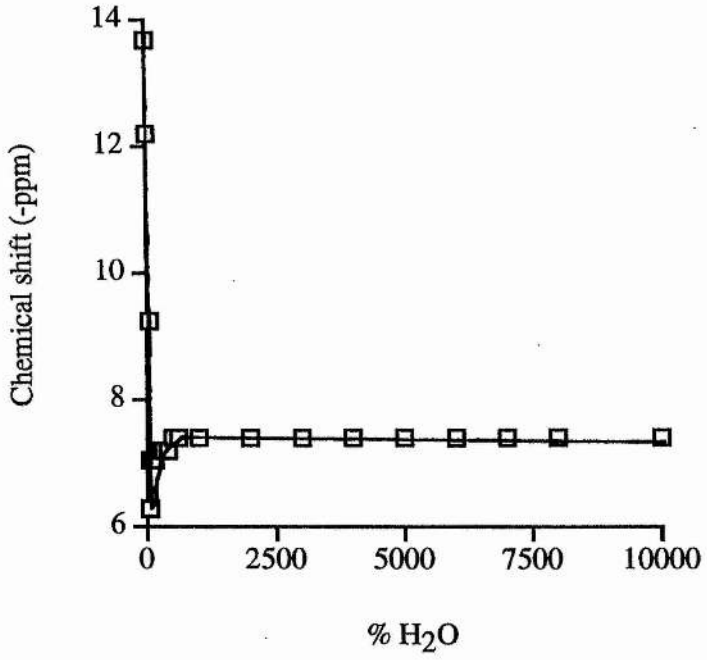

Figure 8.7. Chemical shift versus % hydration for DMRD1.

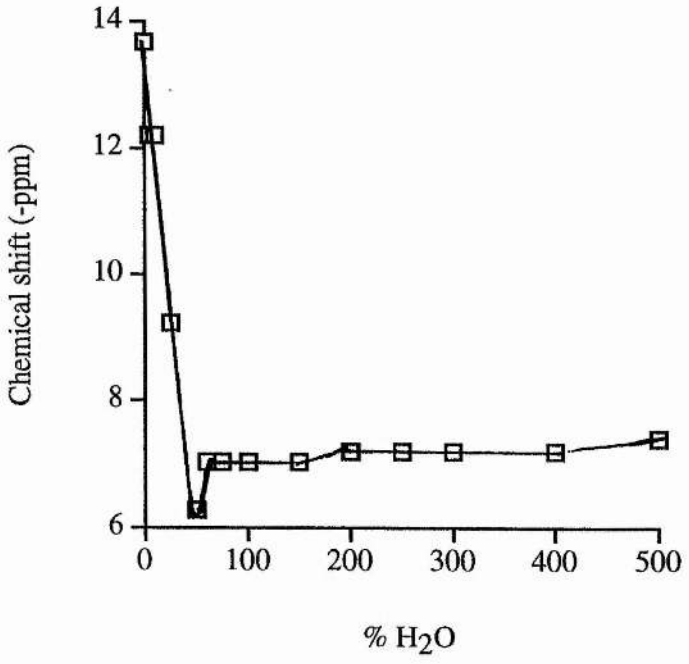

Figure 8.8. Section of graph of chemical shift versus % hydration for DMRD1.

A study was also carried out on dry samples of superabsorbent polymers ASAP 2300 (pre-neutralised) and DMRD1 (post-neutralised) with varying degrees of neutralisation to see what effect this had on the relaxation times of the sodium ion (see table 8.2). Two graphs have been drawn as a representation of all samples investigated (see figure 8.9 and 8.10).

Polymer sample	Degree of Neutralisation %	T_1 Relaxation time (ms)	Chemical shift (ppm)
2300 (Pre-neut)	25	12.14	-15.13
2300 (Pre-neut)	50	4.98	-13.66
2300 (Pre-neut)	75	3.98	-13.29
2300 (Pre-neut)	100	2.47	-12.17
DMRD1 (Post-neut)	25	8.69	-15.87
DMRD1 (Post-neut)	50	7.68	-15.13
DMRD1 (Post-neut)	75	2.45	-13.18
DMRD1 (Post-neut)	100	2.89	-12.17

Table 8.2. ^{23}Na Relaxation times and chemical shifts of dry superabsorbent polymers with varying degrees of neutralisation.

A graph was also plotted of the relaxation time for each degree of neutralisation for both pre- and post-neutralised polymers (see figure 8.11). From the graph and table it can be seen that for both the pre- and post-neutralised superabsorbent polymers the relaxation time decreases as the degree of neutralisation increases. A high frequency shift of the chemical shift is seen for both pre- and post-neutralised superabsorbent polymers indicating a change in the environment of the sodium ions. This was also observed in a study done by Van der Klink et al. where they looked at the ^{23}Na relaxation times and chemical shifts of solutions of poly(acrylic acid) at various degrees of neutralisation.[1]

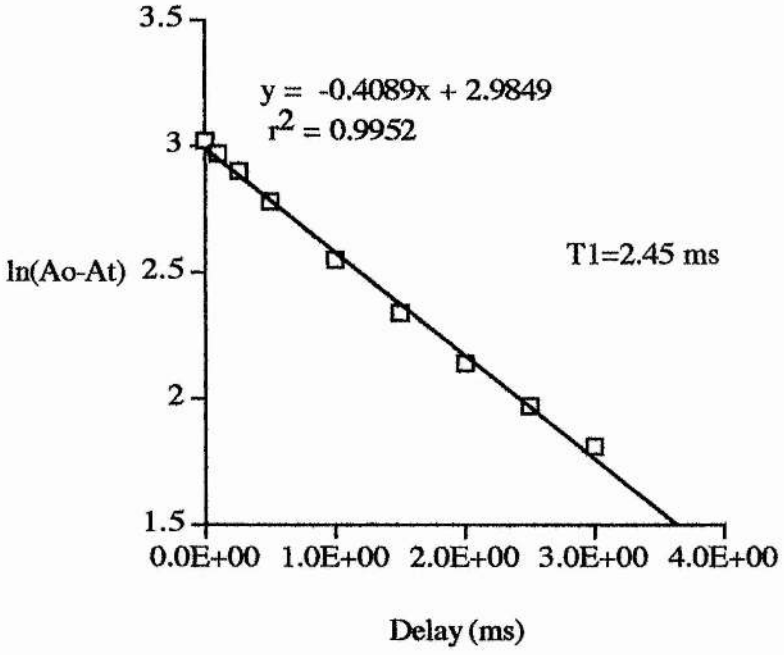

Figure 8.9. ^{23}Na T_1 Relaxation of dry DMRD1 post-neutralised 75 %.

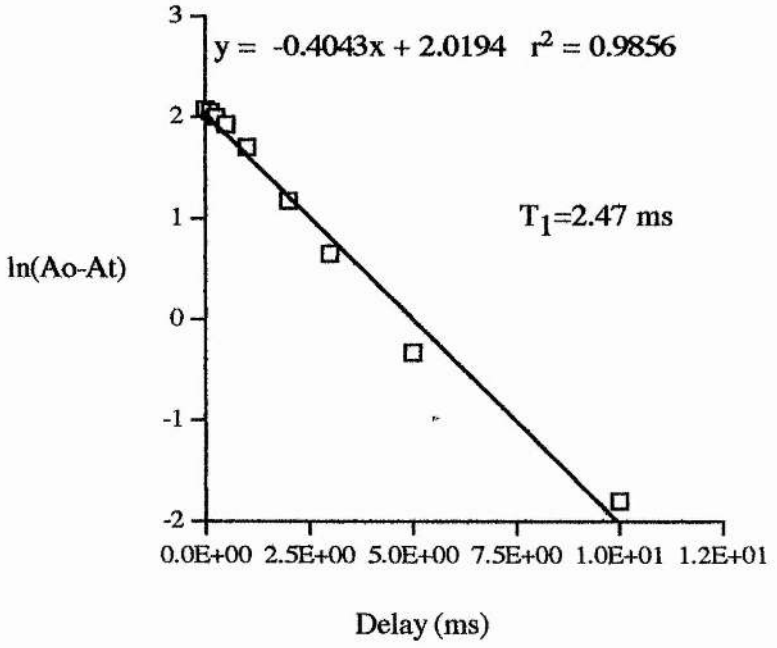

Figure 8.10. ^{23}Na T_1 Relaxation of dry ASAP 2300 pre-neutralised 100 %.

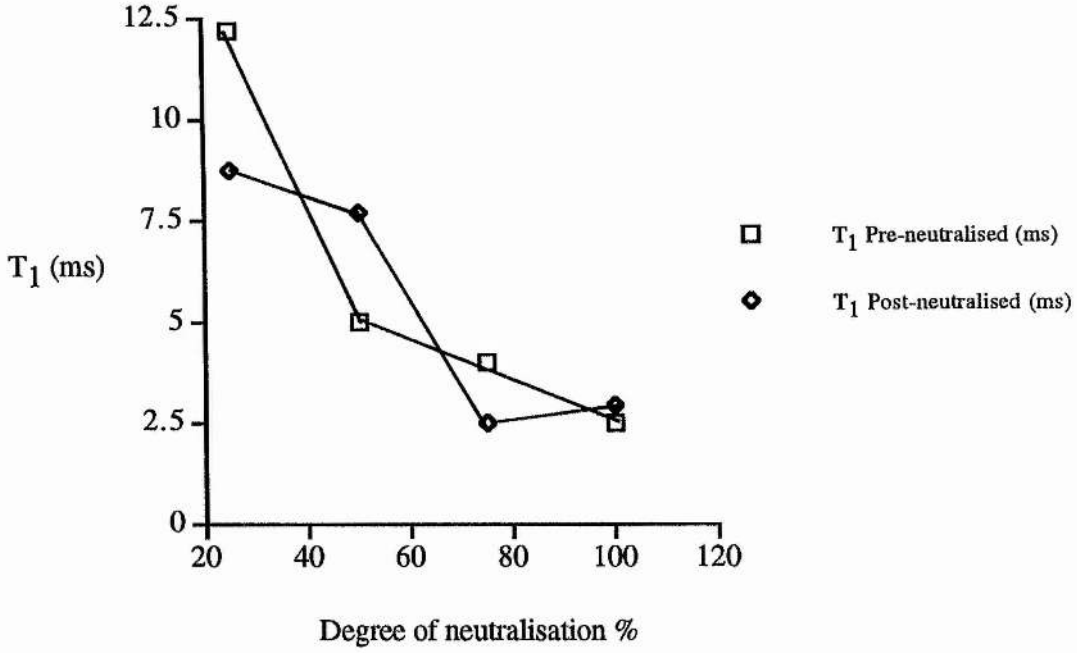

Figure 8.11. ^{23}Na T_1 Relaxation of Pre- and Post-neutralised polymers with varying degrees of neutralisation.

Pre- and post-neutralised polymers with varying degrees of neutralisation were also investigated with various degrees of hydration to look at the effect of hydration on the relaxation time (see tables 8.3 and 8.4). A couple of graphs have been included as a representation of all samples investigated (see figure 8.12 and 8.13).

Degree of hydration %	T_1 (ms) 25 % neutralised	T_1 (ms) 50 % neutralised	T_1 (ms) 75 % neutralised	T_1 (ms) 100 % neutralised
100	2.47	2.21	4.29	2.54
500	16.67	15.99	13.61	15.24
1000	27.38	23.77	27.86	16.13
5000	50.30	40.13	34.88	21.83

Table 8.3. ^{23}Na Relaxation times of hydrated post-neutralised superabsorbent polymers with varying degrees of neutralisation.

Degree of hydration %	T_1 (ms) 25 % neutralised	T_1 (ms) 50 % neutralisation	T_1 (ms) 75 % neutralised	T_1 (ms) 100 % neutralised
100	1.88	1.78	2.40	2.02
500	12.50	13.64	11.83	9.64
1000	32.89	19.72	22.03	13.00
5000	35.21	37.31	21.01	16.64

Table 8.4. ^{23}Na T_1 Relaxation times of hydrated pre-neutralised superabsorbent polymer with varying degrees of neutralisation.

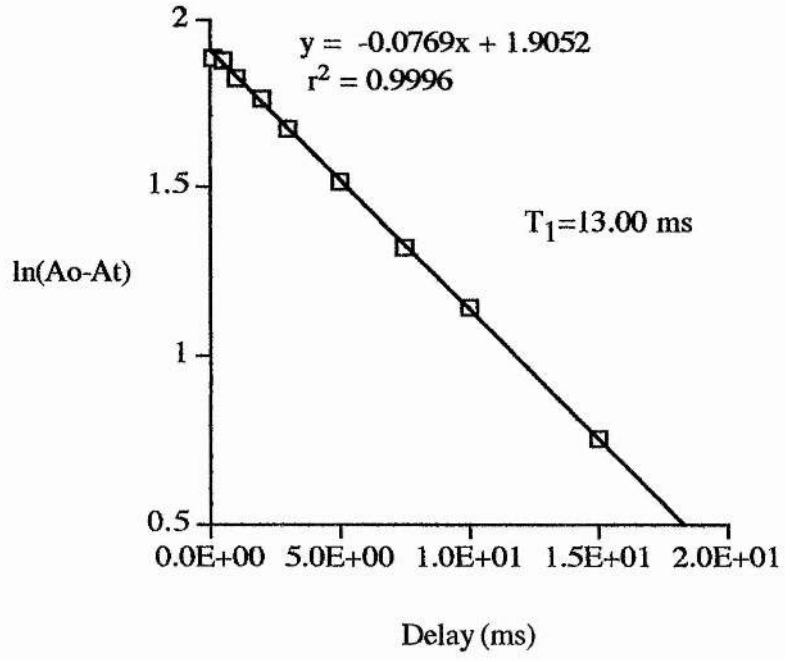

Figure 8.12. ^{23}Na T_1 Relaxation of ASAP 2300 pre-neutralised 100 % and 1000 % hydrated.

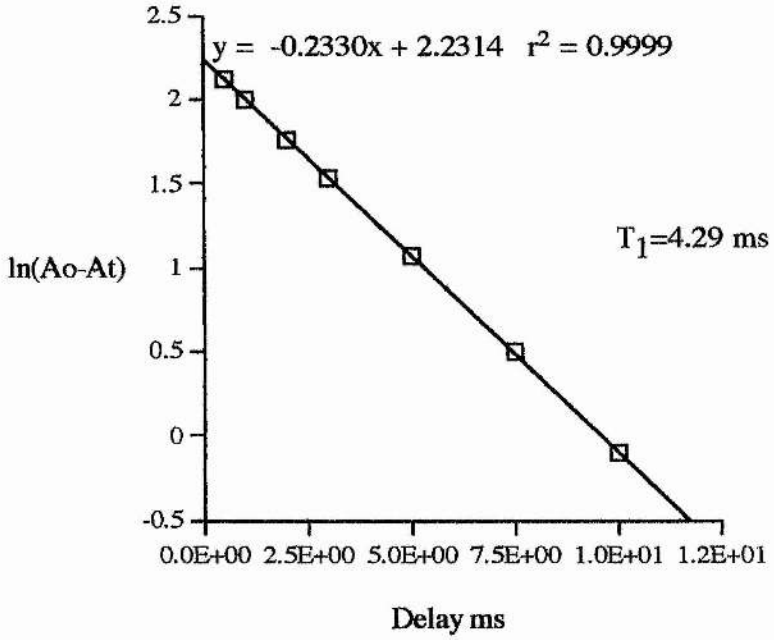

Figure 8.13. ^{23}Na T_1 Relaxation of DMRD1 post-neutralised 75 % and 100 % hydrated

Discussion

The ^{23}Na relaxation times of DMRD1 (with constant degree of neutralisation) at different levels of hydration give some indication of the change in environment of the sodium ions. It can be assumed that the dry polymer where the Na^+ and CO_2^- form contact ion pairs, contains an amount of water that is unable to be completely removed and quantified. Between the hydration levels 0 and 25 % a decrease in the ^{23}Na relaxation time is observed and it can be assumed that in this range the sodium ions are becoming hydrated, with the water molecules forming a hydration sphere around them. The formation of a hydration sphere around the sodium ion causes an increase in the electric field gradient. The water molecules can either participate in the first hydration sphere of the Na^+ or interact with the CO_2^- group. The shortest relaxation

time is observed where the polymer is 25 % hydrated and this is the point of the maximum linewidth.

One repeat unit of the polymer = 94 g which contains one sodium ion

At 25 % hydration the repeat unit will contain 23.5 g H_2O

23.5 g H_2O = 1.306 moles H_2O.

From this calculation it can be seen that very little water needs to be added to the polymer in order to observe the shortest ^{23}Na relaxation time. As further water is added to the polymer the ^{23}Na relaxation time begins to increase. It can be assumed that as the water is added the sodium ions are being further hydrated pushing them slightly away from the CO_2^- group breaking the contact ion pairs. The sodium ions begin to go into solution although most of them are still attached through hydrogen bonding. The section of the graph where the relaxation time begins to level off can be assumed to indicate that the polymer is now in a gel state with the Na^+ effectively floating around as if in solution. The biggest change in chemical shift of the sodium peak is observed as a high frequency shift during the region where the relaxation time is decreasing showing that the immediate environment of the sodium ions is changing as the hydration sphere is formed. As the relaxation time is increasing and levelling off a small low frequency movement in the chemical shift change is seen as a result of the immediate environment of the sodium ions not experiencing any changes.

For dry samples of ASAP 2300 (pre-neutralised) and DMRD1 (post-neutralised) with varying degrees of neutralisation it can be seen that as the degree of neutralisation increases the ^{23}Na relaxation time decreases. A realistic model for the relaxation is perhaps a flexible chain with point charges where a fast counterion motion along a curved rod and/or fast internal motions in the rod would be sufficient to explain the relaxation. An alternative possibility is that the lifetime of the Na^+ ion at the polyion is so short that the exchange dominates the correlation time.

Also seen as the degree of neutralisation increases is a high frequency movement of the chemical shift of approximately 3 ppm. As mentioned before chemical shifts of ^{23}Na are dominated by changes in the paramagnetic shielding term and are generally discussed in terms of the Kondo-Yamashita overlap model.[1] The chemical shifts are dominated by short range overlap effects and should in the absence of specific complex formation covering several groups on the polyion, vary with the degree of neutralisation in parallel with the number of counterions bound. A graph has been included of the chemical shifts against the degree of neutralisation for both pre- and post-neutralised polymers (see figure 8.14).

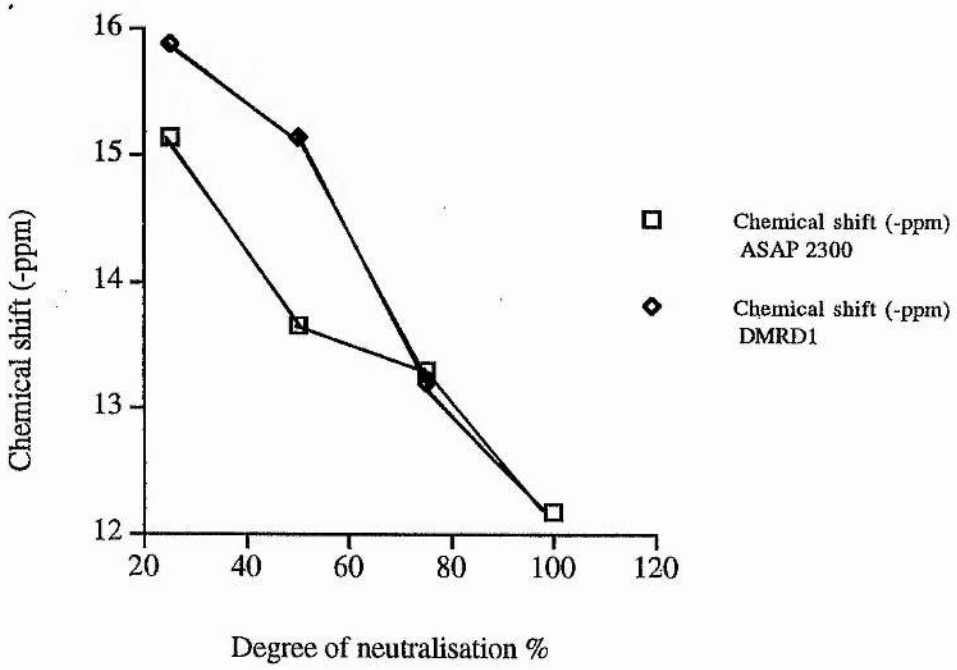

Figure 8.14. Chemical shift of Na peak in pre- and post-neutralised polymers.

The low frequency movement in chemical shift seen for both pre- and post-neutralised polymers as the degree of neutralisation increases is almost linear suggesting that the chemical shift varies linearly with the degree of neutralisation.

The hydration of both pre- and post-neutralised superabsorbent polymers with varying degrees of neutralisation, shows the same characteristic increase in relaxation time as the degree of hydration increases. The relaxation times of hydrated pre- and post neutralised polymers show that the post-neutralised polymer has a faster relaxation time at each of the various degrees of hydration. For both hydrated pre- and post-neutralised polymers a slower increase in the relaxation time is seen when the polymer is neutralised to 100 %. At each different degree of hydration the relaxation time decreases with increasing degree of neutralisation, although some of the relaxation times do not fit into this pattern. This may be due to experimental error within the results. It is therefore difficult to predict changes in the sodium ion environment as both the degree of neutralisation and hydration increases.

^{23}Na relaxational studies have never been carried out on solid crosslinked poly (sodium acrylate) so this study gives some insight into what happens as the polymer becomes hydrated as it does in many of its applications. From measuring the ^{23}Na relaxation times an assumption can be made as to the change in the sodium environment as the polymer becomes further hydrated. It has also been shown that the degree of neutralisation effects the relaxation of the sodium within the polymer as observed in solutions of poly(acrylic acid). A difference between the relaxation times of sodium ions within hydrated pre- and post-neutralised polymers has also been shown through this study, although experimental error will also play a part in these results.

References

1. H. Gustavsson, B. Lindman, T. Bull; *J. Am. Chem. Soc.*, (1978), **100**, 4655-4661.
2. P. Laszlo; *Angew. Chem. Int. Ed.*, (1978), **17**, 254-266.
3. A. J. Vega; Encyclopaedia of NMR, (1996), 3869-3876.
4. T. Tokuniro; *Journal of Magnetic Resonance*, (1988), **76**, 22-29.
5. S. K. Kang, M. S. Jhon; *Macromolecules*, (1993), **26**, 171-176.
6. G. Gunnarsson, H. Gustavsson; *J. Chem. Soc. Faraday Trans. I*, (1982), **78**, 2901-2910.
7. G. J. Templeman, A. L. Van Geet; *J. Am. Chem. Soc.*, (1972), **16**, 5578-5587.

Acknowledgements

There are many people without whose help this project would not have been possible.

Firstly I wish to thank Dr Frank Riddell for all his help and enthusiasm throughout this project. I especially wish to thank him for having faith in me and always reminding me that my project wasn't quite as bad as I thought. I also wish to thank past and present members of lab 408A especially Roger, Jukka and Jennifer who have been my good friends as well as great people to work with. I greatly appreciate the friendship shown to me by Roger at a time when I needed it most. I will also always remember Jukka's "Finnish jokes" and the pointing out of my bad English!! My most fondest memories will be of our group dinners where far too much alcohol was consumed and too many Finnish jokes were told!!!!!!

Special thanks must go to Chemdal and EPSRC for the funding of this project. I also wish to thank all the members of the R&D lab at Chemdal for their friendship and help during my visits. My industrial supervisor Dr John Henderson was extremely helpful and encouraging throughout the project and the visits from Dr Tony Tomlin provided useful discussions.

Sandy Chudek, Gina McKay and Professor Hunter from the University of Dundee must be thanked especially for all their help with the magnetic resonance imaging. I greatly appreciate the time they gave me on their machine and all their assistance with this new technique. Many hours of work were required to set up the best experimental parameters and I thank them for all their effort.

I also received great assistance from many technical members of staff in the department. Many thanks go to Melanja the NMR technician, for her assistance with the ever temperamental "Boris". Bobby and Jim from the workshop must also be

thanked greatly for their assistance in making a device suitable for use in magnetic resonance imaging experiments and for making even the worst days seem worthwhile.

I also thank Mary-Jane Tremayne for all her work on reproducing the images after they were sent across from Dundee and providing me with diagrams to see clearly what was going on.

A big thank you must also go to Dr Mackie for his support and encouragement.

My most special thanks go to my family and closest friends for their constant support and encouragement throughout my PhD.